# COMPUTER MODEL OF THE TWO-PINHOLE INTERFERENCE EXPERIMENT USING TWO-DIMENSIONAL GAUSSIAN WAVE-PACKETS

By

ILUNGA MADIKA ALFRED

A dissertation submitted in partial fulfillment

of the requirements for the degree of

Master of Science in Physics

THE UNIVERSITY OF ZAMBIA

LUSAKA

June, 2019

## COPYRIGHT

## DECLARATION

This dissertation represents my own work, and it has not previously been submitted for a degree, diploma or other qualification at this or any other university.

## APPROVAL

This dissertation of **ILUNGA MADIKA ALFRED** is approved as partial fulfillment of the requirements for the award of the degree of Master of Science in Physics by the University of Zambia.

| | | |
|---|---|---|
| Examiner I | Signature | Date |
| Examiner II | Signature | Date |
| Examiner III | Signature | Date |
| Board of Examiners | Signature | Date |
| Supervisor | Signature | Date |

## ABSTRACT

The current interpretation of quantum mechanics (the Copenhagen interpretation) does not allow a description of underlying physical reality in terms of a single well-defined model. This sometimes leads to paradox and even confusion. In 1952, Bohm introduced an alternative interpretation of quantum mechanics called the **causal interpretation** which does provide a description of underlying physical reality and therefore allows computer modelling of quantum systems. Such computer models have been produced using mainly FORTRAN 77. In this work, we use newer mathematical packages, especially Maple 2015, Mathematica 10.0 and Matlab R2015a, which contain many pre-existing algorithms which make modelling much simpler. We produce a computer model of the two-pinhole matter-interference experiment using $2-D$ Gaussian wave packets. Such a model has not been done before. Another objective is the comparison of various mathematical packages. We do this using each package to produce a computer model of the simpler problem (and already done before) of modelling the two-slit experiment using $1-D$ Gaussian wave-packets. Though no new conceptual results were expected by producing a computer model of the two-pinhole matter-interference experiment using $2-D$ Gaussian wave packets and the Bohm-de Broglie causal interpretation, but we have found that it retains the characteristic features of the two-slit modeled by $1-D$ Gaussian wave packets case.


.

## DEDICATION

I dedicate this work to:

God Almighty my creator, my strong pillar, my source of inspiration, wisdom, knowledge and understanding. He has been the source of my strength throughout this program and on His wings only have I soared.

My father Omer Madika and mother Christine Mwadi, source of my happiness and success in life. May God bless them.

To the kindest person who gave me strength despite the distance: My wife Babaka.

To my brothers ya Felly, Olivier Tshilolo, Henry Kabongo, Guy Ngoy, Junior Mukandila, Sedrick Tshitala, Credo Kabamba and Christian, and my sisters ya Mbeya, Therese and Judith Nseya for their unconditional support and encouragements to pursue my interests.

To my extended family and the many friends, who have been so supportive and encouraged the fulfillment of this work.

To all those who believed in me and prayed for my success, God bless you.

## ACKNOWLEDGMENTS

This thesis would not have been possible without the help and support of a large number of individuals. First and foremost, I would like to thank my family members, especially my beloved wife Nicole Babaka and children Nseya Bellegrace, Kabongo Benel and Nzongola Beniel, who have endured my absence during my research and helped me tremendously in all ways possible. Without your continued help, support and guidance, this would never have been possible. My love for you all can never be quantified.

I have to thank my parents for their love and support throughout my life. Thank you both for giving me strength to reach one of my dreams. My siblings deserve my wholehearted thanks as well.

I am deeply indebted to my research supervisor Prof. PN Kaloyerou, who has given much time, stimulating advice, guidance, encouragement, software and knowledge every step of the way to aid in the completion of this dissertation. I thank him for the accurate advice he put forward and for his patience with me throughout the stages of the research. My thanks to him are limitless for being kind enough to accept directing this work with all his academic engagements. I would also like to thank all the members of staff of physics department (University of Zambia).

I address my special thanks and gratitude to my examiners for having accepted to examine my dissertation.

To all my friends, thank you for your understanding and encouragement in my many moments of crisis. Your friendship makes my life a wonderful experience. I cannot list all the names here, but you are always in my mind.

This thesis is only a beginning of my journey. Thank you, Lord Jesus, for always being there for me.

Finally, I am grateful to have had the privilege of attending the University of Zambia. This experience has afforded me the opportunity to work as a tutor at physics department and the resources for me to achieve great success. Thank you for this opportunity.

# Contents

# List of Figures

# Chapter 1

# Introduction

The current interpretation of quantum mechanics (QM) (the Copenhagen interpretation) does not allow a description of underlying physical reality in terms of a single well-defined model. This sometimes leads to paradox and even confusion.

In 1952, Bohm introduced an alternative interpretation of QM called the causal interpretation (CI) which does provide a description of underlying physical reality and therefore allows computer modelling of quantum systems. Such computer models have been produced using mainly Fortran 77. [1]

In this work, we use newer mathematical packages, especially Maple 2015, Mathematica 10.0 and Matlab R2015a, which contain many pre-existing algorithms which make modelling much simpler. The challenge is to first provide the mathematical model, to derive the equations describing the system based on the CI. We then want to use Maple 2015, Mathematica 10.0 and Matlab R2015a to produce a graphical model. Alternatively, we can use these packages to automatically carry out mathematical steps, and to again produce graphical models. We note that Fortran 77 may still prove to be superior in some cases. Specifically, we want to produce a computer model of the two-pinhole experiment using $2-D$ Gaussian wave packets. These models constitute the new part of the project. Another objective of the project is to evaluate the best package or combination of packages for computer modelling of quantum system. We do this by using each package to produce a computer model of a simple problem (already done by others

[2]) of modeling the two-slit experiment using $1-D$ Gaussian wave-packets.

Though no new conceptual results are expected, we thought it might be interesting to see if the trajectories, now for two-pinhole experiment modeled by $2-D$ Gaussian wave packets, might retain the characteristic features of the two-slit modeled by $1-D$ Gaussian wave packets case.

Let us list our objective in detail:

(1) To compare the software packages Maple 2015, Mathematica 10.0 and Matlab R2015a by using them to reproduce the existing model of the two-slit experiment usng the Bohm-de Broglie CI and using $1-D$ Gaussian wave packet,

(2) To derive the formula, using the Bohm-de Broglie CI needed to model the intensity and quantum potential for the two-pinhole experiment using 2D-Gaussian wave packets,

(3) To derive the coupled nonlinear differential equation used to obtain the trajectories, again using the Bohm-de Broglie CI,

(4) To write a program in Fortran 77 to solve the coupled nonlinear differential equation which describe the trajectories, i.e., to produce the data values needed to plot the trajectories,

(5) To write the Maple programs to produce intensity, quantum potential and trajectories plots using $2-D$ Gaussian wave packet. These various plots constitute the model of the two-pinhole experiment that we seek.

## 1.1 Birth of Quantum Mechanics

Let us fly over the few events that took place at the birth of QM:

- **December 14, 1900. Birth of quantum theory**: Planck, before the German Physical Society, proposed a simple formula in perfect agreement with the experiments on the spectrum of black body radiation. Planck had first obtained his result from empirical arguments, but had noticed that one could deduce the

central point of his argument from statistical thermodynamics by the curious assumption that loaded mechanical oscillators, of frequency $\nu$, could only emit or absorb light energy by discrete amounts (the 'quanta' of energy $nh\nu$).

- **1905. Einstein postulates the photon**: The next big step in the development of quantum theory was Einstein's recognition that energy itself is quantised with the statement that radiant energy is actually quantified; this feature is not an artifact of calculation. This marks the birth of the concept of the photon, which he used to explain the photoelectric effect.

- **1912-1914. Bohr's model of the atom**: Another major step was the introduction of Bohr's model of the atom. Bohr sought a coherent model of the structure of atoms. He was guided by the principle of combination of spectral lines of Ritz, the atomic model of Rutherford (who had, in 1911, discovered the existence of the nucleus), and the quanta of Planck and Einstein. Bohr postulated that the energies of atomic and molecular structures adopt discrete values, and the emission or absorption of light is made only to certain specific light frequencies.

- **1923, Particle-wave duality**: de Broglie hypothesized that, as light has a corpuscular behavior, particles such as electrons can have a wave behavior. This wave hypothesis allowed the interpretation of the quantification of matter as a phenomenon of stationary waves, and restored the continuity so desired by Einstein.

- **1925, Heisenberg's matrix mechanics**: In 1924 Heisenberg, in an astonishing inspiration, and largely imbued with philosophical ideas, developed a theoretical framework, somewhat mysterious, the results of which were astonishing. Max Born recognized quickly in the symbolic multiplication that Heisenberg introduced, the rules of matrix algebra, and in early 1925, the School of Göttingen (Heisenberg, Born, Jordan and Pauli) laid the foundations of matrix mechanics which was given for the first time, the name of *Quanten Mechanik*. Following a Heisenberg lecture in Cambridge in July 1925, Dirac developed independently during the summer of 1925 his own formulation of the theory, based on the property of non-commutative quantum quantities. Dirac's formulation is equivalent to the Göttingen School but more general and elegant.

- **1926, Schrödinger's wave equation**: Erwin Schrödinger acknowledged the work of de Broglie. He was seduced by de Broglie's work, but skeptical about its merits

for reasons of relativistic invariance. Urged by several colleagues, including Debye and Einstein, Schrödinger used his competence in partial differential equations to build, in an astonishing series of eight articles published in 1926, what became known as wave mechanics. In his work, Schrödinger succeeded in developing a partial differential equation, now called the Schrödinger equation which is a cornerstone of wave mechanics. An immediate problem was that the solutions of the Schrödinger equation were complex functions and the physical interpretation was not at all obvious. This led to a number of suggested interpretations. The most prominent of these were the Copenhagen interpretation (consisting of the Born probability rule and Bohr's principle of complementarity (BPC)), de Broglie's theory of the double solution and his pilot wave theory, the Madelung hydrodynamical equation and Schrödinger's electromagnetic interpretation. We note that de Broglie favored the theory of the double solution, and viewed his pilot wave theory alone only as a temporary interpretation, until his theory of the double solution was completed.

- **1927, Bohr's Como Lecture given at the Como Congress, 11 to 20 September**: Bohr gives the first outline of his new conceptual framework of complementarity, followed by a presentation of the uncertainty principle of Heisenberg and the role of measurement in quantum theory. Bohr also adopted the probabilistic interpretation of Max Born of the wave function of Schrödinger. These elements formed the foundations of a new physical understanding of QM. Physicists later called this fusion of ideas 'The Copenhagen interpretation'.

- **1927, Fifth Solvay Congress, 24 to 29 October**: The fifth Solvay Congress was convened to consider the various interpretations of QM. Attending the congress was a highly auspicious group of the world's leading physicists among whom were Lorentz (the chair of the meeting), Bohr, Einstein, Born, Bragg, Brillouin, de Broglie, Compton, Debye, Dirac, Ehrenfest, Heisenberg, Kramers, Planck, Pauli and Schrödinger. Of the interpretations presented, among the most prominent were the Copenhagen interpretation and de Broglie's pilot theory (a truncated version of the double solution). De Broglie was unable to answer a criticism due to Pauli regarding the Fermi rigid rotator (a criticism related to the measurement problem). Partly for this reason and partly, perhaps, because of the general dislike, de Broglie's pilot wave theory was poorly received. In fact, the response was

so negative that de Broglie abandoned his theory in favor of the Copenhagen interpretation. Indeed, at the end of the congress the Copenhagen interpretation was almost universally adopted by the audience. By 1932, and with the introduction of the von Neumann impossibility proof, a realistic interpretation of QM was considered impossible, and the Copenhagen interpretation gained almost total prominence.

- **1932**: The mathematician von Neumann presented a proof [3] that it is impossible for any type of hidden-variable theory (a 'hidden-variable' is any quantity introduced into the description of the system and which can not be reduced to the wave function) to reproduce all of the statistical predictions of the standard quantum theory. This proof is now commonly referred to as 'The von Neumann impossibility proof'. This proof was widely believed to be logically irrefutable, and most physicists paid a lot of lip service to it believing its conclusion to be true, though many never bothered to read it.

- **1925-1932**: The theory of QM in its current form developed during this period, and appears as the result of the exceptional combination of the talents of physicists and mathematicians like Schrödinger, Heisenberg, Born, Bohr, Dirac, Pauli, Hilbert, von Neumann, etc. This remarkable synthesis, followed by crucial experiments that were to quickly anchor the new mechanics, came from work done in the first quarter of the twentieth century. From there, two equivalent approaches of this theory were Born.

- **1935, The Einstein, Podolsky and Rosen (EPR) experiment**: In this experiment, EPR's goal was to refute the Copenhagen interpretation of QM by showing that the wave function does not give a complete description of physical reality. They showed in their thought experiment that either the world is nonlocal in the sense that doing a measurement on the left has a faster than light affect to the right, or QM is incomplete. One of these conclusions is unavoidable if one analyzes the EPR experiment. Because of his theory of special relativity, Einstein rejected the non-locality conclusion, and EPR interpreted their experiment as demonstrating the incompleteness of the Copenhagen interpretation. Einstein's hope was to find a super-theory which would reproduce the predictions of QM (there was no question of disputing the practical success of this theory), and would be determin-

istic. Bohr was able to show the completeness of QM, and as a result the EPR experiment came to be regarded as demonstrating a revolutionary aspect of QM, namely, nonlocality. EPR became EPRB when Bohm offered a version of the EPR thought experiment involving spin, which is much easier to perform experimentally.

- **1952**: In two fundamental 1952 articles, entitled 'A Suggested Interpretation of the Quantum Theory in Terms of 'Hidden' Variables I and II', Bohm introduced the CI of QM. This interpretation is deterministic but is able to reproduce all the statistical results of the quantum theory. Probability enters this deterministic theory because the initial positions can never be determined, and hence are called 'hidden-variables'. The CI provides the description of underlying physical reality in terms of a single well-defined model. Such a model was considered to be impossible according to BPC. In fact, Bohm's CI was resurrection of de Broglie's pilot theory, but Bohm only learned of de Broglie's work after completing his papers. Bohm, however, succeeded in providing an answer to the measurement problem, effectively answering Pauli's Fermi rigid rotator criticism of the 1927 congress which de Broglie failed to do.

- **1952 onwards**: The publication of Bohm's work rekindled the Broglie's interested in the CI. De Broglie's student Vigier also became very interested in the CI. Subsequently, Bohm, Vigier and de Broglie developed various aspects of the CI [4]. Other possible interpretations of the CI were considered. One prominent example was to consider a hydrodynamical model of a subquantum level. In 1955, Bohm, with Schiller and Tiomno, extended the CI to include spin [5]. Takabayasi in 1952 extended Bohm's CI to the Dirac equation [6].

- **1964-66, Bell's Locality Theory**: In the first of his 1952 papers Bohm argued that the von Neumann impossibility proof did not apply to his hidden-variable theory. Motivated by Bohm's argument and the CI in general, Bell showed [7] that the von Neumann impossibility proof, and later versions of this proof by Kochen and Specker [8] are not completely general. Specifically, Bell showed that these impossibility proofs do not apply to nonlocal hidden-variable theories, of which Bohm's CI is an example. In a 1966 paper [9], Bell established an inequality that demonstrates that nonlocal hidden-variable theory can reproduce the statistical results of the quantum theory. Bell's theorem has since been confirmed by numer-

ous experiments following the work of Shimony and others [10] who recast Bell's theorem into a practical form suitable for use with photon polarisations.

- **1982, Aspect, Grangier and Roger (AGR)**: Motivated by Bell's work, and based on EPRB, but using photon polarisation, Aspect et. al [11] performed the first actual EPR experiment and confirmed the non locality of QM.

## 1.2 Suggested Interpretations of QM

At the time of the birth of QM, physicists and mathematicians were very familiar with differential and partial differential equations. Hence, they focused on the Schrödinger equation which is a partial differential wave equation. There were two issues that they had to contend with:

(1) The solutions $\Psi$ of Schrödinger's equation were complex functions and not at all clear to interpret physically,

(2) Experiments revealed a dual particle-wave behaviour of fundamental entities.

These difficulties motivated quite a number of interpretations to be put forward. Among the most prominent were Schrödinger's electromagnetic interpretation, Madelung's Hydrodynamical model, de Broglie's pilot-wave theory and his theory of the double solution, Born's probability rule and BPC and Bohm-de Broglie interpretation.

### 1.2.1 Schrödinger's Electromagnetic Model

At the end of his series of memoirs 'Quantification and eigenvalues' in 1926, Schrödinger proposed a physical interpretation of the function $\Psi$. He wrote, "the meaning of the function $\Psi$ in the configuration space is purely formal: $\Psi$ is the function that satisfies the wave equation. It is necessary to attribute to it a physical sense, more precisely an electromagnetic sense ". It is because this physical sense is related to the physical conditions of the initial problem which was that of the emission of electromagnetic waves by an atomic system and the properties of these waves. This physical significance is therefore expressed in terms of the electric charge density given by the integral over the space covered by the material system of the form $\Psi\Psi^*$, which represents 'a kind of weight function in the space of system configuration'. Underlying this interpretation,

and guiding it, stands the image of the 'wave configuration of the system', constituted by the superposition of 'all the possible kinematic configurations of the system', each intervening with the mentioned weight. It is basically this notion that replaces the notion of trajectory found in the macroscopic approximation. In this way of viewing things, the function $\Psi$ is given an abstract definition over a configuration space, to which is added a physical interpretation as regards its relation to real space: "A determined distribution of the values of $\Psi$ in the configuration space is interpreted as a continuous distribution of electricity (and of electric current density) in real space", specified by Schrödinger in the analytical table of contents prepared in November 1926 edition of his articles [12].

### 1.2.2 The Hydrodynamical Interpretation of QM

The earliest hydrodynamic interpretation was proposed by Erwin Madelung (Ph.D. Göttingen, 1905 [13]). While Schrödinger's attempt to interpret QM found its support primarily in the analogy to wave phenomena, the similarity of the wave equation and its implications for the equations of hydrodynamical flow formed the basis for another early attempt to account for QM processes in terms of classical continuum physics.

The Hydrodynamical interpretation of QM starts by introducing the wavefunction in polar form in the time-independent Schrödinger equation, and taking into account the definition of the velocity field

$$\mathbf{v} = \dot{\mathbf{r}} = \frac{\nabla S}{m} \tag{1.1}$$

and

$$\rho = R^2 = \Psi^* \Psi, \tag{1.2}$$

$$\mathbf{J} = \rho \mathbf{v} = R^2 \frac{\nabla S}{m}, \tag{1.3}$$

where $\rho = \rho(r,t)$ is the probability density and $J = J(r,t)$ is the quantum density current.

By proceeding in this way with

$$\nabla S = \mathbf{p} = m\mathbf{v}, \tag{1.4}$$

equations

$$\frac{\partial R^2}{\partial t} + \nabla . \left( R^2 \frac{\nabla S}{m} \right) = 0, \tag{1.5}$$

$$\frac{\partial S}{\partial t} + \frac{(\nabla S)^2}{2m} + V - \frac{\hbar^2}{2m} \frac{\nabla^2 R}{R} = 0 \tag{1.6}$$

transform to

$$\frac{\partial \rho}{\partial t} + \nabla . \mathbf{J} = 0, \tag{1.7}$$

$$\frac{\partial \mathbf{v}}{\partial t} + (\mathbf{v} . \nabla)\mathbf{v} = -\frac{1}{m} \nabla (V + Q) \tag{1.8}$$

These equations constitute the formal basis of the hydrodynamical interpretation and are in direct correspondence with those of classical fluid mechanics [14].

The hydrodynamic theory of QM was later extended by de Broglie (idea of the 'double solution') and Bohm (idea of 'subquantic medium') and used as a preliminary theoretical scheme for quasicausal interpretations of microphysical phenomena.

### 1.2.3 De Broglie Pilot-Wave Theory and the Theory of Double Solution

In his early work on wave mechanics that goes back to 1923, de Broglie had clearly outlined the need to associate with the motion of any particle the propagation of a wave. But the homogeneous wave he was led to consider, which was to become the wave $\Psi$ of the usual wave mechanics, did not seem to exactly describe physical reality. He noted that the phase of the wave directly related to the particles motion. This feature seemed to de Broglie to have a deep meaning. For this reason, he named this wave, a solution of Schrödinger equation and associated with a particle's motion, the particle 'phase wave'.

It was in his submission of 1927 [15], that de Broglie had the idea that in any problem of wave mechanics two solutions had to be considered. One of the solutions is the phase wave $\Psi$ whose phase can be interpreted physically as giving the motion of the particle. However, due to the continuous nature of its magnitude, it has to be given a probabilistic and subjective meaning. De Broglie supposed that the second wave $u$, having the same phase as the $\Psi$ wave, has a very large amplitude around a small point

in space. It is this singular solution that de Broglie interpreted as representing a particle.

De Broglie developed a reasoning which led him to the conclusion that the phase wave $\Psi$ can be given a hydrodynamical interpretation in which flow lines give the particle's motion. The singular solution $u$ follows one of these flow lines. This is the essence of de Broglie's theory of the double solution: the phase wave $\Psi$ guides the motion of the particle represented by the soliton wave solution $u$.

Thus, de Broglie considered two coupled solutions:

The first, the phase wave, is a solution of the Schrödinger equation and can be written as

$$\Psi = a.e^{\frac{2\pi i}{h}\varphi}, \tag{1.9}$$

where $a$ and $\varphi$ are real and continuous functions.

The second solution is a singular solution of a certain nonlinear equation such that the motion of the soliton wave is guided by solutions of the Schrödinger equation, given by

$$u = f.e^{\frac{2\pi i}{h}\varphi}, \tag{1.10}$$

where $\varphi$ is the same function as in $\Psi$ and where the amplitude $f$ has very high values in a singular region. The formula for the speed of the particle identified in this unique region at each point of its trajectory has the following simple form:

$$\mathbf{v} = -\frac{1}{m}\nabla\varphi, \tag{1.11}$$

where $m$ is the mass of the particle

The wave $u$ is the true description of physical reality: it gives the image of a particle. De Broglie judged it necessary to introduce a strong 'inhomogeneity' located in a very small area within an extended wave phenomenon in which it is intimately incorporated. By postulating a parallelism between the wave $u$ (objective reality) and the wave $\Psi$ (construction of our mind), it seemed possible to him to justify the statistical properties awarded to the $\Psi$ wave. The theory of the double solution restores objectivity, deter-

minism and location.

At the time, de Broglie could not find the nonlinear equation he sought and so he developed his simpler pilot-wave theory as an interim interpretation of the QM.

The pilot-wave theory was meet with severe criticism from Pauli in particular. De Broglie was unable to respond to Pauli's objection, which concerned Fermi's rigid rotator (an objection essentially to do with the measurement problem of QM).

### 1.2.4 The Copenhagen Interpretation

BPC together with the Born probability interpretation form what is called the Copenhagen interpretation and is the most widely accepted interpretation of QM.

Born interpreted the wavefunction as a probability such that $\mid \Psi(x, y, z, t) \mid$ gives the probability of finding a particle at $x, y, z, t$. This Born probability rule is an essential interpretational element which links theory with experiment.

In Copenhagen's interpretation of QM, the wave function of a particle represents all the information on the particle. This wave function is a vector of a Hilbert space representing a quantum state. The linearity of the Hilbert space corresponds to the superposition principle according to which the quantum states can be combined, superposed, as waves and fields do in classical physics. When the wave function is the superposition of several terms, the properties of this particle are not well defined; in particular, the position and speed of a particle are no longer defined individually. Only a measurement made on the particle can specify them by means of a reduction of the wave packet. As long as no measurement is made, the properties of the particle are only known by the probability that a possible measurement will give such and such a value.

Thus, in the Young Slits experiment, the particle has no position before the impact and the position of the impact on the detecting screen can only be deduced from the square of the wave function module statistically, without any possible explanation.

Thus, according to Bohr, an electron is never a particle and never a wave. Rather, in

one experiment the concept of a particle can be used to describe the experiment, but in another mutually exclusive experiment the wave concept may be used for its description, but reality should not be attached to either concept. Bohr achieves consistency at the very heavy price of giving up a description of underlying physical reality.

Bohr never achieved a uniquely definitive statement of the Copenhagen interpretation, and over the years numerous variations of complementarity have evolved. Some even stand in contradiction to Bohr's original complementarity (e.g.: The Wootters-Zurek formulation of complementarity [16], a critique of which has given by Kaloyerou [17] ). Indeed, it is sometimes flippantly said that there are as many interpretations of QM as there are physicists. However there are certain core elements of Bohr's original complementarity that run through Bohr's writings. According to Kaloyerou [17] these core elements can be embodied in four tenets:

(T1) The concept of a precisely definable classical state must be given up (because of the quantum postulate), and a separation of subject (experimental apparatus) and object (quantum system) is impossible. An experiment must therefore be viewed as an unanalyzable whole.

(T2) A single picture is not sufficient to exhaust the description of a quantum system. Rather pairs of complementary concepts are needed. Such complementarity concepts (for example, wave and particle concepts) can only be used in mutually exclusive experimental arrangements. Indeed, it is the experimental arrangement which defines the concept to be used.

(T3) Classical concepts are abstractions to aid thought and to communicate the results of experiment, but cannot be attributed to physical reality.

(T4) A description of physical processes that underlie experiment in terms of a single well defined model is impossible, i.e., a description of underlying physical reality in terms of a single-well defined model is impossible.

### 1.2.5 Bohm-de Broglie interpretation

In this interpretation, the wave function does not represent all the information on the particle; we must add an initial position to describe it completely; it is this position

that is improperly called 'hidden variable' because as Bell says it is the main directly measured variable. In this case, we deduce from the wave function the trajectory of the particle by taking as speed the gradient of the phase of the wave function. This is how we can say with de Broglie that the wave 'drives' the particle. It is not irrelevant to remark that we have a similar result in classical mechanics: the velocity of a particle is indeed equal to the gradient of the action divided by the mass of the particle; we can therefore say that in classical mechanics also the action 'drives' the particle.

An important consequence of the choice of this 'speed' is that it gives the same statistical results as the Copenhagen interpretation, but also and above all it explains the individual impacts of particles, which the Copenhagen interpretation does not.

In the experience of Young's slits, the impact on the detection screen then corresponds to the classical position of the particle. However, this deterministic position depends on the initial position of the particle. As the latter is unknown, the final position can in practice be known only statistically, as the Copenhagen interpretation says.

Thus Bohm showed that von Neumann's impossibility proof did not apply to his model. Later, Bell [9] demonstrated more generally that von Neumann's impossibility proof applied only to local hidden variable theories but not to nonlocal theories such as Bohm showed's.

## 1.3 The von Neumann Impossibility proof

Von Neumann developed a theory of measurement that is similar to that of the Copenhagen interpretation, except that he considered the measuring apparatus as obeying the rules of QM like the measured system.

In his book of 1932 'The Mathematical Foundations of quantum theory' [18], he presented a theorem which appeared to show the impossibility to complete QM by hidden-variables. This impossibility, with its physical interpretation, became almost a postulate of QM, based on von Neumann's indisputable mathematical authority [19].

Let us consider an observable of spin $R$ corresponding to a $2 \times 2$ Hermitian matrix R. If a series of $N$ measurements of $R$ is carried out on particles prepared in an identical

manner (that is to say particles having the same initial wave function), we will get the results:

$$R = r_1, r_2, ..., r_N. \tag{1.12}$$

In agreement with QM, the accuracy of which is not disputed here, these results will have to coincide in each case with one of the two eigenvalues of the matrix $R$.

It is useful to consider also the observable $R^2$ which is by definition an observable which can be measured by first measuring $R$, then taking the square of the result obtained. The $N$ previous measurements of $R$ then also constitute $N$ measurements of $R^2$ that we find equal to:

$$R^2 = r_1^2, r_2^2, ..., r_N^2. \tag{1.13}$$

Let us suppose that the results $r_1, r_2, ..., r_N$ are actually conditioned by a hidden-variable $\lambda$, or more precisely, by the values $\lambda_1, \lambda_2, ..., \lambda_N$ that $\lambda$ possesses immediately before each measurement operation. We can then write:

$$r_1 = r(\lambda_1), r_2 = r(\lambda_2), ..., r_N = r(\lambda_N), \tag{1.14}$$

If we prepare the particles in such a way that $\lambda$ is always the same before each measurement (that is, if $\lambda = \lambda_0$), obviously, we will always obtain the same result:

$$R = r_1, r_2, ..., r_N = r(\lambda_0), r(\lambda_0), ..., r(\lambda_0), \tag{1.15}$$

It follows that for such a set with fixed $\lambda$:

$$\langle R \rangle = \frac{1}{N} \sum_{i=1}^{N} r_i = r(\lambda_0) \tag{1.16}$$

$$\left\langle R^2 \right\rangle = \frac{1}{N} \sum_{i=1}^{N} r_i^2 = r^2(\lambda_0) \tag{1.17}$$

Consequently, the mean squared deviation on the observable $R$, defined in elementary error theory as the square root of the difference between $\langle R^2 \rangle$ and $\langle R \rangle^2$ vanishes:

$$\Delta R = \left(\left\langle R^2 \right\rangle - \left\langle R \right\rangle^2\right)^{\frac{1}{2}} = 0 \tag{1.18}$$

$\Delta R$ is also called dispersion. We will then say that the variable $R$ is without dispersion when the hidden-variable has a fixed value ($\lambda = \lambda_0$ in this case).

More generally, we can consider a situation in which there are several different observables (as for spin 1/2 particles at rest). Let $R, S, T, ...$ be the set of all the observables belonging to the considered particles.

$$R = r_1, r_2, ..., r_N$$

$$S = s_1, s_2, ..., s_N$$

$$T = t_1, t_2, ..., t_N$$

$$...$$

It is useful to consider also the observables $R^2$. Thee are:

$$R^2 = r_1^2, r_2^2, ..., r_N^2$$

$$S^2 = s_1^2, s_2^2, ..., s_N^2$$

$$T^2 = t_1^2, t_2^2, ..., t_N^2$$

$$...$$

In the spirit of a hidden-variable model, we can say that the results obtained by measuring $R$, or $S$, or $T$, ... are fixed by the values of the hidden-variables contained in the set $\lambda, \mu, \nu, ....$ We find: $\Delta R = \Delta S = \Delta T = ... = 0$. This is an obvious consequence of the fact that these observables have well-defined (fixed) values.

Since all the observables of the particles forming the statistical set have zero dispersion, we say that we are dealing with a set without dispersion. We do not need the fact that the different observables can be represented by non-commuting matrices. This simply means that it is not possible to build an instrument capable of measuring them simultaneously. But if we have two such observables $R$ and $S$ represented by the two non-commutative matrices $R$ and $S$ of $2 \times 2$ dimensions and only one hidden-variable

$\lambda$ of fixed value $\lambda_0$ (the extension of the following reasoning to several hidden-variables being immediate), we will perform on a part of the system the measurement of $R$ and on the rest of the system, the measurement of $S$. In the first case, we will always find $r_0$ and in the second, always $s_0$. Moreover, we will always have $\Delta R = \Delta S = 0$, which does not lead to a contradiction with the non-commutativity of the matrices $R$ and $S$, since the measurements of $R$ and $S$ must be carried out on different subsystems. If we believe in hidden-variables, we can always think that a given set is a union of sets without dispersion. The familiar result of QM (i.e., $\Delta R \times \Delta S = \hbar$) will appear for the whole set, but not for its non-scattering parts. The practical difficulty of preparing sets without dispersion is not involved here. What is important is that we can logically design each given set as a union of subsets without dispersion.

It was precisely against the existence of such sets that von Neumann's theorem was directed. If we succeed in showing that it is in default in a concrete physical situation, it will ipso facto lose its generality.

The von Neumann's theorem axioms are [20]:

(A.1) there is a bijection between spinSpin observables and $2 \times 2$ Hermitian matrices,

(A.2) if the observable $R$ corresponds to the matrix R, then the observable $f(R)$ corresponds to the matrix $f(R)$,

(A.3) if $R$ and $S$ are any observables and if $a$ and $b$ are real numbers, the following relation (expressing the linearity of the mean) is true:

$$\langle aR + bS \rangle = a \langle R \rangle + b \langle S \rangle \tag{1.19}$$

From these three axioms, von Neumann deduced that sets without dispersion can not exist.

Let us now turn to the proof of von Neumann's theorem, that is, there can not be hidden-variables if the three axioms stated above are true.

Let us suppose there is a hidden-variable $\lambda$ that determines the results of the measurements of all possible spin components. Let us consider a set in which $\lambda$ has a fixed

value $\lambda_0$, that is to say a set without dispersion. Let $R$, $S$ and $T$ be three observables of respective matrices $R$, $S$ and $T$, of dimension $2 \times 2$. Measurements of these observables in a set without dispersion necessarily lead to the conclusion that:

$R$ has a fixed value $r_0 = r(\lambda_0)$ which is an eigenvalue of $R$

$S$ has a fixed value $s_0 = s(\lambda_0)$ which is an eigenvalue of $S$

$T$ has a fixed value $t_0 = t(\lambda_0)$ which is an eigenvalue of $T$.

In particularizing this general conclusion, we can assume that: $R = \sigma_1$, $S = \sigma_2$ and $T =$
$sigma \times \mathbf{n}$ with $\mathbf{n} = (1, 1, 0)$. Hence, $T = R + S$. Thus, the eigenvalues of $T$ are: $\lambda_{1,2} = \pm\sqrt{2}$.

Applying $(A.3)$, we deduce that $\langle T \rangle = \langle R \rangle + \langle S \rangle$. This relation can not be satisfied however, since the eigenvalues of $R$ are $\lambda_{1,2} = \pm 1$, the eigenvalues of $S$ are: $\lambda_{1,2} = \pm 1$ and the eigenvalues of $T$ are $\lambda_{1,2} = \pm\sqrt{2}$. No choice of signs allows us to write the relation $\pm\sqrt{2} = \pm 1 \pm 1$.

Starting from the von Neumann axioms and the existence of sets without dispersion we are thus led to an absurd conclusion. If we believe that the axioms are correct we must conclude, therefore, that there are no sets without dispersion. As we have seen in this section, it amounts to saying that QM can not be completed by means of hidden-variables.

## 1.4 Von Neumann's Theorem is not General Enough

If we superficially consider $(A.1)$, $(A.2)$ and $(A.3)$, nothing seems false. $(A.1)$ establishes a very simple correspondence between spin observables and $2 \times 2$ Hermitian matrices: if this axiom was false, then we would be obliged to construct a different theory of QM that makes this bijection a fundamental basis of its formalism. $(A.3)$ postulates the linear properties of the averages which are true in QM and which also seem valid in classical physics. To verify this, let us consider a set of classical particles placed in an external field and suppose that they are moving at different speeds. The general relation $E = T + V$ expresses the total energy $E$ as the sum of the kinetic energy $T$ and the potential energy $V$. For $N$ individual particles, we measure $T$ (and we find $T_1, T_2, ..., T_N$) and $V$ (and we

find $V_1, V_2, ..., V_N$) and we calculate $E_1 = T_1 + V_1, E_2 = T_2 + V_2, ..., E_N = T_N + V_N$ as: $\langle E \rangle = \langle T \rangle + \langle V \rangle$.

Thus, in this example, $(A.3)$ is also true for classical physics. However, it is this axiom which is insufficient when we consider other types of classical measurements.

To put this clearly, we will consider a concrete model of spin 1/2 particles and measure their spin. This model reproduces all the predictions of QM (results, probabilities) and presents itself as a model that causally complements QM, which the von Neumann theorem precisely attempts to prohibit.

The properties of this model are contained in the following three hypotheses:

(H.1) Spin 1/2 particles can be simulated by rotating spheres that are supposed to propagate along the $x$-axis. The proper angular momentum $\lambda$ of each sphere (spin) is assumed to be in the plane $(y, z)$ perpendicular to the direction of propagation,

(H.2) In order to reproduce the probabilistic properties of the state $\begin{pmatrix} 1 \\ 0 \end{pmatrix}$ of quantum mechanics, we will assume that a statistical set of such spheres has a vector distribution $\lambda$ for which the density $\rho(\theta)$ of the angle $\theta$ that they form with the $z$ axis is given by:

$$\rho(\theta) = \begin{cases} \frac{1}{2}\cos\theta & \text{if } -\frac{\pi}{2} < \theta < \frac{\pi}{2} \\ 0 & otherwise \end{cases} \tag{1.20}$$

(H.3) An instrument designed to measure the quantum observable $R$ operates in the following way: it measures the sign of the projection of $\lambda$ on $\beta$, multiplies the result obtained by $\mid \beta \mid$ and adds $\alpha$ to the result.

This formulated model leads to many interesting consequences:

(i) The measurement method defined in (H.3) implies that the results obtained will not be different from $\alpha \pm \mid \beta \mid$, which guarantees that there is no disagreement with the results of quantum mechanics,

(ii) As a special case of the previous result and as a consequence of (1.20), if we measure $\sigma_3$ (we have $\alpha = 0, \beta = \vec{k}$ (unit vector of the $z$ axis)), the angle $\theta$ between $\lambda$ and $\beta$ is in all cases between $-\frac{\pi}{2} < \theta < \frac{\pi}{2}$ which implies that the projection of $\lambda$ on $\beta$ (that is to say $\mid \lambda \mid \cos\theta$) is never negative (see the hatched part of the Figure below). It follows that all the measurements will give $\sigma_3 = +1$, a result coherent with the fact that the state $\begin{pmatrix} 1 \\ 0 \end{pmatrix}$ is an eigenstate of $\sigma_3$ for the eigenvalue $r = +1$.

(iii) It is easy to verify that the probability density (1.20), which is never negative because $(\theta) =\mid \Psi(x) \mid^2$, is correctly normalized.

Finally, we can calculate the probabilities $p_1$ and $p_2$ to find the results $\alpha + \mid \beta \mid$ and $\alpha - \mid \beta \mid$ respectively when the general observable $R$ is measured. Let us note that (H.3) comprises two parts: a true measure when the sign of $\lambda\,\beta$ is defined and a quasi-automatic process which consists of multiplying this sign by $\mid \beta \mid$ and add $\alpha$ to the result. Thus $p_1$ and $p_2$ coincide respectively with the probabilities of finding $\lambda\,\beta = +1$ and $\lambda\,\beta = -1$.

To calculate $p_1$, it is enough to calculate the integral of $\rho(\theta)$ on the area $\sigma_0$ hatched of the Figure below, because according to the (H.2), $\lambda' s$ are only in the upper semi circle.

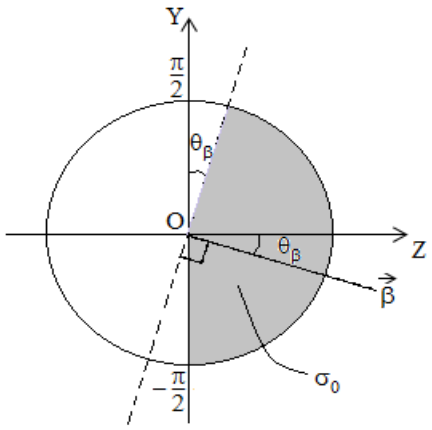


Figure 1.1: *Area $\sigma_0$ hatched*

Limits of integration are: $-\dfrac{\pi}{2} \leq \sigma_0 \leq \dfrac{\pi}{2}$

$$p_1 = \int_{\sigma_0} \frac{1}{2} \cos\theta \; d\theta = \frac{1}{2} \left[ \sin\left(\frac{\pi}{2} - \theta_\beta\right) - \sin\left(-\frac{\pi}{2}\right) \right] = \frac{1}{2}(1 + \cos\theta_\beta) \tag{1.21}$$

Since $p_1 + p_2 = 1$, then

$$p_2 = \frac{1}{2}(1 - \cos\theta_\beta) \tag{1.22}$$

In addition, according to the definition of the scalar product,

$$\vec{k} \cdot \vec{\beta} = \mid \vec{k} \mid \mid \vec{\beta} \mid \cos\theta_\beta \tag{1.23}$$

Equation (1.23) can also be written as:

$$\cos\theta_\beta = \frac{\beta_3}{\mid \vec{\beta} \mid} \tag{1.24}$$

(1.24) in (1.21):

$$p_1 = \frac{1}{2} \left( 1 + \frac{\beta_3}{\mid \vec{\beta} \mid} \right) \tag{1.25}$$

(1.24) in (1.22):

$$p_2 = \frac{1}{2} \left( 1 - \frac{\beta_3}{\mid \vec{\beta} \mid} \right) \tag{1.26}$$

This model thus produces measurements results and probabilities in perfect agreement with quantum mechanics. In addition, the result of an act of measurement of $\alpha I + \sigma \, \beta$ on a given sphere is completely fixed by the value of $\lambda$ for this sphere. Thus, in this model, the measurements are causal processes and we have obtained a causal generalization of the spin 1/2.

Thus, this model achieves exactly what the von Neumann theorem forbids. We must therefore discuss the validity of the axioms on which this theorem is based, in the light of this model. The hidden-variable is here the vector $\lambda$.

# Chapter 2

# Bohm's 1952 Causal Interpretation

This chapter presents the first comprehensive exposition of the interpretation of QM suggested by de Broglie in 1927 (pilot-wave theory) and independently reintroduced by Bohm in 1952, who also resolved the objection due to Fermi which caused de Broglie to initially abandon his pilot-wave theory. Actually, Bohm had independently rediscovered and made more coherent de Broglie's 1927 pilot-wave model; this interpretation has thus also been called the Bohm-de Broglie theory. Other names which denote different versions of the approach, include 'the CI', 'Bohmian mechanics' and 'the ontological interpretation' [21]. In this work we refer to this approach as 'the Bohm theory'.

The Copenhagen interpretation is self-consistent, but it involves an assumption that cannot be tested experimentally, viz., that the most complete possible specification of an individual system is in terms of a wave function that determines only probable results of actual measurement processes. The only way of investigating the truth of this assumption is by trying to find some other interpretation of the QM in terms of at present 'hidden' variables [22], which in principle determine the precise behavior of an individual system, but which are in practice averaged over in measurements of the types that can now be carried out. This suggested interpretation leads to precisely the same results for all physical processes as does the Copenhagen interpretation. Nevertheless, the suggested interpretation provides a broader conceptual framework than the Copenhagen interpretation, because it makes possible a precise and continuous description of all processes, even at the quantum level. This broader conceptual framework allows more general mathematical formulations of the theory than those allowed by the Copenhagen interpretation. Now, the usual mathematical formulation seems to lead to insoluble dif-

ficulties when it is extrapolated into the domain of distances of the order of $10^{-13}$cm or less [22]. It is therefore entirely possible that the interpretation suggested here may be needed for the resolution of these difficulties. Therefore, it is not necessary to give up a precise, rational, and objective description of individual systems at a quantum level of accuracy.

## 2.1 Introduction

The Copenhagen interpretation is based on an assumption having very far-reaching implications, viz., that the physical state of an individual system is completely specified by a wave function that determines only the probabilities of actual results that can be obtained in a statistical ensemble of similar experiments. This assumption has been the object of severe criticisms, notably on the part of Einstein, who had always believed that, even at the quantum level, there must exist precisely definable elements or dynamical variables determining (as in classical physics) the actual behavior of each individual system, and not merely its probable behavior. What bothered him most was the elimination of determinism from fundamental physics. Since these elements or variables are not now included in the QM and have not yet been detected experimentally, Einstein had always regarded the present form of the QM as incomplete, although he admitted its internal consistency [22]. The incompleteness is provided by the $\Psi$-function, and his advocacy of a definite counter-interpretation. To illustrate what he meant by 'incomplete', Einstein [23] considered the case of radioactive decay in which an $\alpha$-particle is emitted from an atom localized practically at a point. This system may be modelled by a closed potential barrier which at $t = 0$ encloses the $\alpha$-particle. As time passes, the wavefunction, initially finite only inside the barrier, leaks into the surrounding space. According to the Copenhagen interpretation this function yields the probability that at some instant the particle is found in a certain portion of the external space. Yet the wave may take many centuries to expand into the outer space whereas the particle may be found there after only a relatively short time. The wave function does not therefore imply any assertion concerning the time instant of the disintegration of the radioactive atom. That is, it does not describe the actual individual event revealed by the detector, including its cause. If it is reasonable to suppose that the individual atom really does have a definite moment of decay, one may conclude, according to Einstein, that the $\Psi$-function does not provide a complete description of the individual; it must be considered

incomplete. Einstein amplified his example of incompleteness to the macroscopic scale [24]).

Most physicists have felt that objections such as those raised by Einstein are not relevant, first, because the present form of the QM with its usual probability interpretation is in excellent agreement with an extremely wide range of experiments, at least in the domain of distances larger than $10^{-13}$cm, and, secondly, because it was the first time that the Bohm-de Broglie CI was suggested. The purpose of this chapter is to suggest that the Bohm-de Broglie CI that can permit us to conceive of each individual system as being in a precisely definable state, whose changes with time are determined by definite laws, analogous to the classical equations of motion. Quantum-mechanical probabilities are regarded (like their counterparts in classical statistical mechanics) as only a practical necessity and not as a manifestation of an inherent lack of complete determination in the properties of matter at the quantum level. As long as the present general form of Schrödinger's equation is retained, the physical results obtained with the suggested Bohm-de Broglie CI are precisely the same as those obtained with the Copenhagen interpretation. We shall see that the Bohm-de Broglie CI allows modifications of the mathematical formulation which could not even be described in terms of the Copenhagen interpretation. Moreover, the modifications can quite easily be formulated in such a way that their effects are insignificant in the atomic domain, where the present QM is in such good agreement with experiment, but of crucial importance in the domain of dimensions of the order of $10^{-13}$cm, where the present theory is totally inadequate.

## 2.2 Why a CI is Called for

The formalism of the QM leads to results that agree with experiment with great accuracy and covers an extremely wide range of phenomena. As yet, there are no experimental indications of any domain in which it might break down. Nevertheless, there still remain a number of basic questions concerning its fundamental significance which are obscure and confused. We can outline a few of them:

(i) Though the QM treats statistical ensembles in a satisfactory way, we are unable to describe individual quantum processes without bringing in unsatisfactory assumptions, such as the collapse of the wave function.

(ii) There is by now the well-known nonlocality that has been brought out by Bell [25] in connection with the EPR experiment.

(iii) There is the mysterious 'wave-particle duality' in the properties of matter that is demonstrated in a quantum interference experiment.

(iv) Above all, there is the inability to give a clear notion of what the reality of a quantum system could be.

All that is clear about the QM is that it contains an algorithm for computing the probabilities of experimental results. But it gives no physical account of individual quantum processes. Indeed, without the measuring instruments in which the predicted results appear, the equations of the QM would be just pure mathematics that would have no physical meaning at all. Thus QM merely gives us (generally statistical) knowledge of how our instruments will function. From this we can make inferences that contribute to our knowledge, for example, of how to carry out various technical processes.

It follows from this that QM can say little or nothing about reality itself. In philosophical terminology, it does not give what can be called an ontology for a quantum system.

## 2.3 The Copenhagen Interpretation

The two mutually consistent assumptions on which the Copenhagen interpretation is based are:

(i) The wave function with its probability interpretation determines the most complete possible specification of the state of an individual system.

(ii) The process of transfer of a single quantum from an observed system to a measuring apparatus is inherently unpredictable, uncontrollable, and unanalyzable.

and it centers around the uncertainty principle [22].

The problem which Heisenberg faced in 1927 was twofold:

1. Does the formalism allow for the fact that the position of a particle and its velocity are determinable at a given moment only with a limited degree of precision?

2. Would such imprecision, if admitted by the theory, be compatible with the optimum accuracy obtainable in experimental measurements?

For the first question, Heisenberg [13] resorted to the Dirac-Jordan transformation theory as follows. For a Gaussian distribution of the position coordinate $q$ the state function or 'probability amplitude', as Heisenberg called it, is given by the expression

$$\Psi(q) = const. \exp\left[-\frac{q^2}{2(\delta q)^2}\right], \tag{2.1}$$

where $\delta q$, the half-width of the Gaussian hump, denotes (according to Born's probabilistic interpretation) the distance in which the particle is situated and hence the indeterminacy in position ($\delta q = \sqrt{2}\Delta q$ where $\Delta q$ is the standard deviation). In accordance with the transformation theory the momentum distribution is $|\varphi(p)|^2$ where $\varphi(p)$ is obtained by the Fourier transformation:

$$\varphi(p) = \int_{-\infty}^{+\infty} \exp\left(-\frac{2\pi ipq}{h}\right) \Psi(q)\, dq \tag{2.2}$$

Substituting (2.1) in (2.2), we get:

$$\varphi(p) = \int_{-\infty}^{+\infty} \exp\left[-\frac{1}{2}\left(\frac{4\pi ipq}{h} + \frac{q^2}{(\delta q)^2}\right)\right]\, dq, \tag{2.3}$$

and knowing that:

$$-\frac{1}{2}\left(\frac{2\pi ip\delta q}{h} + \frac{q}{\delta q}\right)^2 - \frac{2\pi^2 p^2 (\delta q)^2}{h^2} = -\frac{1}{2}\left(\frac{4\pi ipq}{h} + \frac{q^2}{(\delta q)^2}\right), \tag{2.4}$$

we get

$$\varphi(p) = \exp\left[-\frac{2\pi^2 p^2 (\delta q)^2}{h^2}\right] \int_{-\infty}^{+\infty} \exp\left[-\frac{1}{2}\left(\frac{2\pi ip\delta q}{h} + \frac{q}{\delta q)}\right)^2\right]\, dq, \tag{2.5}$$

Substituting $2\pi ip\delta q/h + q/\delta q = y$ and integrating, we get

$$\varphi(p) = const. \exp\left[-\frac{2\pi^2 p^2 (\delta q)^2}{h^2}\right], \tag{2.6}$$

and in accordance with the equation (2.1), we may also write:

$$\Psi(p) = const. \exp\left[-\frac{p^2}{2(\delta p)^2}\right] \tag{2.7}$$

If we compare expressions (2.6) and (2.7), we get:

$$\delta p \delta q = \frac{h}{2\pi} \tag{2.8}$$

For the second question, Heisenberg asked whether a close examination of measuring processes themselves does not lead to a result which violates the restriction imposed by the relation (2.8); Heisenberg analyzed what has since become known as the 'gamma-ray microscope experiment'. His point of departure here was the operational view that a scientific concept is a condensed code of operations and its meaning, in the last analysis, a definite relation between sense impressions of the observer. To understand the meaning of the concept 'place' or 'position' of a particle, such as an electron, one has to refer to a definite experiment by which 'the position' is to be determined; otherwise the concept has no meaning. One may, for example, illuminate the electron and observe it under the microscope. Since in accordance with the optical laws of resolution the precision increases the smaller the wave length of the radiation (illumination), a gamma-ray microscope promises maximum accuracy in position determination. Such a procedure, however, involves the Compton effect. At the moment of the position determination, that is, when the quantum of light is being diffracted by the electron, the latter changes its momentum discontinuously. This change is greater the smaller the wave length of light, that is, the more precise the position determination. Hence, at the moment when the position of the electron is being ascertained its momentum can be known only up to a magnitude that corresponds to the discontinuous change; thus, the more accurate the position determination, the less accurate the momentum determination and vice versa. Heisenberg also showed by an analysis of a Stern-Gerlach experiment for the determination of the magnetic moment of an atom that the uncertainty in measuring the energy $\Delta E$ is smaller the longer the time $\Delta t$ spent by the atom in crossing the deviating field. Since the potential energy $E$ of the deviating force cannot be allowed to change within the width $d$ of the atomic beam by more than the energy difference $\Delta E$ of the stationary states, if the energy of these states is to be measured $\Delta E/d$ is the maximum value of the deviating force; the angular deviation $\varphi$ of the beam of atoms with momentum $p$ is then given by $\Delta E \Delta t/dp$; since, however, $\varphi$ must be at least as large as the natural diffraction at the slit defining the width $d$ of the beam, that is, $\lambda/d$

, where according to the de Broglie relation $\lambda = h/p$, Heisenberg concluded that:

$$\frac{\lambda}{d} = \frac{h}{pd} \lesssim \frac{\Delta E \Delta t}{dp}, \tag{2.9}$$

or

$$\Delta E \Delta t \gtrsim h \tag{2.10}$$

This equation (2.10), Heisenberg concluded, "shows how an accurate determination of energy can be obtained only by a corresponding indeterminacy in time."

In formulating the BPC, Bohr suggests that at the atomic level we must renounce our hitherto successful practice of conceiving of an individual system as a unified and precisely definable whole, all of whose aspects are simultaneously and unambiguously accessible to our conceptual gaze. Such a system of concepts which is sometimes called a 'model', need not be restricted to pictures, but may also include, for example, mathematical concepts, as long as these are supposed to be in a precise (i.e., one-to-one) correspondence with the objects that are being described. The principle of complementarity requires us, however, to renounce even mathematical models. Thus, in Bohr's point of view, the wave function is in no sense a conceptual model of an individual system, since it is not in a precise (one-to-one) correspondence with the behavior of this system, but only in a statistical correspondence.

In place of a precisely defined conceptual model, the BPC states that we are restricted to complementarity pairs of inherently imprecisely defined concepts, such as position and momentum, particle and wave, etc. The maximum degree of precision of definition of either member of such a pair is reciprocally related to that of the opposite member. This need for an inherent lack of complete precision can be understood in two ways. First, it can be regarded as a consequence of the fact that the experimental apparatus needed for a precise measurement of one member of a complementary pair of variables must always be such as to preclude the possibility of a simultaneous and precise measurement of the other member. Secondly, the assumption that an individual system is completely specified by the wave function and its probability interpretation implies a corresponding unavoidable lack of precision in the very conceptual structure, with the aid of which we can think about and describe the behavior of the system.

It is only at the classical level that we can correctly neglect the inherent lack of precision in all of these conceptual models; for here, the incomplete determination of physical properties implied by the uncertainty principle produces effects that are too small to be of practical significance. Our ability to describe classical systems in terms of precisely definable models is, however, an integral part of the theory. For without such models, we would have no way to describe, or even to think of, the result of an observation, which is of course always finally carried out at a classical level of accuracy. If the relationships of a given set of classically describable phenomena depend significantly on the essentially quantum-mechanical properties of matter however, then BPC states that no single model is possible which could provide a precise and rational analysis of the connections between these phenomena. In such a case, there is no way to attempt to describe in detail how future phenomena arise out of past phenomena. Instead, we should simply accept without further analysis the fact that future phenomena do in fact somehow manage to be produced in a way that is however necessarily beyond the possibility of a detailed description. The only aim of a mathematical theory is then to predict the statistical relations, if any, connecting these phenomena.

## 2.4 Criticism of the Copenhagen Interpretation

The Copenhagen interpretation gives up the possibility of conceiving precisely what might determine the behavior of an individual system at the quantum level, without providing adequate proof that such a renunciation is necessary. The Copenhagen interpretation is admittedly consistent; but the mere demonstration of such consistency does not exclude the possibility of other equally consistent interpretations, which would involve additional elements or parameters permitting a detailed causal and continuous description of all processes, and not requiring us to forego the possibility of conceiving the quantum level in precise terms. As a matter of fact, whenever we have previously had recourse to statistical theories, we have always ultimately found that the laws governing the individual members of a statistical ensemble could be expressed in terms of just such hidden variables. For example, from the point of view of macroscopic physics, the coordinates and momenta of individual atoms are hidden variables, which in a large scale system manifest themselves only as statistical averages.

## 2.5 New Physical Interpretation of Schrödinger's Equation

For simplicity, we will only develop the basic principles of the CI in the context of a one-body system.

Let us begin by considering the standard Wentzel-Kramers-Brillouin approximation (WKB) for the classical limit in QM.

As a reminder, the WKB approximation, taking its name from its inventors Wentzel, Kramers and Brillouin, is a method developed in 1926 that allows an approximate solution of the Schrödinger equation. The aim of this approximation is to regain the classical regime when $\hbar$ is set to 0, since the wave function oscillates very rapidly. For this, we consider a solution of the Schrödinger equation of the form:

$$\Psi(x) = \exp\left[\frac{i}{\hbar}\sigma(x)\right], \tag{2.11}$$

where $\sigma(x)$ is a function of the position variable. By introducing it into the Schrödinger equation we obtain

$$\frac{i\hbar}{2m}\sigma'' - \frac{1}{2m}\sigma'^2 + E - V = 0 \tag{2.12}$$

We are therefore faced with a second-order differential equation for $\sigma$. As a reminder, at the classical limit, $\hbar$ towards 0. Thus, $\sigma$ can be rewritten as a power series of $\hbar$. We then have:

$$\sigma = \sigma_0 + \frac{\hbar}{i}\sigma_1 + \left(\frac{\hbar}{i}\right)^2\sigma_2 + ... + \left(\frac{\hbar}{i}\right)^n\sigma_n \tag{2.13}$$

It is at this precise moment that the WKB approximation comes into play. Indeed, the precision of this will depend on the number of terms that are taken into account in the previous development. Thus, for example, if the order is 0, one takes only $\sigma = \sigma_0$. This order, called the 'classical approximation', consists of keeping no term in $\hbar$.

By introducing (2.13) into (2.12) we obtain

$$\frac{-1}{2m}\sigma_0'^2 + E - V = 0 \Longrightarrow \sigma_0' = \pm\sqrt{2m(E-V)} \Longrightarrow \sigma_0 = \pm\int \sqrt{2m(E-V)}\, dx$$

Thus, we identify: $\sqrt{2m(E-V)}$ as the classical phase of the particle.

In order to motivate the introduction of the particle concept into QM we shall decompose the Schrödinger equation into two real equations in a particular way by applying the standard WKB approximation and writing the wave function in polar form:

$$\Psi = R\cos\left(\frac{S}{h}\right) + iR\sin\left(\frac{S}{h}\right) = R\exp\left(i\frac{S}{h}\right), \tag{2.14}$$

Here $R = R(x,t)$ is a real amplitude function (amplitude function is by definition nonnegative $R \geq 0), (\forall\ x,t)$ and $S = S(x,t)$ is a real phase function of space and time, and $\hbar = \frac{h}{2\pi}$ where $h$ is Planck's constant. $S$ thus has the dimension of action and is measured in units of $\hbar$ and $R$ is the square root of a density function. Writing $\Psi$ in terms of its real and imaginary parts

$$\Psi = \Psi_1 + i\Psi_2 \tag{2.15}$$

we have

$$R = (\Psi_1^2 + \Psi_2^2)^{\frac{1}{2}} = (\Psi^*\Psi)^{\frac{1}{2}} \tag{2.16}$$

$$\frac{S}{\hbar} = \arctan(\frac{\Psi_2}{\Psi_1}) = \frac{1}{2i}\ln(\frac{\Psi}{\Psi^*}) \tag{2.17}$$

We insert (2.14) into Schrödinger's equation

$$i\hbar\frac{\partial\Psi}{\partial t} = -(\frac{\hbar^2}{2m})\nabla^2\Psi + V(x)\Psi, \tag{2.18}$$

where $V(x)$ is the classical potential. Multiplying through by $\exp(iS/h)$, we obtain respectively by separating into real and imaginary parts

$$\frac{\partial S}{\partial t} = -\left[\frac{(\nabla S)^2}{2m} + V(x) - \frac{\hbar^2}{2m}\frac{\nabla^2 R}{R}\right] \tag{2.19}$$

and

$$\frac{\partial R}{\partial t} = -\frac{1}{2m}[R\nabla^2 S + 2\nabla R.\nabla S] \tag{2.20}$$

In order to obtain the WKB approximation, we note that in the classical limit in which there is a wave packet of width much greater than the wavelength $\lambda$, the term $-\hbar^2/2m.\nabla^2 R/R$ will be very small compared with the term $(\nabla S)^2/2m$. We therefore neglect it and obtain:

$$\frac{\partial S_c}{\partial t} = -\left[\frac{(\nabla S_c)^2}{2m} + V(x)\right] \tag{2.21}$$

In the above we have written $S = S_c$ to indicate that we are dealing with the classical Hamilton-Jacobi equation representing a particle with a vector field momentum:

$$\mathbf{p} = m\mathbf{v} = \nabla S_c, \tag{2.22}$$

which moves normal to the wave front $S_c = const.$ $\mathbf{v}$ is a vector field velocity which defines at each point of space and at each instant the tangent to a possible particle trajectory passing through that point. The trajectories are orthogonal to the surfaces $S = constant$ and may be found by integrating the differential equation:

$$m\dot{\mathbf{x}} = \mathbf{p}(x,t)|_{x=x(t)} \tag{2.23}$$

$$\dot{\mathbf{x}} = \frac{1}{m}\nabla S(x,t)\ |_{x=x(t)} \tag{2.24}$$

It follows then that equation (2.19) can be regarded as a conservation equation for the probability in an ensemble of such particles, all moving normal to the same wave front with a probability density

$$P = R^2 \tag{2.25}$$

We then obtain by replacing (2.25) in (2.19) and (2.20)

$$\frac{\partial S}{\partial t} + \frac{(\nabla S)^2}{2m} + V(x) - \frac{\hbar^2}{4m}\left[\frac{\nabla^2 P}{P} - \frac{1}{2}\frac{(\nabla P)^2}{P^2}\right] = 0. \tag{2.26}$$

$$\frac{\partial P}{\partial t} + \nabla.\left(P\frac{\nabla S}{m}\right) = 0, \tag{2.27}$$

In the classical limit ($\hbar \to 0$), (2.26) and (2.27) are subject to a very simple interpretation. The function $S(x)$ is a solution of the Hamilton-Jacobi equation. If we consider an ensemble of particle trajectories which are solutions of the equations of motion, then it is a well-known theorem of mechanics that if all of these trajectories are normal to any given surface of constant $S$, then they are normal to all surfaces of constant $S$ and $\nabla S(x)/m$ will be equal to the velocity vector $\mathbf{v}(x)$ for any particle passing the point $x$. Equation (2.27) can therefore be re-expressed as

$$\frac{\partial P}{\partial t} + \nabla.(P\mathbf{v}) = 0 \tag{2.28}$$

This equation indicates that it is consistent to regard $P(x)$ as the probability density for particles in our ensemble. For in that case, we can regard $P\mathbf{v}$ as the mean current of particles in this ensemble, and Eq. (2.28) then simply expresses the conservation of probability.

It seems natural at this point to ask whether this kind of ontology could not be extended to the quantum domain. Thus we note the quantum equation (2.19) differs from the classical equation (2.21) only by the term $-\hbar^2/2m.\nabla^2 R/R$ which evidently can be regarded as playing the role of an additional potential in what we may call the quantum Hamilton-Jacobi equation . To bring this out we shall define what we call the function $Q$ that we will call the 'quantum potential energy' or simply the 'quantum potential'.

$$Q = -\frac{\hbar^2}{2m}\frac{\nabla^2 R}{R} \tag{2.29}$$

However, it is important to realize that the notion of an individual particle in the Bohm theory is very different from what we would expect from the classical perspective. For although the Bohmian quantum individual particle has a well defined energy, that energy is not a local energy. This is consistent with Niels Bohr's views in two ways:

- The particle is never separated from the quantum field. It is an invariant feature of the total underlying process. This is consistent with Bohr's notion of the 'impossibility of subdividing quantum phenomena' in the sense that the whole experimental arrangement must be taken into account [26].

- The individual particle is not a localised point-like object. As Bohr remarks [26] the

quantum process is a 'closed indivisible phenomenon'. The energy is not localised at a point. In fact complementarity can be taken to imply that energy transcends space-time. Nevertheless there is a centre of energy, a generalisation of the centre of mass which can be given a position in space-time. It is this centre that moves with the Bohm momentum.

These ideas are not consistent with a classical physics of a particle. Further explanations about differences individual particles in the Bohm theory and classical theory are given in [27].

Substituting (2.29) in (2.19), the quantum Hamilton-Jacobi equation becomes:

$$\frac{\partial S}{\partial t} + \frac{(\nabla S)^2}{2m} + V + Q = 0 \tag{2.30}$$

The equation (2.20) still expresses the conservation of probability, but for an ensemble of particles which satisfies (2.30) rather than (2.21).

Let us now discuss this ontology in a more systematic way. Its key points are:

1. The electron actually is a particle with a well-defined position $\mathbf{x}(t)$ which varies continuously and is causally determined.

2. This particle is never separated from a new type of quantum field that fundamentally affects it. This field is given by $R$ and $S$ or alternatively by $\Psi = R\exp\left(i\frac{S}{h}\right)$, where $\Psi$ satisfies Schrödinger's equation (rather than for example Maxwell's equation), so that it too changes continuously and is causally determined.

3. The particle has an equation of motion

$$m\frac{d\mathbf{v}}{dt} = -\nabla V(\mathbf{x}) - \nabla Q \tag{2.31}$$

   This means that the forces acting on it are not only the classical force $-\nabla V$, but also the quantum force $-\nabla Q$.

4. The particle momentum is restricted to $\mathbf{p} = \nabla S$. Since the quantum field $\Psi$ is single valued it follows that:

$$\oint_{(c)} \mathbf{p} \cdot \, d\mathbf{x} = \oint_{(c)} \nabla S \cdot \, d\mathbf{x} = \oint_{(c)} dS = nh \tag{2.32}$$

5. In a statistical ensemble of particles selected so that all have the same quantum field $\Psi$, the probability density is $P = R^2$.

   Given that the particle is always accompanied by its quantum field $\Psi$, we may say that the combined system of particle plus field is causally determined.

## 2.6 Introduction of the Particle

We have rewritten the field equation (2.18) for the complex amplitude $\Psi$ as a pair of real equations (2.19) and (2.27). The latter are mathematically equivalent to the former if we impose conditions such as (2.32) on the new variables. The purpose of this exercise is to facilitate the physical interpretation of the Schrödinger equation.

We propose to associate with the physical wave $\Psi$ propagating in space a point particle of mass $m$ which pursues a trajectory $\mathbf{x} = \mathbf{x}(t)$. Since wave and particle depend on the same parameter $m$ (and more generally on the charge $e$, magnetic moment $\mu$, etc.) and, as we shall see, the former exerts a force on the latter, it is appropriate to treat the wave and particle as aspects of a single physical system. To see the connection between the wave and particle we treat (2.19) as a particular instance of the generalized Hamilton-Jacobi theory:

$$\frac{\partial S}{\partial t} = -\left[\frac{(\nabla S)^2}{2m} + V + V'(S, \partial_i S, \partial_{ij} S, \partial_{ijk} S, ...)\right], \tag{2.33}$$

where $\partial_{ij} S = \partial^2 S / \partial x_i \partial x_j \;\; \forall \, i, j = 1, 2, 3, ....$ In addition to the usual external potential $V(x, t)$, a new type of energy $V'(x, t)$ is introduced into the Hamilton-Jacobi equation which depends explicitly on $S$ and on various orders of the derivatives of $S$.

Eq. (2.19) has the form of the classical Hamilton-Jacobi equation apart from the extra term (2.29)

From the point of view of the particle we may then interpret (2.30) as an equation for its total energy. The latter is defined by:

$$E(x(t),t) = -\frac{\partial S(\mathbf{x},t)}{\partial t} \mid_{\mathbf{x}=\mathbf{x}(t)} \tag{2.34}$$

and is given by the sum of the kinetic energy

$$\frac{(\nabla S)^2}{2m}|_{\mathbf{x}=\mathbf{x}(t)} = \frac{1}{2}m\dot{x}^2 \tag{2.35}$$

and the total (quantum plus classical) potential energy is

$$[V(\mathbf{x},t) + Q(x,t)]|_{\mathbf{x}=\mathbf{x}(t)} = V(\mathbf{x}(t),t) + Q(\mathbf{x}(t),t) \tag{2.36}$$

In this way we introduce a phase space with coordinates $(\mathbf{x}, \mathbf{p})$ into QM. The system trajectory is defined by the equation $\mathbf{p} = \nabla S(\mathbf{x}, t)$.

Now clearly $Q$ is not a pre-assigned function of the coordinates in the way that $V$ is. It depends on the total quantum state and although it is expressed in terms of just $R$, $Q$ is inextricably coupled to $S(x,t)$. Indeed if we specify $R_0(\mathbf{x})$ and treat $\nabla S$ as a given function of $x$ and $t$, we can in principle solve (2.27) for $R(x,t)$ in terms of $\nabla S$.

Substituting the result into (2.29) yields $Q$ in terms of $R_0$ and the derivatives of $S$. We obtain then for (2.30) an equation of the type (2.33).

To show that it is nevertheless consistent to regard $Q$ as a potential on the same footing as $V$ in respect of the particle motion, we apply the operator $V$ to (2.30) and find, after some rearrangement, the field equation

$$\left[\frac{\partial}{\partial t} + \left(\frac{1}{m}\right)\nabla S.\nabla\right]\nabla S = -\nabla(V+Q) \tag{2.37}$$

Making the identification of $\nabla S/m$ with particle velocity as in (2.24) we find by evaluating (2.37) along the trajectory

$$\frac{d}{dt}(m\dot{\mathbf{x}}) = -\nabla(V+Q)|_{\mathbf{x}=\mathbf{x}(t)} \tag{2.38}$$

where

$$\frac{d}{dt} = \frac{\partial}{\partial t} + \dot{\mathbf{x}}\cdot\nabla \tag{2.39}$$

represents the time rate of change with respect to a point moving with the particle.

Eq.(2.38) has the form of Newton's second law, in which the particle is subject to a quantum force $-\nabla Q$ in addition to the classical force $-\nabla V$. The effective potential acting on the particle is $(Q+V)$ not $V$. Newton's first law, that a body persists in a state of uniform motion unless acted on by a resultant force, follows as a special case of (2.38).

Either (2.24) or (2.38) may be considered as the particle 'law of motion'. In practice, it is easier to solve the former.

In this theory of motion the initial velocity of the particle is determined by the initial field $\Psi_0(\mathbf{x})$. The latter implies an initial single-valued momentum field

$$\mathbf{p}_0(x) = \nabla S_0(\mathbf{x}) \tag{2.40}$$

so that, if the initial position is specified, the initial velocity is uniquely given by

$$\dot{\mathbf{x}}(0) = \frac{1}{m}\nabla S_0(\mathbf{x})|_{\mathbf{x}=\mathbf{x}(t)} \tag{2.41}$$

It follows that the only information that must be added to that contained in the fields in order to obtain a unique orbit for all time is $\mathbf{x}_0$. Specification of $\mathbf{x}$ and $\Psi$ at a certain time then defines the 'state' of an individual system (although we shall occasionally use the expression 'quantum state' to denote just the wave). Given $\mathbf{p}_0$, we may, in principle, invert (2.40) to find the corresponding $\mathbf{x}_0 s$. Note that the choice of $\mathbf{x}_0$ is arbitrary except that it cannot lie in a nodal region, for at these points $\nabla S_0$ is undefined.

The initial phase function thus has through its gradient a meaning for the particle. At this stage the initial field $R_0(\mathbf{x})$ has no significance for the particle; as a special case of the general theory it may be ascribed the meaning of a density of particles in the ensemble (in the case that $R(\mathbf{x},t) = R_0(\mathbf{x})$ for all t, this field defines the quantum potential).

It is emphasized that the law of motion (2.24) is postulated and then shown to be consistent. Why then should it be relevant to QM? The reason is simple: the velocity field $\mathbf{v}(\mathbf{x},t)$ is proportional to what is termed in QM the 'probability density current', defined by

$$\mathbf{j} = \frac{\hbar}{2mi}\Psi^*\nabla\Psi \tag{2.42}$$

We have

$$\mathbf{j}(\mathbf{x}, t) = R^2\mathbf{v} \tag{2.43}$$

so that the current lies along the tangent to each point of a trajectory. Hence the trajectories $\mathbf{x}(t)$ are the lines along which probability conventionally 'flows'.

Having defined the momentum and total energy of the particle, it is natural to define its angular momentum about a point at the origin of coordinates as the value of the field quantity

$$L(\mathbf{x}, t) = \mathbf{x}.\nabla S(\mathbf{x}, t) \tag{2.44}$$

evaluated along the trajectory:

$$L(\mathbf{x}(t), t) = \mathbf{x}(t) \cdot m\dot{\mathbf{x}}(t) \tag{2.45}$$

To summarize, an individual material system comprises the following two components:

(a) A wave having an amplitude and phase at each spacetime point. Its law of motion is (2.18),

(b) A mass point pursuing a spacetime trajectory. Its law of motion is (2.24) or (2.38).

An ensemble of mass points is associated with each wave. In the Copenhagen interpretation each system in the ensemble described by $\Psi$ is considered to be in the same state. Here they are distinguished by their initial locations.

From this definition we may associate various properties with the respective system components (e.g., field energy and particle momentum). To establish the connection between the two aspects of matter we have rewritten the complex Schrödinger equation in a manner that is suggestive of a physical interpretation, as a coupled system of equations for the real fields $R$ and $S$. These fields play several roles simultaneously:

1. They are associated with two physical fields propagating in spacetime and define, along with the particle, an 'individual physical system'.

2. They enter into the definition of properties associated with a particle (momentum, energy and angular momentum). These are not arbitrarily specified but are a specific combination of field variables and are closely related to the associated quantum mechanical operators. To obtain a particle property one evaluates the relevant function along a trajectory.

3. They enter as causal agents in the particle equation of motion, via the quantum potential.

4. They have other meanings which ensure the consistency of the theory with its Copenhagen interpretation and its connection with classical mechanics. $S$ is a generalized Hamilton-Jacobi function.

The wave equation does two things: it determines the spacetime dependence of the $\Psi$-field, and it tells us how the physical properties of a particle embedded in that field evolve (by Eqs. (2.34) and (2.35) for example). In practice, it is easier to solve the wave equation in its linear form (2.18) and treat the variables $R$ and $S$ as derived quantities.

Since the set of equations (2.18) and (2.24) uniquely specifies the future (and past) continuous evolution of the field and particle system, the theory forms the basis of a 'CI' of QM.

## 2.7 Applications of the Quantum Potential Approach

The quantum potential approach can be used to model quantum effects without requiring the Schrödinger equation to be explicitly solved, and it can be integrated in simulations, such as Monte Carlo simulations using the hydrodynamic and drift diffusion equations [28]. This is done in the form of a 'hydrodynamic' calculation of trajectories: starting from the density at each 'fluid element', the acceleration of each 'fluid element' is computed from the gradient of $V$ and $Q$, and the resulting divergence of the velocity field determines the change to the density.[29]

The approach using Bohmian trajectories and the quantum potential is used for calculating properties of quantum system which cannot be solved exactly, which are often approximated using semi-classical approaches. Whereas in mean-field approaches the potential for the classical motion results from an average over wave functions, this approach does not require the computation of an integral over wave functions.[30]

The expression for the quantum force has been used, together with Bayesian statistical analysis and expectation-maximisation methods, for computing ensembles of trajectories that arise under the influence of classical and quantum forces.[31]

# Chapter 3

# Mathematics of the Two-slit Experiment

## 3.1 Introduction

In spite of the undoubted success of the quantum formalism, its interpretation continues to present difficulties for it does not provide a description of underlying physical reality.

However, Bohm in 1952 introduced an alternative interpretation of QM called the C.I. which does provide a description of underlying physical reality and therefore allows computer modelling of quantum systems. We would like firstly to determine the expression of the Gaussian wave packet as given in [32]. Then, using $1-D$ Gaussian wave packet we want to calculate the formula for the intensity, the quantum potential and trajectories for the two-slit experiment and thereby reproduce the computer model of this experiment first produced by Philippidis, Dewdney and Hiley in 1979 [2]. Finally, it might be interesting to attempt an extension by modelling each pinhole by a $2-D$ Gaussian wave packet.

## 3.2 Derivation of the Gaussian Wave Packet

### 3.2.1 Motion of Pulses of Light

Before we develop the de Broglie theory of matter waves, we shall find it helpful to discuss the motion of light rays and to show in some detail the connection between the path

of the ray and the underlying waves which make up the ray. This is of interest, not only for its own sake, but also because it provides a picture of the processes involved on the basis of the relatively familiar light waves and also because it illustrates the necessary mathematical methods.

Let us begin with a pulse of light that might be defined for example by a shutter opened for a limited time $\tau$. In general, such a pulse is $2-D$, having a length $c\tau$ in the direction of motion of the pulse, and a diameter that depends on the narrowest aperture through which the light has gone and also on the divergence of the beam of rays as it passes through this aperture. If the dimensions of the pulse are large compared with a wavelength, but small compared with the dimensions of the apparatus, then the light beam acts like a particle (or a group of particles) localized in the pulse and moving with the speed of light.

We shall first consider a case in which a parallel beam of light strikes with normal incidence a shutter that remains open for a time so short that $c\tau$ is much less than the diameter of the pulse. This is essentially a $1-D$ case, since no important effects occur that involve the directions normal to the motion of the pulse. The pulse then simply travels with velocity $c$ in its original direction of motion, which we take to be the $x$-direction.

Now, an ordinary plane wave of definite wavelength $\lambda$ is spread over all space and therefore cannot be used to describe the motion of a pulse, which is localized in a comparatively narrow region. To obtain a wave that is restricted to a definite region of space, we must construct what is known as a wave packet. A wave packet comprises a group of waves of slightly different wavelengths, with phases and amplitudes so chosen that they interfere constructively over only a small region of space, outside of which they produce amplitude that reduces to zero rapidly as a result of destructive interference. The amplitude $\varepsilon$ of a $1-D$ wave packet (representing, for example, the $z$-component of the electric field) will in general resemble the curve shown in (Fig 3.1).

We can construct a wave packet by taking a plane wave and integrating it over a small range of wavelengths. Let us take, for example,

$$E_z(x) = \int_{k_0-\Delta k}^{k_0+\Delta k} e^{ik(x-x_0)}\, dk = \frac{2\sin[\Delta k(x-x_0)]}{(x-x_0)} e^{ik_0(x-x_0)} \tag{3.1}$$

Figure 3.1: *A wave packet*

When plotted as a function of $(x - x_0)$, the real part of $E_z(x)$ looks like the curve shown in (Fig 3.2) ($\Delta k << k_0$).

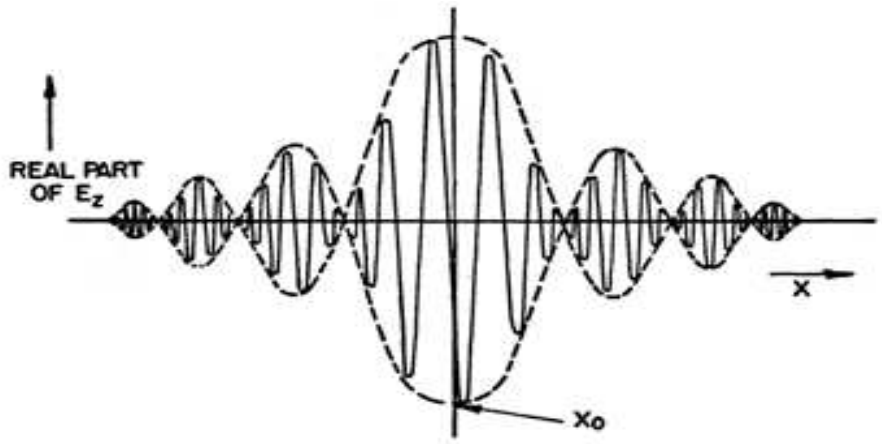


Figure 3.2: *The real part of* $E_z(x)$

We see that the amplitude of oscillation reaches a maximum at $x = x_0$, and goes down to zero when $x - x_0 = \dfrac{\pi}{\Delta k}$, after which it is a rapidly decreasing oscillatory function. We have thus obtained a wave packet that is concentrated in a packet. In a function like the preceding one, the real and the imaginary parts each oscillate rapidly as a function of $(x - x_0)$. The intensity of the wave is proportional to the square of the maximum amplitude of oscillation. If, as is usually the case, the wavelength ($\lambda = \dfrac{\pi}{\Delta k}$) is much

less than the width of the packet $\Delta k$, this maximum is approximated very closely by the square of the absolute value of the complex function $E_z(x)$. Thus, we get:

$$I = E_z(x)^* E_z(x) = \frac{4\sin^2[\Delta k(x - x_0)]}{(x - x_0)^2} \tag{3.2}$$

To obtain a more general type of packet, we multiply $e^{ik(x-x_0)}$ by a weighting function, $f(k-k_0)$, which is large near $k-k_0 = 0$ and dies out rapidly beyond some short distance $\Delta k$. For the present, we consider only functions which do not oscillate rapidly inside the region $\Delta k$, so that a graph of $f(k - k_0)$ resembles the curve shown in (Fig 3.3).

Figure 3.3: *Graph of* $f(k - k_0)$

Note that the use of a weighting function is, in a qualitative way, equivalent to integrating over a small range of wavelengths. We now assert that the following wave packet is concentrated in a packet:

$$\Psi = \int_{-\infty}^{+\infty} f(k - k_0) e^{ik(x-x_0)}\, dk \tag{3.3}$$

To prove this, we note that at $x = x_0$, the argument of the exponential is zero for all $k$, hence all contributions to the integral coming from different values of $k$ add up in phase, and the result is large. As $(x - x_0)$ becomes large, $e^{ik(x-x_0)}$ becomes a rapidly oscillating function of $k$, and its integral tends to cancel out. Thus, $\Psi$ is a function that is large only near $x = x_0$. At places far from $x = x_0$, the contributions of different $k$ values interfere destructively. Hence, any function defined in this way has the form of a wave packet.

As an example, let us choose

$$f(k-k_0) = \exp\left[-\frac{(k-k_0)^2}{2(\Delta k)^2}\right] \tag{3.4}$$

This is chosen because it leads to simple mathematical results. We then get

$$\Psi = \int_{-\infty}^{+\infty} f(k-k_0)e^{ik(x-x_0)}\, dk = \sqrt{2\pi}\Delta k \exp\left[ik_0(x-x_0) - \frac{(x-x_0)^2}{2}(\Delta k)^2\right] \tag{3.5}$$

The intensity becomes:

$$I = \Psi^*\Psi = 2\pi(\Delta k)^2 \exp\left[-(x-x_0)^2(\Delta k)^2\right] \tag{3.6}$$

We note that a Gaussian function in $k$-space leads to a Gaussian function in $x$-space. The Gaussian function is the only one having this peculiar symmetry in $x$ and $k$-space. We note also that the resulting packet has a maximum at $x = x_0$ and clearly becomes negligible for large values of $(x - x_0)$.

### 3.2.2 The Width of a Wave Packet

At this point, we are ready to calculate what determines the width of a given wave packet. This problem is of special interest because the results are applied later in connection with the derivation of the uncertainty principle.

Let us begin with our two examples given above. In the first of these, the intensity is

$$I \sim \frac{\sin^2[\Delta k(x-x_0)]}{(x-x_0)^2} \tag{3.7}$$

This quantity becomes fairly small when $(x - x_0)$ takes on values appreciably larger than $\frac{1}{\Delta k}$ or when

$$x - x_0 > \frac{1}{\Delta k} \tag{3.8}$$

In a similar way, the intensity in the second example

$$I \sim 2\pi(\Delta k)^2 \exp\left[-(x-x_0)^2(\Delta k)^2\right] \tag{3.9}$$

becomes small when

$$(x - x_0)^2 > \frac{1}{(\Delta k)^2} \tag{3.10}$$

Since, in both cases, $\Delta k$ is a measure of the range of wave numbers $k$ present in the packet, we obtain the result that the product of the width of the packet in $k$-space, and its width in $x$-space is of the order of unity, or, mathematically speaking

$$\Delta x.\Delta k \cong 1 \tag{3.11}$$

This means that a packet with a narrow range in $k$-space must be very broad in $x$-space and vice versa.

It is easy to show that this result holds for any packet of the form (3.3), where $f(k - k_0)$ is a smooth function that does not oscillate too rapidly. To do this, consider the function given in eq.(3.3). We see that contributions of difference $k$ tend to interfere constructively as long as $k(x - x_0) < 1$,but that for larger values of $k$ they tend to oscillate and get out of phase. Since $f$ is large in only a limited region $\Delta k$ we conclude that destructive interference becomes important when $|x - x_0| > \frac{1}{\Delta k}$. Thus, we obtain once again the result that $\Delta x.\Delta k \cong 1$.

We can summarize the preceding results in simpler terms by noting that in order to make up a packet that is small beyond a region $\Delta x$, it is necessary to add up a range of waves involving functions such as $\cos[k(x - x_0)]$ and $\cos[(k - \Delta k)(x - x_0)]$, which can be in phase at $x = x_0$, but are out of phase at $x = x_0 + \Delta x$, so that we must have $(x - x_0)\Delta k > 1$. Note however that this result required that we add up waves of the same sign. If $f(k - k_0)$ is a rapidly oscillating function, the result does not necessarily follow.

Similar results can be obtained relating the time $\Delta t$ that is required for a pulse to pass a given point, to the range of angular frequencies $\Delta\omega$ needed to form such a pulse. Thus, the electric field at a given point can be expressed as

$$E = \int f(\omega - \omega_0)e^{-i\omega(t-t_0)}\ d\omega \tag{3.12}$$

Such a function will be a pulse that is large only near $t = t_0$ and which has a width $\Delta t$ obeying the relation

$$\Delta\omega.\Delta t \cong 1 \tag{3.13}$$

The fact that a pulse requires a range of frequencies is responsible, for example, for the 'band width' of a radio transmitter. To carry audio-frequency pulses on a radio wave, it is necessary to allow the frequency of the radio wave to shift by an amount of the order of magnitude of the audio frequencies that we wish to carry. If the receiver is tuned to accept a band width $\Delta\omega$, the shortest pulse that can be received has a duration $\Delta t \cong \dfrac{1}{\Delta\omega}$.

### 3.2.3 Group Velocity

We now treat the problem of how a wave packet moves through space. To do this, we make use of the fact that for light in free space, a wave of propagation vector $k$ oscillates with frequency $\omega = ck$. Thus, we write

$$E(x,t) = \int_{-\infty}^{+\infty} f(k-k_0)e^{ik(x-x_0-ct)}\ dk \tag{3.14}$$

Note that $E$ is a function only of $(x - x_0 - ct)$; this means that the pulse travels at the velocity $c$ without changing its shape. This is of course a well-known result.

The motion of the wave packet is caused by the change of phase of all of the different wavelengths, resulting from the multiplication by the term $\exp(-ickt)$. Thus, when $t \neq 0$, the waves cease to add up in phase at $x = x_0$ but instead they are all in phase at the point $x = x_0 + ct$. The change of position of the wave packet is therefore caused by the change of conditions for constructive and destructive interference

.

Suppose now that the packet enters a dispersive medium which has an index of refraction $n(\lambda)$. The angular frequency

$$\omega = \frac{2\pi c}{\lambda n(\lambda)} \tag{3.15}$$

is in general a fairly complicated function of $\lambda$ and therefore of $k$. To denote this we

write $\omega = \omega(k)$. The electric field is then given by

$$E(x,t) = \int_{-\infty}^{+\infty} f(k-k_0) e^{ik(x-x_0-i\omega(k)t)}\, dk \tag{3.16}$$

Let us consider how the packet as a whole moves. In order to find the position of the maximum of the packet, we note that as in free space there will be at each instant of time one point where waves of different $k$ do not tend to interfere destructively. This will happen wherever the phase of the exponential $\varphi = k(x-x_0) - \omega(k)t$ has an extremum. At this point there will be a range of $k$ values for which all the waves have nearly the same phase; hence there will be constructive interference. To find this point, we set

$$\frac{\partial \varphi}{\partial k} = 0 \tag{3.17}$$

This gives

$$x - x_0 = t\frac{\partial \omega(k)}{\partial k} \tag{3.18}$$

which means that the maximum of the wave packet moves through space with the velocity

$$v_g = \left(\frac{\partial \omega(k)}{\partial k}\right)_{k=k_0} \tag{3.19}$$

The quantity $v_g$ is called the group velocity because it denotes the speed of motion of a group of waves collected together in the form of a packet. This is in contrast to the phase velocity $v_p = \lambda v = \dfrac{\omega}{k}$, which is precisely the speed with which a point of constant phase moves when $\omega$ and $k$ are defined. In general, the phase velocity has little physical significance. For example, the speed of transmission of a signal through a dielectric is given by the group velocity, as is also the speed of transport of energy.

For the special case $\omega = ck$ which holds in free space, one obtains $v_g = c = v_p$. Only if $\omega$ is proportional to $k$ is the group velocity equal to the phase velocity.

### 3.2.4 Spread of Wave Packets

We have already seen that we cannot in general expect a wave packet to be transmitted through a dielectric without change in shape. The problem of solving for the change of shape by taking into account the specific dependence of $\omega$ on $k$ is usually too com-

plicated to be solved exactly. If $f(k-k_0)$ has a narrow enough peak however, a good approximation is obtained by expanding $\omega(k)$ as a series of powers of $k-k_0$. This is because the main contributions to the integral come in a region of the order of the width of the peak in $f(k-k_0)$. Thus, we obtain

$$\omega(k) = \omega(k_0) + \left(\frac{\partial\omega(k)}{\partial k}\right)_{k=k_0}(k-k_0) + \frac{1}{2}\left(\frac{\partial^2\omega(k)}{\partial k^2}\right)_{k=k_0}(k-k_0)^2 + ... \tag{3.20}$$

Setting $\omega(k_0) = \omega_0$; $\left(\frac{\partial\omega(k)}{\partial k}\right)_{k=k_0} = v_g$ and $\left(\frac{\partial^2\omega(k)}{\partial k^2}\right)_{k=k_0} = \alpha$, we obtain

$$\omega(k) = \omega_0 + v_g(k-k_0) + \frac{1}{2}\alpha(k-k_0)^2 + ... \tag{3.21}$$

Inserting (3.21) in (3.16) gives:

$$E(x,t) = \int_{-\infty}^{+\infty} f(k-k_0)\exp\left[ik(x - x_0 - i[\omega_0 + v_g(k-k_0) + \frac{1}{2}\alpha(k-k_0)^2]t)\right]\ dk \tag{3.22}$$

After rearrangement, one obtains

$$\begin{aligned} E(x,t) &= \exp\left[i[k_0(x-x_0) - \omega_0 t]\right] \\ &\times \int_{-\infty}^{+\infty} f(k-k_0)\exp\left[i(k-k_0)(x-x_0-v_g t) - \frac{i}{2}\alpha t(k-k_0)^2\right]\ dk \end{aligned} \tag{3.23}$$

where $k - k_0 = K$. Then $dk = dK$

(3.23) becomes

$$\begin{aligned} E(x,t) &= \exp\left[i[k_0(x-x_0) - \omega_0 t]\right] \\ &\times \int_{-\infty}^{+\infty} f(K)\exp\left[iK(x-x_0-v_g t)(x-x_0-v_g t) - \frac{i}{2}\alpha t K^2\right]\ dK \end{aligned} \tag{3.24}$$

If $\alpha = 0$, then $E(x,t)$ is a function only of $x - x_0 - v_g t$, and the pulse does not change

its shape. In order to show how the $\alpha$ term affects the pulse, let us consider the special case

$$f(K) = \exp\left[-\frac{K^2}{2(\Delta k)^2}\right] \tag{3.25}$$

given in [32].

Substituting (3.25) in (3.24) gives

$$\begin{aligned} E &= \exp\left[i[k_0(x-x_0)-\omega_0 t]\right] \\ &\times \int_{-\infty}^{+\infty} \exp\left[-\frac{K^2}{2(\Delta k)^2}\right] \exp\left[iK(x-x_0-v_g t) - \frac{i}{2}\alpha t K^2\right]\, dK \\ &= \exp\left[i[k_0(x-x_0)-\omega_0 t]\right] \\ &\times \int_{-\infty}^{+\infty} \exp\left[-\left[-iK(x-x_0-v_g t) + \frac{K^2}{2}\left(i\alpha t + \frac{1}{(\Delta k)^2}\right)\right]\right]\, dK \end{aligned} \tag{3.26}$$

Since

$$\begin{aligned} &-\left[-i\frac{(x-x_0-v_g t)(\Delta k)}{\sqrt{2[1+i\alpha t(\Delta k)^2]}} + K\sqrt{\frac{1}{2}\left(i\alpha t + \frac{1}{(\Delta k)^2}\right)}\right]^2 - \left[\frac{(x-x_0-v_g t)(\Delta k)}{\sqrt{2[1+i\alpha t(\Delta k)^2]}}\right]^2 = \\ &-\left[-iK(x-x_0-v_g t) + \frac{K^2}{2}\left(i\alpha t + \frac{1}{(\Delta k)^2}\right)\right] \end{aligned} \tag{3.27}$$

we get

$$\begin{aligned} E &= \exp\left[i[k_0(x-x_0)-\omega_0 t] - \left[\frac{(x-x_0-v_g t)(\Delta k)}{\sqrt{2[1+i\alpha t(\Delta k)^2]}}\right]^2\right] \\ &\times \int_{-\infty}^{+\infty} \exp\left[-\left[-i\frac{(x-x_0-v_g t)(\Delta k)}{\sqrt{2[1+i\alpha t(\Delta k)^2]}} + K\sqrt{\frac{1}{2}\left(i\alpha t + \frac{1}{(\Delta k)^2}\right)}\right]^2\right]\, dK \end{aligned} \tag{3.28}$$

Substituting $-i\frac{(x-x_0-v_g t)(\Delta k)}{\sqrt{2[1+i\alpha t(\Delta k)^2]}} + K\sqrt{\frac{1}{2}\left(i\alpha t + \frac{1}{(\Delta k)^2}\right)} = u$ and integrating, we

get

$$E = \sqrt{2\pi \left[\frac{(\Delta k)^2}{1 + i\alpha t(\Delta k)^2}\right]} \exp\left[i[k_0(x - x_0) - \omega_0 t] - \left[\frac{(x - x_0 - v_g t)^2(\Delta k)^2}{2[1 + i\alpha t(\Delta k)^2]}\right]\right] \quad (3.29)$$

We can transform the argument of the exponential to a simpler form by multiplying both the numerator and the denominator by $1 - i\alpha t(\Delta k)^2$. We get

$$\begin{aligned} E &= \sqrt{2\pi \left[\frac{(\Delta k)^2}{1 + i\alpha t(\Delta k)^2}\right]} \exp[i[k_0(x - x_0) - \omega_0 t]] \\ &\times \exp\left[-\frac{(x - x_0 - v_g t)^2(\Delta k)^2}{2[1 + \alpha^2 t^2(\Delta k)^4]}\right] \times \exp\left[\frac{i\alpha t(\Delta k)^4(x - x_0 - v_g t)^2}{2[1 + \alpha^2 t^2(\Delta k)^4]}\right] \end{aligned} \quad (3.30)$$

Expression (3.30) was first given by Bohm [32]. For easy plotting, we need to re-adjust some terms in this formula by the replacement $\Delta k = \frac{1}{\Delta x_0}$ in the above formula to obtain

$$\begin{aligned} E &= \sqrt{2\pi \left[\frac{1}{\Delta x_0^2 + i\alpha t}\right]} \exp[i[k_0(x - x_0) - \omega_0 t]] \\ &\times \exp\left[-\frac{(x - x_0 - v_g t)^2}{2\left[\Delta x_0^2 + \alpha^2 t^2 \frac{1}{\Delta x_0^2}\right]}\right] \times \exp\left[\frac{i\alpha t(x - x_0 - v_g t)^2}{2[\Delta x_0^4 + \alpha^2 t^2]}\right] \end{aligned} \quad (3.31)$$

Using

$$\Delta x^2 = \Delta x_0^2 + \alpha^2 t^2 \frac{1}{\Delta x_0^2} \quad (3.32)$$

and

$$\Delta x_1^2 = \Delta x_0^4 + \alpha^2 t^2 \quad (3.33)$$

We find that

$$E = \sqrt{2\pi\left[\frac{1}{\Delta x_0^2 + i\alpha t}\right]}\exp[i[k_0(x-x_0)-\omega_0 t]] \times \exp\left[-\frac{(x-x_0-v_g t)^2}{2\Delta x^2}\right] \times \exp\left[\frac{i\alpha t(x-x_0-v_g t)^2}{2\Delta x_1^2}\right] \quad (3.34)$$

## 3.3 Mathematical Model of the Two-slit Experiment Using $1-D$ Gaussian

### 3.3.1 Intensity and Quantum Potential

Einstein's two-slit experiment (see Figure 3.4) has now become a classic example for exhibiting the peculiar particle-wave duality of the QM. It is well known that using the arrangement of Figure 3.4, Einstein sought to determine the electron trajectory without destroying the interference pattern. The important point here is that this experiment dealt with the mutually exclusive situations of either perfect particle knowledge or perfect wave knowledge.

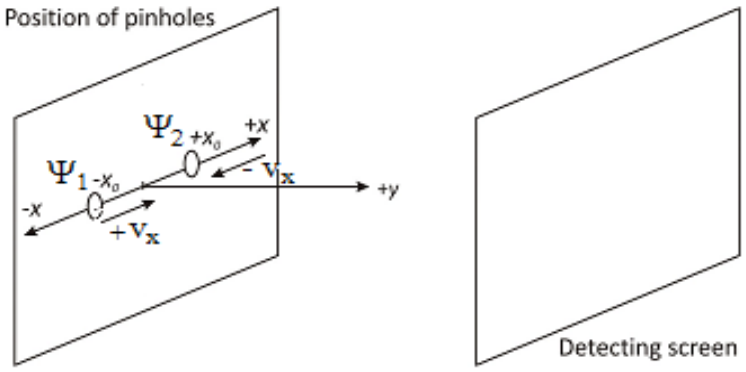


Figure 3.4: *Einstein's two-slit experiment showing the orientation of the axes and the position of the two-slit*

The two-slits represented by the $1-D$ Gaussian wave packets $\Psi_{1x} = \Psi_1(x,y,t)$ and $\Psi_{2x} = \Psi_2(x,y,t)$ are functions of $x$ while the $y$-behavior is represented by a plane wave. The total Gaussian wave packet is the sum of the two Gaussian wave packets

$$\Psi_x = \Psi_{1x} + \Psi_{2x} \tag{3.35}$$

where $\Psi_x = \Psi(x, y, t)$,

(i) The Gaussian wave packet $\Psi_{1x}$ is

$$\begin{aligned}
\Psi_{1x} &= \tilde{R}_1 \sqrt{\frac{2\pi}{\Delta x_0^2 + i\alpha t}} \times \exp\left[\frac{-(x + x_0 - v_x t)^2}{2\Delta x^2}\right] \\
&\times \exp\left\{i\left[k_x(x + x_0) - \omega_x t + k_y y + \frac{\alpha t (x + x_0 - v_x t)^2}{2\Delta x_1^2}\right]\right\} \\
&= \tilde{R}_1 A_x \exp\left[\frac{-(x + x_0 - v_x t)^2}{2\Delta x^2}\right] \\
&\times \exp\left\{i\left[k_x(x + x_0) - \omega_x t + k_y y + \frac{\alpha t (x + x_0 - v_x t)^2}{2\Delta x_1^2}\right]\right\} \\
&= A_x \bar{\Psi}_{1x}
\end{aligned} \tag{3.36}$$

where

$$\tilde{R}_1 = \cos^2\theta \tag{3.37}$$

is a constant amplitude

$$A_x = \sqrt{\frac{2\pi}{\Delta x_0^2 + i\alpha t}} \tag{3.38}$$

and

$$\begin{aligned}
\bar{\Psi}_{1x} &= \bar{\Psi}_1(x, y, t) \\
&= \tilde{R}_1 \exp\left[\frac{-(x + x_0 - v_x t)^2}{2\Delta x^2}\right] \times \exp\left\{i\left[k_x(x + x_0) - \omega_x t + k_y y + \frac{\alpha t (x + x_0 - v_x t)^2}{2\Delta x_1^2}\right]\right\} \\
&= \bar{R}_{1x} \exp\left[i\left(\frac{S_{1x}}{\hbar}\right)\right]
\end{aligned} \tag{3.39}$$

with

$$\begin{aligned}\frac{S_{1x}}{\hbar} &= \frac{S_1(x,y,t)}{\hbar} \\ &= k_x(x+x_0) - \omega_x t + k_y y + \frac{\alpha t(x+x_0-v_x t)^2}{2\Delta x_1^2} \end{aligned} \tag{3.40}$$

and

$$\begin{aligned}\bar{R}_{1x} &= \bar{R}_1(x,t) \\ &= \tilde{R}_1 \exp\left[\frac{-(x+x_0-v_x t)^2}{2\Delta x^2}\right] \\ &= \tilde{R}_1 \exp\left[\frac{-x(x_0-v_x)t}{\Delta x^2}\right] \exp\left[\frac{-x^2 - x_0 - ^2 - v_x^2 t^2 + 2x_0 v_x t}{2\Delta x^2}\right] \\ &= e_x R_{1fx} \end{aligned} \tag{3.41}$$

Here

$$\begin{aligned} e_x &= e(x,t) \\ &= \exp\left[\frac{-x^2 - x_0^2 - v_x^2 t^2 + 2x_0 v_x t}{2\Delta x^2}\right] \end{aligned} \tag{3.42}$$

and

$$\begin{aligned} R_{1fx} &= R_{1f}(x,t) \\ &= \tilde{R}_1 \exp\left[\frac{-x(x_0-v_x t)}{\Delta x^2}\right] \end{aligned} \tag{3.43}$$

(ii) The Gaussian wave packet $\Psi_{2x}$ is

$$
\begin{aligned}
\Psi_{2x} &= \tilde{R}_2 \sqrt{\frac{2\pi}{\Delta x_0^2 + i\alpha t}} \times \exp\left[\frac{-(x - x_0 + v_x t)^2}{2\Delta x^2}\right] \\
&\times \exp\left\{i\left[-k_x(x - x_0) - \omega_x t + k_y y + \frac{\alpha t (x - x_0 + v_x t)^2}{2\Delta x_1^2}\right]\right\} \\
&= \tilde{R}_2 A_x \exp\left[\frac{-(x - x_0 + v_x t)^2}{2\Delta x^2}\right] \\
&\times \exp\left\{i\left[-k_x(x - x_0) - \omega_x t + k_y y + \frac{\alpha t (x - x_0 + v_x t)^2}{2\Delta x_1^2}\right]\right\} \\
&= A_x \bar{\Psi}_{2x} \qquad (3.44)
\end{aligned}
$$

where

$$
\tilde{R}_2 = \sin^2\theta \qquad (3.45)
$$

is a constant amplitude. Also

$$
\begin{aligned}
\bar{\Psi}_{2x} &= \tilde{R}_2 \exp\left[\frac{-(x - x_0 + v_x t)^2}{2\Delta x^2}\right] \times \exp\left\{i\left[-k_x(x - x_0) - \omega_x t + k_y y + \frac{\alpha t (x - x_0 + v_x t)^2}{2\Delta x_1^2}\right]\right\} \\
&= \bar{R}_{2x} \exp\left[i\left(\frac{S_{2x}}{\hbar}\right)\right] \qquad (3.46)
\end{aligned}
$$

where

$$
\begin{aligned}
\frac{S_{2x}}{\hbar} &= \frac{S_2(x, y, t)}{\hbar} \\
&= -k_x(x - x_0) - \omega_x t + k_y y + \frac{\alpha t (x - x_0 + v_x t)^2}{2\Delta x_1^2} \qquad (3.47)
\end{aligned}
$$

and

$$\begin{aligned}\bar{R}_{2x} &= \tilde{R}_2 \exp\left[\frac{-(x-x_0+v_x t)^2}{2\Delta x^2}\right] \\ &= \tilde{R}_2 \exp\left[\frac{x(x_0-v_x)t}{\Delta x^2}\right] \exp\left[\frac{-x^2-x_0-^2-v_x^2t^2+2x_0v_xt}{2\Delta x^2}\right] \\ &= e_x R_{2fx} \end{aligned} \tag{3.48}$$

with

$$\begin{aligned}R_{2fx} &= R_{2f}(x,t) \\ &= \tilde{R}_2 \exp\left[\frac{x(x_0-v_x t)}{\Delta x^2}\right] \end{aligned} \tag{3.49}$$

The superposition of $\Psi_1(x,y,t)$ and $\Psi_2(x,y,t)$ gives (3.35). Then the expression of the intensity becomes

$$\begin{aligned}\bar{R}_x^2 &= \bar{R}^2(x,y,t) \\ &= \mid \bar{\Psi}_x \mid^2 \\ &= \bar{\Psi}_x^* \bar{\Psi}_x \end{aligned} \tag{3.50}$$

Substituting (3.35) in (3.50) we get

$$\bar{R}_x^2 = \bar{\Psi}_{1x}^* \bar{\Psi}_{1x} + \bar{\Psi}_{2x}^* \bar{\Psi}_{2x} + \bar{\Psi}_{1x}^* \bar{\Psi}_{2x} + \bar{\Psi}_{2x}^* \bar{\Psi}_{1x} \tag{3.51}$$

After replacing equations (3.39) and (3.46) in (3.51), we get

$$\bar{R}_x^2 = \bar{R}_{1x}^2 + \bar{R}_{2x}^2 + 2\bar{R}_{1x}\bar{R}_{2x}\cos(S_{12x}) \tag{3.52}$$

where

$$\begin{aligned}S_{12x} &= S_{12}(x,y,t) \\ &= \frac{S_{1x}}{\hbar} - \frac{S_{2x}}{\hbar} = 2k_x x + \frac{2\alpha t x(x_0 - v_x t)}{\Delta x_1^2} \end{aligned} \tag{3.53}$$

Hence, we can write the expression for the intensity as

$$R_x^2 = A_x^* A_x \bar{R}_x^2 \tag{3.54}$$

According to equation (2.29), the expression for the quantum potential becomes

$$\begin{aligned} Q(x,y,t) &= -\frac{\hbar^2}{2m}\frac{1}{\bar{R}_x}\frac{\partial^2 \bar{R}_x}{\partial x^2} \\ &= -\frac{\hbar^2}{2m}\left\{\frac{1}{2\bar{R}_x^2}\frac{\partial^2(\bar{R}_x^2)}{\partial x^2} - \left[\frac{1}{2\bar{R}_x^2}\frac{\partial(\bar{R}_x)^2}{\partial x}\right]^2\right\} \\ &= Q_1(x,y,t) + Q_2(x,y,t) + Q_3(x,y,t) + Q_4(x,y,t) \end{aligned} \tag{3.55}$$

where

$$Q_1(x,y,t) = \frac{\hbar^2}{8m\bar{R}_x^4}\left\{-2T_{1x}\bar{R}_{1x}^2 - 2T_{2x}\bar{R}_{2x}^2 + 4\bar{R}_{1x}\bar{R}_{2x}\left[-\frac{x\cos(S_{12x})}{\Delta x^2} - TT_x\sin(S_{12x})\right]\right\}^2 \tag{3.56}$$

$$Q_2(x,y,t) = -\frac{\hbar^2}{4m\bar{R}_x^2}\left\{\bar{R}_{1x}^2\left[4T_{1x}^2 - \frac{2}{\Delta x^2}\right] + \bar{R}_{2x}^2\left[4T_{2x}^2 - \frac{2}{\Delta x^2}\right]\right\} \tag{3.57}$$

$$Q_3(x,y,t) = -\frac{\hbar^2}{2m\bar{R}_x^2}\left\{\bar{R}_{1x}\bar{R}_{2x}\left[T_{1x}^2 - \frac{2}{\Delta x^2} + 2T_{1x}T_{2x} + T_{2x}^2\right]\cos(S_{12x})\right\} \tag{3.58}$$

$$Q_4(x,y,t) = \frac{2\hbar^2}{m\bar{R}_x^2}\left\{\bar{R}_{1x}\bar{R}_{2x}\left[-\frac{2x\ TT_x}{\Delta x^2}\sin(S_{12x}) + (TT_x)^2\cos(S_{12x})\right]\right\} \tag{3.59}$$

with

$$\begin{aligned} T_{1x} &= T_1(x,t) \\ &= \frac{x + x_0 - v_x t}{\Delta x^2} \end{aligned} \tag{3.60}$$

$$\begin{aligned} T_{2x} &= T_2(x,t) \\ &= \frac{x - x_0 + v_x t}{\Delta x^2} \end{aligned} \tag{3.61}$$

and

$$\begin{aligned} TT_x &= TT(x,t) \\ &= \frac{\alpha t(x_0 - v_x t)}{\Delta x_1^2} + k_x \end{aligned} \tag{3.62}$$

### 3.3.2 Trajectories

Particle trajectories can be obtained by integrating equation (2.24), with given initial positions. In the present case, this means integrating the following differential equation, assuming a Gaussian distribution of initial particle positions at each slit (i.e., the probability distribution given by equation (3.50) for t=0) [33]:

$$\vec{r}(t) = x(t)\vec{i} + y(t)\vec{j} \tag{3.63}$$

$$\vec{v}(t) = v_x(t)\vec{i} + v_y(t)\vec{j} \tag{3.64}$$

We see that the differential equation we must solve to obtain the trajectory (3.63) are

$$v_y(t) = \frac{\partial y(t)}{\partial t} = \frac{\hbar k_y}{m} \quad \Rightarrow \quad y(t) = \frac{\hbar k_y t}{m} + c \tag{3.65}$$

solved analytically, and

$$v_x(t) = \frac{\partial x(t)}{\partial t} = \frac{p_x}{m} = \frac{\nabla S_x}{m} = \frac{1}{m}\frac{\partial S_x}{\partial x} \tag{3.66}$$

which is a nonlinear equation. To solve this we must use expression (2.17) and differentiate it with respect to $x$ where

$$S_x = \frac{\hbar}{2i} \ln\left(\frac{\Psi_x}{\Psi_x^*}\right) \tag{3.67}$$

We obtain

$$\frac{\partial S_x}{\partial x} = \hbar \left( \frac{f_{1x} - f_{2x}}{f_{3x}} + f_{4x} \right) \tag{3.68}$$

$$\begin{aligned} f_{1x} &= f_1(x,t) \\ &= \left[ \frac{\alpha t(x_0 - v_x t)}{\Delta x_1^2} + k_x \right] (R_{1fx}^2 - R_{2fx}^2) \end{aligned} \tag{3.69}$$

$$\begin{aligned} f_{2x} &= f_2(x,t) \\ &= \frac{2(x_0 - v_x t) R_{1fx}^2}{\Delta x^2} \sin(S_{12x}) \end{aligned} \tag{3.70}$$

$$\begin{aligned} f_{3x} &= f_3(x,t) \\ &= R_{1fx}^2 + R_{2fx}^2 + 2R_{1fx}R_{2fx}\cos(S_{12x}) \end{aligned} \tag{3.71}$$

$$\begin{aligned} f_{4x} &= f_4(x,t) \\ &= \frac{\alpha t x}{\Delta x_1^2} \end{aligned} \tag{3.72}$$

Notice that the expressions for $R_{1fx}$ and $R_{2fx}$ can be found in expressions (3.43) and (3.49) respectively.

$$\begin{aligned} v_x(t) &= \frac{dx}{dt} \\ &= \frac{1}{m}\frac{\partial S_x}{\partial x} \\ &= \alpha \left( \frac{f_{1x} - f_{2x}}{f_{3x}} + f_{4x} \right) \end{aligned} \tag{3.73}$$

where

$$\alpha = \frac{\hbar}{m} \tag{3.74}$$

The solution (particle trajectories) of the differential equation (3.73) may be obtained numerically.

## 3.4 Mathematical Model of the Two-pinhole Experiment Using $2-D$ Gaussian

### 3.4.1 Intensity and Quantum Potential

By considering the $Z$-component of the Einstein's two-slit experiment, Figure 3.4 becomes Figure 3.5 below.

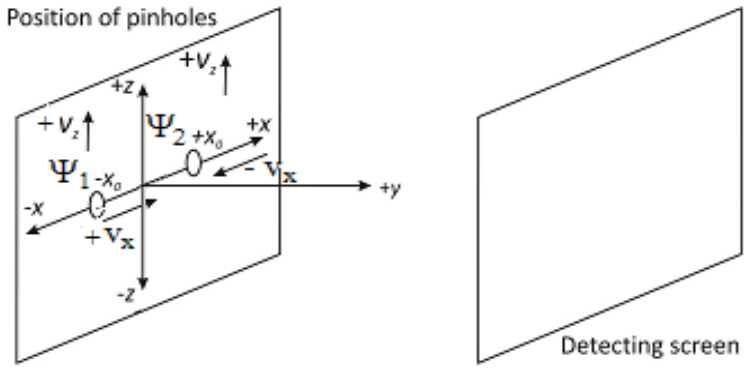


Figure 3.5: *Einstein's two-slit experiment in $XZ$-plane*

The two circles represent the $2-D$ Gaussian wave packets $\Psi_1$ and $\Psi_2$. $\Psi_1$ starts at $(x = -x_0, y = 0, z = -z_0 = 0)$ at $t = 0$ and moves to the right and up while $\Psi_2$ starts at $(x = +x_0, y = 0, z = z_0 = 0)$ at $t = 0$ and moves to the left and up.

The two-pinholes represented by the $2-D$ Gaussian wave packets $\Psi_1 = \Psi_1(x, y, z, t)$ and $\Psi_2 = \Psi_2(x, y, z, t)$ are functions of $x$ and $z$ while the $y$-behavior is represented by a plane wave. The total Gaussian wave packet is the sum of the two Gaussian wave packets

$$\Psi = \Psi_1 + \Psi_2 \tag{3.75}$$

where $\Psi = \Psi(x, y, z, t)$, $\Psi_1 = \Psi_1(x, y, z, t)$ and $\Psi_2 = \Psi_2(x, y, z, t)$

The pinholes are represented by $2 - D$ Gaussian wave packets $\Psi_1$ and $\Psi_2$ given by the following:

(i) The Gaussian wave packet in the first pinhole is given by:

$$\Psi_1 = \Psi_{1x}\Psi_{1z} \tag{3.76}$$

where

$$\begin{aligned}
\Psi_{1x} &= \tilde{R}_1\sqrt{\frac{2\pi}{\Delta x_0^2 + i\alpha t}} \times \exp\left[\frac{-(x + x_0 - v_x t)^2}{2\Delta x^2}\right] \\
&\times \exp\left\{i\left[k_x(x + x_0) - \omega_x t + k_y y + \frac{\alpha t(x + x_0 - v_x t)^2}{2\Delta x_1^2}\right]\right\} \\
&= A_x\tilde{R}_1 \times \exp\left[\frac{-(x + x_0 - v_x t)^2}{2\Delta x^2}\right] \times \exp\left\{i\left[\frac{S_{1x}}{\hbar}\right]\right\}
\end{aligned} \tag{3.77}$$

with

$$A_x = \sqrt{\frac{2\pi}{\Delta x_0^2 + i\alpha t}} \tag{3.78}$$

and

$$\frac{S_{1x}}{\hbar} = k_x(x + x_0) - \omega_x t + k_y y + \frac{\alpha t(x + x_0 - v_x t)^2}{2\Delta x_1^2} \tag{3.79}$$

We also have

$$\begin{aligned}\Psi_{1z} &= \tilde{R}_1\sqrt{\frac{2\pi}{\Delta z_0^2+i\alpha t}}\times\exp\left[\frac{-(z+z_0-v_zt)^2}{2\Delta z^2}\right]\\ &\times \exp\left\{i\left[k_z(z+z_0)-\omega_z t+k_y y+\frac{\alpha t(z+z_0-v_zt)^2}{2\Delta z_1^2}\right]\right\}\\ &= A_z\tilde{R}_1\times\exp\left[\frac{-(z+z_0-v_zt)^2}{2\Delta z^2}\right]\times\exp\left\{i\left[\frac{S_{1z}}{\hbar}\right]\right\} \qquad (3.80)\end{aligned}$$

with

$$A_z=\sqrt{\frac{2\pi}{\Delta z_0^2+i\alpha t}} \qquad (3.81)$$

and

$$\frac{S_{1z}}{\hbar}=k_z(z+z_0)-\omega_z t+k_y y+\frac{\alpha t(z+z_0-v_zt)^2}{2\Delta z_1^2} \qquad (3.82)$$

After replacing (3.77) and (3.80) in (3.76), we obtain

$$\begin{aligned}\Psi_1 &= A_xA_z\tilde{R}_1^2\times\exp\left[\frac{-(x+x_0-v_xt)^2}{2\Delta x^2}\right]\times\exp\left[\frac{-(z+z_0-v_zt)^2}{2\Delta z^2}\right]\\ &\times \exp\left[i\left(\frac{S_{1x}}{\hbar}+\frac{S_{1z}}{\hbar}\right)\right] \qquad (3.83)\end{aligned}$$

(ii) The Gaussian wave packet in the second pinhole is given by

$$\Psi_2=\Psi_{2x}\Psi_{2z} \qquad (3.84)$$

where

$$\begin{aligned}\Psi_{2x} &= \tilde{R}_2\sqrt{\frac{2\pi}{\Delta x_0^2+i\alpha t}}\times\exp\left[\frac{-(x-x_0+v_xt)^2}{2\Delta x^2}\right]\\ &\times \exp\left\{i\left[-k_x(x-x_0)-\omega_xt+k_yy+\frac{\alpha t(x-x_0+v_xt)^2}{2\Delta x_1^2}\right]\right\}\\ &= A_x\tilde{R}_2\times\exp\left[\frac{-(x-x_0+v_xt)^2}{2\Delta x^2}\right]\times\exp\left\{i\left[\frac{S_{2x}}{\hbar}\right]\right\} \qquad (3.85)\end{aligned}$$

with

$$A_x=\sqrt{\frac{2\pi}{\Delta x_0^2+i\alpha t}} \qquad (3.86)$$

and

$$\frac{S_{2x}}{\hbar}=-k_x(x-x_0)-\omega_xt+k_yy+\frac{\alpha t(x-x_0+v_xt)^2}{2\Delta x_1^2} \qquad (3.87)$$

We also have

$$\begin{aligned}\Psi_{2z} &= \tilde{R}_2\sqrt{\frac{2\pi}{\Delta z_0^2+i\alpha t}}\times\exp\left[\frac{-(z-z_0+v_zt)^2}{2\Delta z^2}\right]\\ &\times \exp\left\{i\left[-k_z(z-z_0)-\omega_zt+k_yy+\frac{\alpha t(z-z_0+v_zt)^2}{2\Delta z_1^2}\right]\right\}\\ &= A_z\tilde{R}_2\times\exp\left[\frac{-(z-z_0+v_zt)^2}{2\Delta z^2}\right]\times\exp\left\{i\left[\frac{S_{2z}}{\hbar}\right]\right\} \qquad (3.88)\end{aligned}$$

with

$$A_z=\sqrt{\frac{2\pi}{\Delta z_0^2+i\alpha t}} \qquad (3.89)$$

and

$$\frac{S_{2z}}{\hbar}=-k_z(z-z_0)-\omega_zt+k_yy+\frac{\alpha t(z-z_0+v_zt)^2}{2\Delta z_1^2} \qquad (3.90)$$

After replacing (3.85) and (3.88) in (3.84), we obtain

$$\begin{aligned}\Psi_2 &= A_x A_z \tilde{R}_2^2 \times \exp\left[\frac{-(x-x_0+v_x t)^2}{2\Delta x^2}\right] \times \exp\left[\frac{-(z-z_0+v_z t)^2}{2\Delta z^2}\right] \\ &\times \exp\left[i\left(\frac{S_{2x}}{\hbar}+\frac{S_{2z}}{\hbar}\right)\right] \end{aligned} \tag{3.91}$$

Since intensity is given by the expression:

$$\begin{aligned} R^2 &= R^2(x,y,z,t) \\ &= \mid \Psi \mid^2 \\ &= \Psi^* \Psi \end{aligned} \tag{3.92}$$

then by replacing (3.75) in (3.92), we obtain

$$R^2 = \Psi_1^* \Psi_1 + \Psi_2^* \Psi_2 + \Psi_1^* \Psi_2 + \Psi_2^* \Psi_1 \tag{3.93}$$

The final expression for $R^2$ will be obtained by replacing (3.83) and (3.91) in (3.93).

Since in two dimensions

$$\nabla^2 = \frac{\partial^2}{\partial x^2} + \frac{\partial^2}{\partial z^2} \tag{3.94}$$

equation (2.29) becomes

$$Q(x,y,z,t) = Q_x(x,y,z,t) + Q_z(x,y,z,t) \tag{3.95}$$

where

$$Q_x(x,y,z,t) = -\frac{\hbar^2}{2m}\frac{1}{R}\frac{\partial^2 R}{\partial x^2} \tag{3.96}$$

and

$$Q_z(x,y,z,t) = -\frac{\hbar^2}{2m}\frac{1}{R}\frac{\partial^2 R}{\partial z^2} \tag{3.97}$$

Since

$$\frac{\partial R^2}{\partial x} = 2R\frac{\partial R}{\partial x} \tag{3.98}$$

then

$$\frac{\partial R}{\partial x} = \frac{1}{2R}\frac{\partial R^2}{\partial x} \tag{3.99}$$

and

Since

$$\frac{\partial^2 R^2}{\partial x^2} = 2\left(\frac{\partial R}{\partial x}\right)^2 + 2R\frac{\partial^2 R}{\partial x^2} \tag{3.100}$$

then

$$\frac{\partial^2 R}{\partial x^2} = \frac{1}{2R}\frac{\partial^2 R^2}{\partial x^2} - \frac{1}{R}\left(\frac{\partial R}{\partial x}\right)^2 \tag{3.101}$$

Using (3.99) in (3.101)

$$\frac{\partial^2 R}{\partial x^2} = R\left[\frac{1}{2R^2}\frac{\partial^2 R^2}{\partial x^2} - \left(\frac{1}{2R^2}\frac{\partial R^2}{\partial x}\right)^2\right], \tag{3.102}$$

(3.102) in (3.96)

$$Q_x(x,y,z,t) = -\frac{\hbar^2}{2m}\left[\frac{1}{2R^2}\frac{\partial^2 R^2}{\partial x^2} - \left(\frac{1}{2R^2}\frac{\partial R^2}{\partial x}\right)^2\right] \tag{3.103}$$

and (3.92) in (3.103)

$$Q_x(x,y,z,t) = -\frac{\hbar^2}{2m}\left[\frac{1}{2(\Psi^*\Psi)}\frac{\partial^2}{\partial x^2}(\Psi^*\Psi) - \left(\frac{1}{2(\Psi^*\Psi)}\frac{\partial}{\partial x}(\Psi^*\Psi)\right)^2\right] \tag{3.104}$$

we obtain after simplification

$$Q_x(x,y,z,t) = -\frac{\hbar^2}{2m}\left[\left(\frac{1}{2\Psi^*}\frac{\partial^2\Psi^*}{\partial x^2} + \frac{1}{2\Psi}\frac{\partial^2\Psi}{\partial x^2} + \frac{1}{\Psi^*\Psi}\frac{\partial\Psi^*}{\partial x}\frac{\partial\Psi}{\partial x}\right) - \left(\frac{1}{2\Psi^*}\frac{\partial\Psi^*}{\partial x} + \frac{1}{2\Psi}\frac{\partial\Psi}{\partial x}\right)^2\right] \tag{3.105}$$

where

$$\Psi = \Psi_1 + \Psi_2 \tag{3.106}$$

$$\frac{\partial \Psi}{\partial x} = \frac{\partial \Psi_1}{\partial x} + \frac{\partial \Psi_2}{\partial x} \tag{3.107}$$

$$\frac{\partial^2 \Psi}{\partial x^2} = \frac{\partial^2 \Psi_1}{\partial x^2} + \frac{\partial^2 \Psi_2}{\partial x^2} \tag{3.108}$$

and, using equation (3.83), we find that

$$\frac{\partial \Psi_1}{\partial x} = \left\{ \frac{-(x + x_0 - v_x t)}{\Delta x^2} + i \left[ k_x + \frac{\alpha t (x + x_0 - v_x t)}{\Delta x_1^2} \right] \right\} \Psi_1 \tag{3.109}$$

and

$$\frac{\partial^2 \Psi_1}{\partial x^2} = \left( -\frac{1}{\Delta x^2} + i \frac{\alpha t}{\Delta x_1^2} \right) \Psi_1 + \left\{ \frac{-(x + x_0 - v_x t)}{\Delta x^2} + i \left[ k_x + \frac{\alpha t (x + x_0 - v_x t)}{\Delta x_1^2} \right] \right\}^2 \Psi_1 \tag{3.110}$$

Using equation (3.91), we get

$$\frac{\partial \Psi_2}{\partial x} = \left\{ \frac{-(x - x_0 + v_x t)}{\Delta x^2} + i \left[ -k_x + \frac{\alpha t (x - x_0 + v_x t)}{\Delta x_1^2} \right] \right\} \Psi_2 \tag{3.111}$$

$$\frac{\partial^2 \Psi_2}{\partial x^2} = \left( -\frac{1}{\Delta x^2} + i \frac{\alpha t}{\Delta x_1^2} \right) \Psi_2 + \left\{ \frac{-(x - x_0 + v_x t)}{\Delta x^2} + i \left[ -k_x + \frac{\alpha t (x - x_0 + v_x t)}{\Delta x_1^2} \right] \right\}^2 \Psi_2 \tag{3.112}$$

Using the same calculations as above for the $z$-axis, we find that

$$Q_z(x, y, z, t) = -\frac{\hbar^2}{2m} \left[ \left( \frac{1}{2\Psi^*} \frac{\partial^2 \Psi^*}{\partial z^2} + \frac{1}{2\Psi} \frac{\partial^2 \Psi}{\partial z^2} + \frac{1}{\Psi^* \Psi} \frac{\partial \Psi^*}{\partial z} \frac{\partial \Psi}{\partial z} \right) - \left( \frac{1}{2\Psi^*} \frac{\partial \Psi^*}{\partial z} + \frac{1}{2\Psi} \frac{\partial \Psi}{\partial z} \right)^2 \right] \tag{3.113}$$

where

$$\Psi = \Psi_1 + \Psi_2 \tag{3.114}$$

$$\frac{\partial \Psi}{\partial z} = \frac{\partial \Psi_1}{\partial z} + \frac{\partial \Psi_2}{\partial z} \tag{3.115}$$

$$\frac{\partial^2\Psi}{\partial z^2} = \frac{\partial^2\Psi_1}{\partial z^2} + \frac{\partial^2\Psi_2}{\partial z^2} \tag{3.116}$$

and likewise, using equation (3.83), we obtain

$$\frac{\partial\Psi_1}{\partial z} = \left\{ \frac{-(z + z_0 - v_z t)}{\Delta z^2} + i\left[k_z + \frac{\alpha t(z + z_0 - v_z t)}{\Delta z_1^2}\right]\right\}\Psi_1 \tag{3.117}$$

$$\frac{\partial^2\Psi_1}{\partial z^2} = \left(-\frac{1}{\Delta z^2} + i\frac{\alpha t}{\Delta z_1^2}\right)\Psi_1 + \left\{ \frac{-(z + z_0 - v_x t)}{\Delta z^2} + i\left[k_z + \frac{\alpha t(z + z_0 - v_z t)}{\Delta z_1^2}\right]\right\}^2\Psi_1 \tag{3.118}$$

Using equation (3.91), we get:

$$\frac{\partial\Psi_2}{\partial z} = \left\{ \frac{-(z - z_0 + v_z t)}{\Delta z^2} + i\left[-k_z + \frac{\alpha t(z - z_0 + v_z t)}{\Delta z_1^2}\right]\right\}\Psi_2 \tag{3.119}$$

$$\frac{\partial^2\Psi_2}{\partial z^2} = \left(-\frac{1}{\Delta z^2} + i\frac{\alpha t}{\Delta z_1^2}\right)\Psi_2 + \left\{ \frac{-(z - z_0 + v_z t)}{\Delta z^2} + i\left[-k_z + \frac{\alpha t(z - z_0 + v_z t)}{\Delta z_1^2}\right]\right\}^2\Psi_2 \tag{3.120}$$

### 3.4.2 Trajectories

The parametric equation of a trajectory is:

$$\vec{r}(t) = x(t)\vec{i} + y(t)\vec{j} + z(t)\vec{k} \tag{3.121}$$

$$\vec{v}(t) = v_x(t)\vec{i} + v_y(t)\vec{j} + v_z(t)\vec{k} \tag{3.122}$$

The differential equations we must solve to obtain the trajectory (3.63) are

$$v_y(t) = \frac{\partial y(t)}{\partial t} = \frac{\hbar k_y}{m} \;\Rightarrow\; y(t) = \frac{\hbar k_y t}{m} + c \tag{3.123}$$

and

$$v_x(t) = \frac{\partial x(t)}{\partial t} = \frac{p_x}{m} = \frac{\nabla S}{m} = \frac{1}{m}\frac{\partial S}{\partial x}, \tag{3.124}$$

$$v_z(t) = \frac{\partial z(t)}{\partial t} = \frac{p_z}{m} = \frac{\nabla S}{m} = \frac{1}{m}\frac{\partial S}{\partial z} \tag{3.125}$$

which are non-linear equation. Therefore to solve them, we will do the same as before, i.e.

$$S = \frac{\hbar}{i}\ln\left(\frac{\Psi}{\Psi^*}\right) \tag{3.126}$$

$$\frac{\partial S}{\partial x} = \hbar\left(\frac{f_{1x} - f_{2x}}{f_{3x}} + f_{4x}\right) \tag{3.127}$$

$$\frac{\partial S}{\partial z} = \hbar\left(\frac{f_{1z} - f_{2z}}{f_{3z}} + f_{4z}\right) \tag{3.128}$$

where

$$\begin{aligned} f_{1x} &= f_1(x,t) \\ &= \left[\frac{\alpha t(x_0 - v_x t)}{\Delta x_1^2} + k_x\right](R_{1f}^2 - R_{2f}^2) \end{aligned} \tag{3.129}$$

$$\begin{aligned} f_{1z} &= f_1(z,t) \\ &= \left[\frac{\alpha t(z_0 - v_z t)}{\Delta z_1^2} + k_z\right](R_{1f}^2 - R_{2f}^2) \end{aligned} \tag{3.130}$$

$$\begin{aligned} f_{2x} &= f_2(x,t) \\ &= \frac{2(x_0 - v_x t)R_{1f}^2}{\Delta x^2}\sin(S_{12}) \end{aligned} \tag{3.131}$$

$$\begin{aligned} f_{2z} &= f_2(z,t) \\ &= \frac{2(z_0 - v_z t)R_{1f}^2}{\Delta x^2}\sin(S_{12}) \end{aligned} \tag{3.132}$$

$$\begin{aligned} f_{3x} &= f_3(x,t) \\ &= R_{1f}^2 + R_{2f}^2 + 2R_{1f}R_{2f}\cos(S_{12}) \end{aligned} \tag{3.133}$$

$$\begin{aligned} f_{3z} &= f_3(z,t) \\ &= R_{1f}^2 + R_{2f}^2 + 2R_{1f}R_{2f}\cos(S_{12}) \end{aligned} \tag{3.134}$$

$$\begin{aligned} f_{4x} &= f_4(x,t) \\ &= \frac{\alpha t x}{\Delta x_1^2} \end{aligned} \tag{3.135}$$

$$\begin{aligned} f_{4z} &= f_4(z,t) \\ &= \frac{\alpha t z}{\Delta z_1^2} \end{aligned} \tag{3.136}$$

$$v_x(t) = \alpha\left(\frac{f_{1x} - f_{2x}}{f_{3x}} + f_{4x}\right) \tag{3.137}$$

$$v_z(t) = \alpha\left(\frac{f_{1z} - f_{2z}}{f_{3z}} + f_{4z}\right) \tag{3.138}$$

Notice that

$$R_{1f} = R_{1fx}R_{1fz} \tag{3.139}$$

$$R_{2f} = R_{2fx}R_{2fz} \tag{3.140}$$

# Chapter 4

# Assessment of Computer Software for Use in Computer Modeling of Quantum System

## 4.1 Introduction

In this chapter, the aim is to reproduce graphs of the intensity, the quantum potential and the trajectories as originally produced by Philippidis, Dewdney and Hiley, using newer mathematical packages like Maple 2015, Mathematica 10.0 and Matlab R2015a which contain many pre-existing algorithms, making modeling much simpler. We shall establish which mathematical package gives the best plots in order to apply it to the two-pinhole experiment using $2-D$ Gaussian wave packets in the following chapter.

To get the intensity plot and the quantum potential plot with our mathematical packages (Maple 2015, Mathematica 10.0 and Matlab R2015a, we will use for $1-D$ plot the formula (3.54) for the intensity and (3.55) for the quantum potential.

To get the quantum trajectories, we are first going to solve the nonlinear differential equation for the trajectories (3.73) using a numerical method (the fourth-order Runge-Kutta method (RK)). The choice of this numerical method is due to the fact that RK is well suited to the computer because it needs no special starting procedure,makes light demand on storage, and repeatedly uses the same straightforward computational

procedure. It is numerically stable. To get the Maple 2015, the Mathematica 10.0 and the Matlab R2015a plots, we used data points coming from the implementation of the RK method in Fortran 77.

## 4.2 Data from Experiments by Jönson

In order to obtain a clear visualization of the shape of the quantum potential under steady-state conditions, we have carried out numerical computations using data from the experiments performed by Jönsson [2].

(D1). The energy of the electrons is taken to be $45\,keV$ and we have used the velocities $V_x = 1.3 \times 10^8\, ms^{-1}$ and $V_y = (\pm)1.5 \times 10^2\, ms^{-1}$.

(D2). The separation between the centres of the two-slit, $A$ and $B$, is $1.0 \times 10^{-4}\, cm$ and their half-width is taken to be $0.1 \times 10^{-4}\, cm$.

(D3). The quantum potential was calculated in the region between the slits and the screen bounded by $0 < x \leq 35\, cm$ and $-1.9 \times 10^{-4}\, cm < y \leq 1.9 \times 10^{-4}\, cm$.

## 4.3 Maple 2015 Plots of the Intensity, quantum potential and Trajectories

**Intensity**

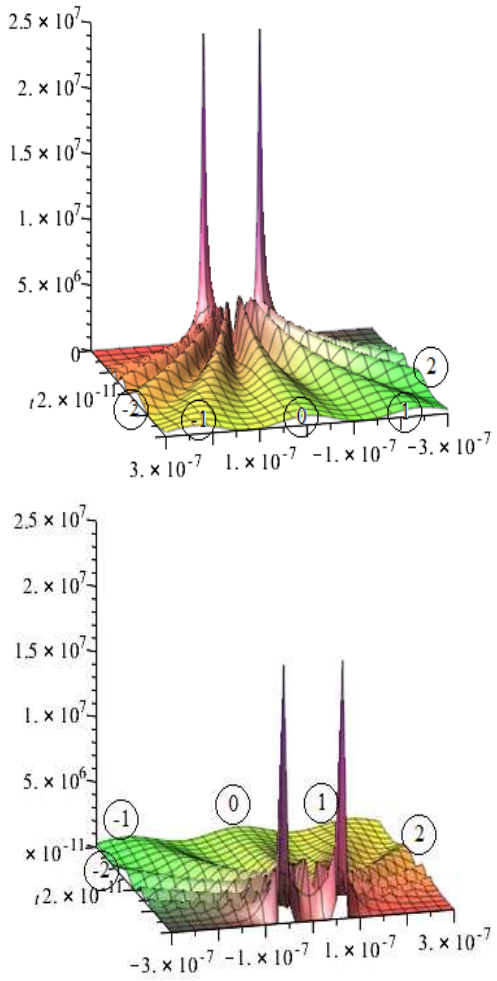


Figure 4.1: *Intensity plot for the two-slit experiment viewed from the detection screen (up) and from the slits (down). The two small peaks on the right and on the left correspond to the two-slit*

Figure 4.1 represents the intensity plot $R_x^2$ versus $x$ of the two-slit experiment calculated using Maple 2015. To get this plot we used the formula (3.54).

We also fixed these intervals: $0 \leq t \leq 5 \times 10^{-11}$; $-3 \times 10^{-7} \leq x \leq 3 \times 10^{-7}$ and $-1 \leq R_x^2 \leq 2.5 \times 10^7$. Orientations are: for the figure on the left: [75,75,0] and for the figure on the right: [-105,75,0].

The plot starts at $t = 0$, where the Gaussian wave packets are found in the two-slit which act as sources with high amplitude represented by the two high peaks in the figure. At $t \neq 0$, the Gaussian wave packets are spread as in the case of a diffraction by only one slit. Their amplitude decreases as $t$ is increases. Once the Gaussian wave packet reaches the screen we observe from those figures a series of alternative plateaus and valleys corresponding respectively to bright (maxima) and dark (minima) fringes. We have represented the plateaus by marking them by numbers inside a circle while the valleys are not marked. In other words, we can say that nodes (dark fringes or valleys correspond to the points for which the Gaussian wave packets resulting respectively from the two-slit are in opposition of phase and interfere destructively. The bellies of vibrations (bright fringes or plateaus) occur at the points where the waves resulting from the two-slit are in phase and interfere constructively.

We also observe from these figures that if we consider the $Yaxis$ as the symmetry axis, then the variation of intensity $R_x^2$ against $Yaxis$ on the screen has bright fringes near the symmetry line with this brightness decreasing as we move away from this axis along the screen. Notice also that the trajectories never cross the central symmetry axis.

**quantum potential**

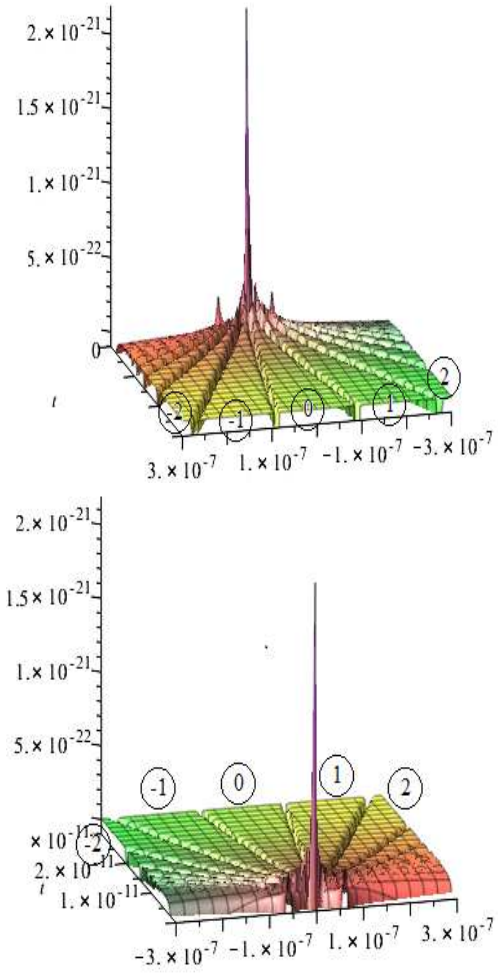


Figure 4.2: *quantum potential plot for the two-slit experiment viewed from the detection screen (up), and from the slits (down). The two small peaks, on the right and on the left, correspond to the two-slit*

In Figure 4.2, we have fixed the following intervals: $0 \leq t \leq 5 \times 10^{-11}$; $-3 \times 10^{-7} \leq x \leq 3 \times 10^{-7}$ and $0 \leq Q \leq 2 \times 10^{-21}$. Orientations are: for the left figure: [75,75,0] and for the right figure: [-105,75,0].

We observe from the same figure at $t = 0$ the presence of high values of the quantum potential at the two-slit. But this quantum potential is highest on the symmetric plane.

Since the quantum potential is a quantum field which does not exist before the Gaussian wave packet reaches the two-slit ($Q = 0$), no force acts on it, and so the particles are driven in a straight line in accordance with the principle of inertia. The amplitude of the Gaussian wave packet has a constant modulus $R$. The situation changes however if the plane wave reaches the two-slit: it suffers a diffraction and after the two-slit it diverges in space as shown in figures above. Its amplitude is not constant any more in space and one has in general $Q \neq O$. This implies that the wave exerts a force on the and curves its trajectory even when the wave moves away from the slit. This is as expected since energy (partner with the particles) is distributed on the screen according to the interference pattern (with plateaus or maxima numbered inside a circle and valleys or minima, not numbered). Indeed, the quantum potential exists between the screen with two-slit ($t = 0$) and the last screen ($t \neq 0$), even without the presence of particle. It serves to guide the particles.

**Trajectories**

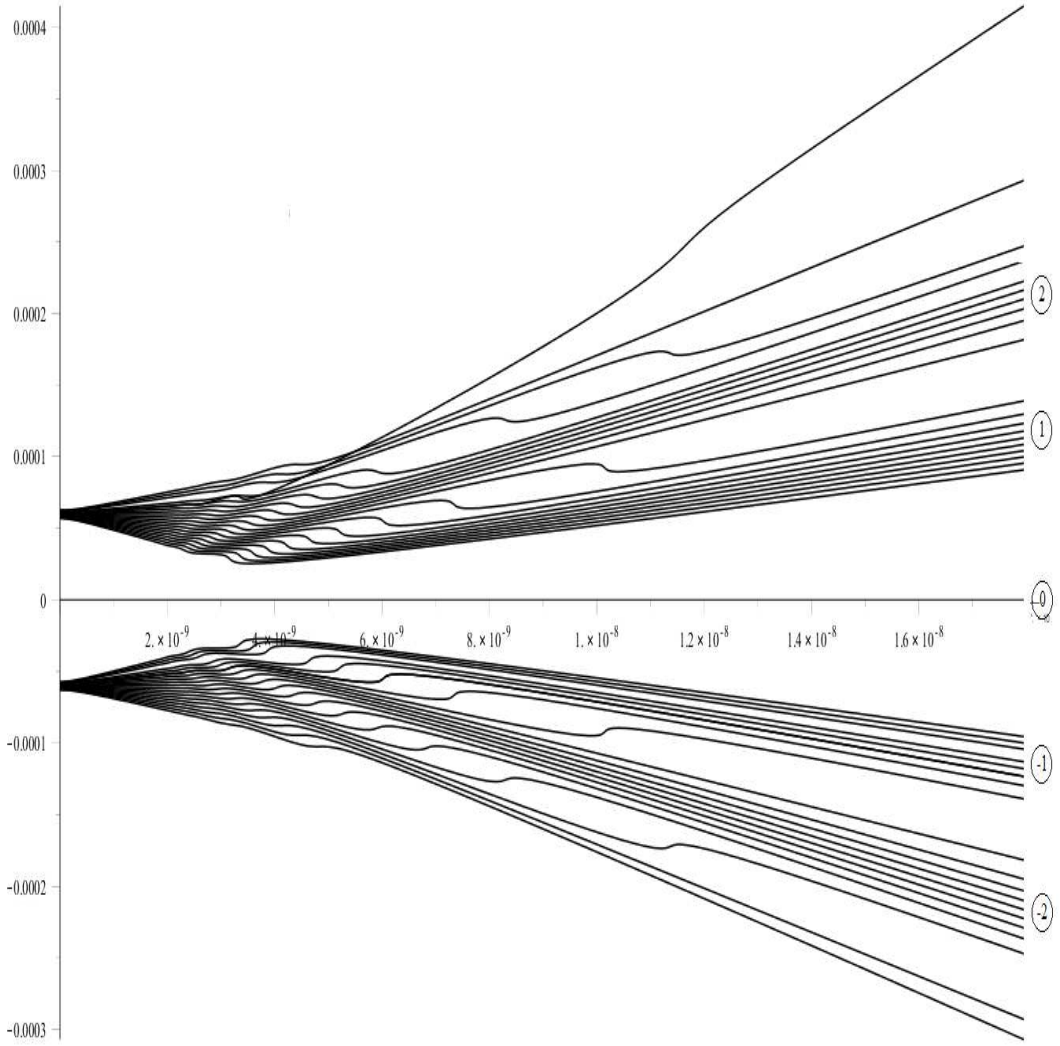


Figure 4.3: *Particle trajectories for the two-slit experiment*

The path of each electron is clearly shown from the first screen up to the last.

From each slit, the trajectories of particles spread and follow the paths already traced by the quantum potential field. As we can see from the Figure (Fig 4.2), the quantum potential has a maximum amplitude in the region close to the symmetry line (labeled '0') at $t = 0$ even if no particles passes through.

It is interesting to note that no trajectory crosses the symmetry plane. This means that all the particles observed on the top/bottom part of the second screen come from the top/bottom slit. It is a result fraught with philosophical implications for those who believe that the experiment with double slits does not imply any simple interpretation. The approach by the quantum potential considers specific particles and each particle of the unit follows a well-defined trajectory which passes by one or the other of the two-slit. This unit produces the figure for interferences and at the same time shows that the final position of the particle on the screen enables us to deduce by which slit it really passed through. It is thus possible to maintain the concept of trajectory, while accounting for the interferences. There is no bigger mystery as that of knowing how a particle crossing a slit 'knows' if the other slit is opened. Information is carried by the quantum potential so that we do not have any more a conceptual difficulty in the interpretation of the results obtained with the experiments of interferences with very low intensities.

## 4.4 Mathematica 10.0 Plots of the Intensity, Quantum Potential and Trajectories

**Intensity**

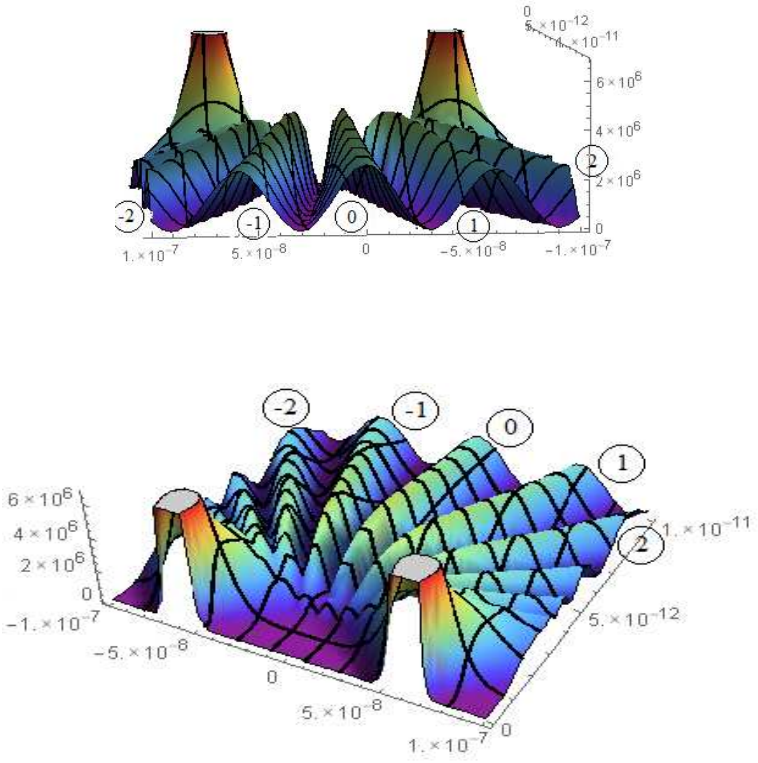


Figure 4.4: *Intensity plot for the two-slit experiment viewed from the detection screen (up), and from the slits (down)*

In Figure 4.4, we have fixed these intervals at $0 \leq t \leq 1 \times 10^{-11}$; $-1 \times 10^{-7} \leq x \leq 1 \times 10^{-7}$ and $0 \leq R_x^2 \leq 6 \times 10^6$. At $t = 0$, we can observe the presence of the Gaussian wave packet on the two-slit with a short amplitude compared to the two peaks of the Maple 2015 intensity plot. At $t \neq 0$, as the Gaussian spreads from the two-slit, the amplitude of the intensity from the two-slit remain almost constant when we expect them to decrease as the Gaussian leaves the two-slit. On the last screen, we can observe the presence of plateaus and valleys.

**quantum potential**

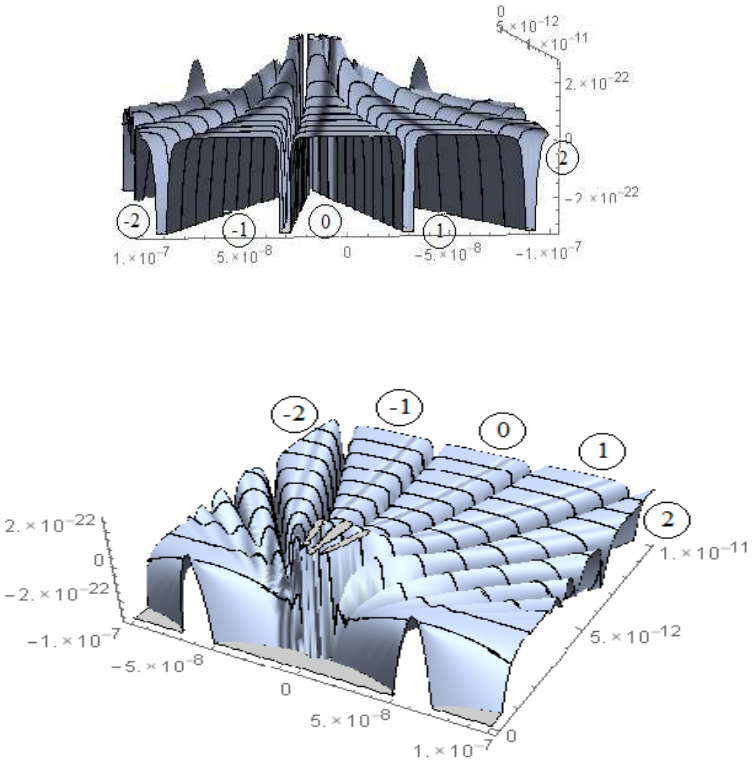


Figure 4.5: *quantum potential plot for the two-slit experiment viewed from the detection screen (up), and from the slits (down)*

We have fixed in Figure (Fig 4.5) the intervals $0 \leq t \leq 1 \times 10^{-11}$; $-1 \times 10^{-7} \leq x \leq 1 \times 10^{-7}$ and $-1 \times 10^{-7} \leq Q \leq 2 \times 10^{-22}$. At $t = 0$ there is no high value of the quantum potential at the two-slit compare to any other places along the first screen, except on the symmetry plane. But in the Maple 2015 quantum potential plot (Fig 4.2) we were able to observe easily the presence of high value of the quantum potential in those two regions than any other place along the first screen except on the symmetry plane. The quantum potential is not high in the symmetry plane. But, as the time $t$ increases, the quantum potential spreads like in case of Figure 4.2.

**Trajectories**

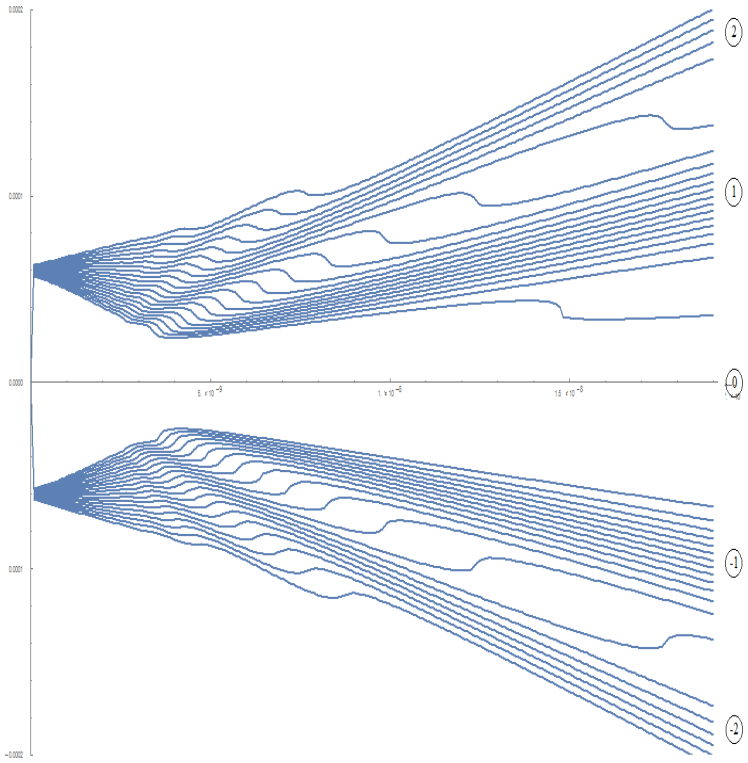


Figure 4.6: *Particle trajectories for the two-slit experiment*

The Mathematica trajectories plot is less clear compare to the corresponding Maple trajectories plot (see Figure 4.3)

## 4.5 Matlab R2015a Plots of the Intensity, Quantum Potential and Trajectories

**Intensity**

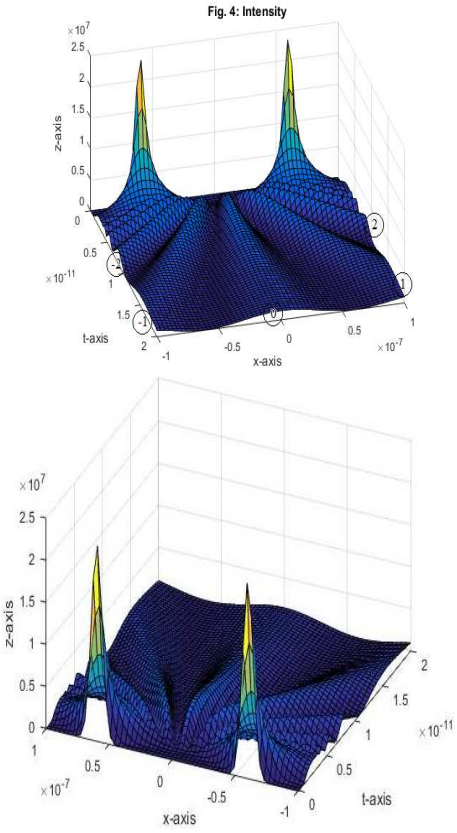


Figure 4.7: *Intensity plot for the two-slit experiment viewed from the detection screen (up), and from the slits (down)*

In Figure 4.7, we have fixed these intervals: $0 \leq t \leq 2 \times 10^{-11}$; $-1 \times 10^{-7} \leq x \leq 1 \times 10^{-7}$ and view(75,40). The spread of the Gaussian wave packet is quite similar with Maple 2015 intensity plot (Fig 4.1).

**quantum potential**

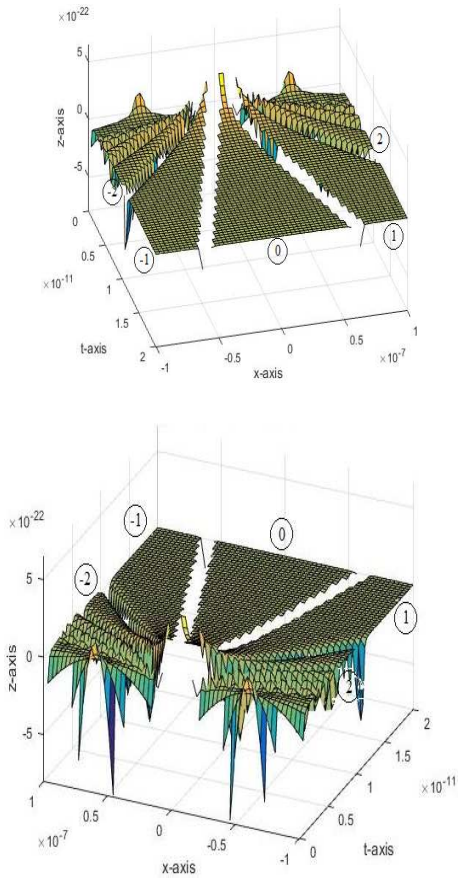


Figure 4.8: *quantum potential plot for the two-slit experiment viewed from the detection screen (up), and from the slits (down)*

We have fixed, in Figure 4.8, the intervals $0 \leq t \leq 2\times10^{-11}$; $-1\times10^{-7} \leq x \leq 1\times10^{-7}$; $-5 \times 10^{-22} \leq Q \leq 5 \times 10^{-22}$ and view(75,40).

We observe at $t = 0$ the presence of a high value of the quantum potential in the two-slit like in the Maple 2015 quantum potential plot. But in the Mathematica 10.0 quantum potential plot, we could not see that.

**Trajectories**

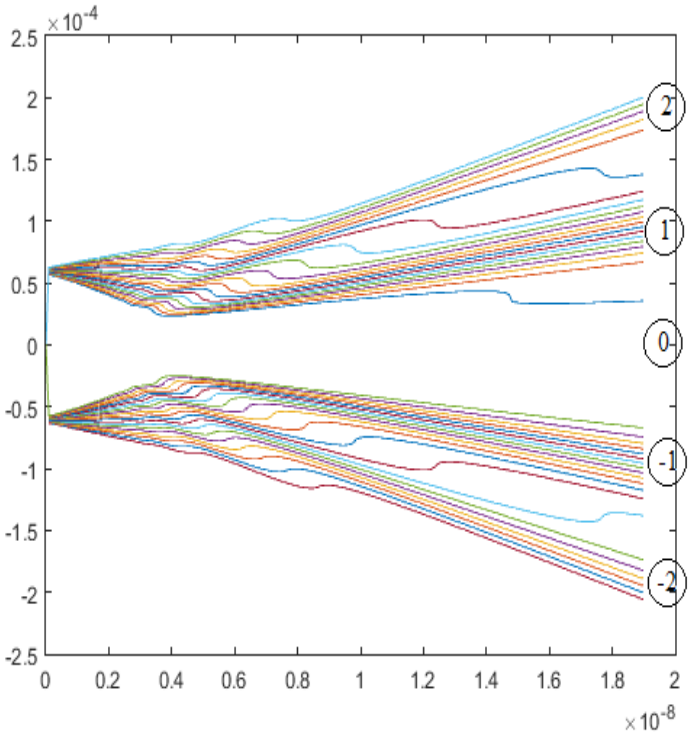


Figure 4.9: *Particle trajectories for the two-slit experiment*

The Matlab trajectories plot is less clear compare to the Maple trajectories plot (Figure 4.3) and the Maple trajectories plot (Figure 4.6)

## 4.6 Conclusion

We have plotted $1-D$ intensities, quantum potentials and trajectories using Maple 2015, Mathematica 10.0 and Matlab R2015a with the aim of selecting the best mathematical package. We have selected Maple 2015 because it produced the best plot. Therefore, we will only use this mathematical package in the the next chapter for the computer model of the two-slit experiment where $2-D$ Gaussian wave packets represent the slits.

# Chapter 5

# Computer Model of the Two-Pinhole Experiment Using $2-D$ $XZ$ Gaussian Wave Packets

## 5.1 Introduction

From the previous chapter, we have realised that the best mathematical package among the three for the plots is Maple 2015.

Now, our aim is to apply this software to plot the intensities, the intensity contours, the quantum potential, the quantum potential contours and trajectories for $2-D$ Gaussian wave packets passing through two-pinhole. We consider the following cases: Equal widths and equal amplitudes (EWEA), equal widths and unequal amplitudes (EWUA), unequal widths and equal amplitudes (UWEA), and finally unequal widths and unequal amplitudes (UWUA).

Below we show the replacements we must make between the $1-D$ and $2-D$ cases

(i) Equation (3.78) becomes

$$A_{Nx} = \sqrt{\frac{2\pi}{\Delta x_{N0}^2 + i\alpha t}} \tag{5.1}$$

(ii) Equation (3.81) becomes

$$A_{Nz} = \sqrt{\frac{2\pi}{\Delta z_{N0}^2 + i\alpha t}} \tag{5.2}$$

(iii) Equation (3.86) becomes

$$A_{Px} = \sqrt{\frac{2\pi}{\Delta x_{P0}^2 + i\alpha t}} \tag{5.3}$$

(iv) Equation (3.89) becomes

$$A_{Pz} = \sqrt{\frac{2\pi}{\Delta z_{P0}^2 + i\alpha t}} \tag{5.4}$$

(v) Equation (3.79) becomes

$$\frac{S_{1x}}{\hbar} = k_x(x + x_0) - \omega_x t + k_y y + \frac{\alpha t(x + x_0 - v_x t)^2}{2\Delta x_{N1}^2} \tag{5.5}$$

(vi) Equation (3.82) becomes

$$\frac{S_{1z}}{\hbar} = k_z(z + z_0) - \omega_z t + k_y y + \frac{\alpha t(z + z_0 - v_z t)^2}{2\Delta z_{N1}^2} \tag{5.6}$$

(vii) Equation (3.87) becomes

$$\frac{S_{2x}}{\hbar} = -k_x(x - x_0) - \omega_x t + k_y y + \frac{\alpha t(x - x_0 + v_x t)^2}{2\Delta x_{P1}^2} \tag{5.7}$$

(viii) Equation (3.90) becomes

$$\frac{S_{2z}}{\hbar} = -k_z(z - z_0) - \omega_z t + k_y y + \frac{\alpha t(z - z_0 + v_z t)^2}{2\Delta z_{P1}^2} \tag{5.8}$$

(ix) Equation (3.83) becomes

$$\begin{aligned} \Psi_1 &= \tilde{R}_1^2 \times A_{Nx} \exp\left[\frac{-(x + x_0 - v_x t)^2}{2\Delta x_N^2}\right] \times A_{Nz} \exp\left[\frac{-(z + z_0 - v_z t)^2}{2\Delta z_N^2}\right] \\ &\times \exp\left[i\left(\frac{S_{1x}}{\hbar} + \frac{S_{1z}}{\hbar}\right)\right] \end{aligned} \tag{5.9}$$

(x) Equation (3.91) becomes

$$\begin{aligned}\Psi_2 &= \tilde{R}_2^2 \times A_{Px} \exp\left[\frac{-(x - x_0 + v_x t)^2}{2\Delta x_P^2}\right] \times A_{Pz} \exp\left[\frac{-(z - z_0 + v_z t)^2}{2\Delta z_P^2}\right] \\ &\times \exp\left[i\left(\frac{S_{2x}}{\hbar} + \frac{S_{2z}}{\hbar}\right)\right] \end{aligned} \tag{5.10}$$

where, from the expressions

(a) Equation (3.32), yields

$$\Delta x_N^2 = \Delta x_{N0}^2 + \frac{\alpha^2 t^2}{\Delta x_{N0}^2} \tag{5.11}$$

$$\Delta z_N^2 = \Delta z_{N0}^2 + \frac{\alpha^2 t^2}{\Delta z_{N0}^2} \tag{5.12}$$

$$\Delta x_P^2 = \Delta x_{P0}^2 + \frac{\alpha^2 t^2}{\Delta x_{P0}^2} \tag{5.13}$$

$$\Delta z_P^2 = \Delta z_{P0}^2 + \frac{\alpha^2 t^2}{\Delta z_{P0}^2} \tag{5.14}$$

and

(b) (3.33) gives

$$\Delta x_{N1}^2 = \Delta x_{N0}^4 + \alpha^2 t^2 \tag{5.15}$$

$$\Delta z_{N1}^2 = \Delta z_{N0}^4 + \alpha^2 t^2 \tag{5.16}$$

$$\Delta x_{P1}^2 = \Delta x_{P0}^4 + \alpha^2 t^2 \tag{5.17}$$

$$\Delta z_{P1}^2 = \Delta z_{P0}^4 + \alpha^2 t^2 \tag{5.18}$$

Hence, for plotting the intensity, we are going to replace (5.9) and (5.10) in (3.93).

We can make this final modification (corresponding to a normalised function):

$$R_N^2 = \frac{1}{NSQ} R^2 \tag{5.19}$$

In order to differentiate electrons passing through one or another pinhole, let us now rewrite the following equations:

(3.109) becomes

$$\frac{\partial \Psi_1}{\partial x} = \left\{ \frac{-(x + x_0 - v_x t)}{\Delta x_N^2} + i \left[ k_x + \frac{\alpha t (x + x_0 - v_x t)}{\Delta x_{N1}^2} \right] \right\} \Psi_1 \tag{5.20}$$

Equation (3.117) becomes

$$\frac{\partial \Psi_1}{\partial z} = \left\{ \frac{-(z + z_0 - v_z t)}{\Delta z_N^2} + i \left[ k_z + \frac{\alpha t (z + z_0 - v_z t)}{\Delta z_{N1}^2} \right] \right\} \Psi_1 \tag{5.21}$$

Equation (3.111) becomes

$$\frac{\partial \Psi_2}{\partial x} = \left\{ \frac{-(x - x_0 + v_x t)}{\Delta x_P^2} + i \left[ -k_x + \frac{\alpha t (x - x_0 + v_x t)}{\Delta x_{P1}^2} \right] \right\} \Psi_2 \tag{5.22}$$

Equation (3.119) becomes

$$\frac{\partial \Psi_2}{\partial z} = \left\{ \frac{-(z - z_0 + v_z t)}{\Delta z_P^2} + i \left[ -k_z + \frac{\alpha t (z - z_0 + v_z t)}{\Delta z_{P1}^2} \right] \right\} \Psi_2 \tag{5.23}$$

Equation (3.110) becomes

$$\frac{\partial^2 \Psi_1}{\partial x^2} = \left( -\frac{1}{\Delta x_N^2} + i \frac{\alpha t}{\Delta x_{N1}^2} \right) \Psi_1 + \left\{ \frac{-(x + x_0 - v_x t)}{\Delta x_N^2} + i \left[ k_x + \frac{\alpha t (x + x_0 - v_x t)}{\Delta x_{N1}^2} \right] \right\}^2 \Psi_1 \tag{5.24}$$

Equation (3.118) becomes

$$\frac{\partial^2 \Psi_1}{\partial z^2} = \left( -\frac{1}{\Delta z_N^2} + i \frac{\alpha t}{\Delta z_{N1}^2} \right) \Psi_1 + \left\{ \frac{-(z + z_0 - v_x t)}{\Delta z_N^2} + i \left[ k_z + \frac{\alpha t (z + z_0 - v_z t)}{\Delta z_{N1}^2} \right] \right\}^2 \Psi_1 \tag{5.25}$$

Equation (3.112) becomes

$$\frac{\partial^2\Psi_2}{\partial x^2} = \left(-\frac{1}{\Delta x_P^2} + i\frac{\alpha t}{\Delta x_{P1}^2}\right)\Psi_2 + \left\{\frac{-(x - x_0 + v_x t)}{\Delta x_P^2} + i\left[-k_x + \frac{\alpha t(x - x_0 + v_x t)}{\Delta x_{P1}^2}\right]\right\}^2 \Psi_2 \tag{5.26}$$

Equation (3.120) becomes

$$\frac{\partial^2\Psi_2}{\partial z^2} = \left(-\frac{1}{\Delta z_P^2} + i\frac{\alpha t}{\Delta z_{P1}^2}\right)\Psi_2 + \left\{\frac{-(z - z_0 + v_z t)}{\Delta z_P^2} + i\left[-k_z + \frac{\alpha t(z - z_0 + v_z t)}{\Delta z_{P1}^2}\right]\right\}^2 \Psi_2 \tag{5.27}$$

Substituting (5.20) and (5.22) in (3.107) gives

$$\begin{aligned}\frac{\partial\Psi}{\partial x} &= \left\{\frac{-(x + x_0 - v_x t)}{\Delta x_N^2} + i\left[k_x + \frac{\alpha t(x + x_0 - v_x t)}{\Delta x_{N1}^2}\right]\right\}\Psi_1 \\ &+ \left\{\frac{-(x - x_0 + v_x t)}{\Delta x_P^2} + i\left[-k_x + \frac{\alpha t(x - x_0 + v_x t)}{\Delta x_{P1}^2}\right]\right\}\Psi_2 \end{aligned} \tag{5.28}$$

Substituting (5.21) and (5.23) in (3.115) gives

$$\begin{aligned}\frac{\partial\Psi}{\partial z} &= \left\{\frac{-(z + z_0 - v_z t)}{\Delta z_N^2} + i\left[k_z + \frac{\alpha t(z + z_0 - v_z t)}{\Delta z_{N1}^2}\right]\right\}\Psi_1 \\ &+ \left\{\frac{-(z - z_0 + v_z t)}{\Delta z_P^2} + i\left[-k_z + \frac{\alpha t(z - z_0 + v_z t)}{\Delta z_{P1}^2}\right]\right\}\Psi_2 \end{aligned} \tag{5.29}$$

Substituting (5.24) and (5.26) in (3.108) gives

$$\begin{aligned}\frac{\partial^2\Psi}{\partial x^2} &= \left(-\frac{1}{\Delta x_N^2} + i\frac{\alpha t}{\Delta x_{N1}^2}\right)\Psi_1 + \left\{\frac{-(x + x_0 - v_x t)}{\Delta x_N^2} + i\left[k_x + \frac{\alpha t(x + x_0 - v_x t)}{\Delta x_{N1}^2}\right]\right\}^2\Psi_1 \\ &+ \left(-\frac{1}{\Delta x_P^2} + i\frac{\alpha t}{\Delta x_{P1}^2}\right)\Psi_2 + \left\{\frac{-(x - x_0 + v_x t)}{\Delta x_P^2} + i\left[-k_x + \frac{\alpha t(x - x_0 + v_x t)}{\Delta x_{P1}^2}\right]\right\}^2\Psi_2 \end{aligned} \tag{5.30}$$

Substituting (5.25) and (5.27) in (3.116) gives

$$\begin{aligned}\frac{\partial^2\Psi}{\partial z^2} &= \left(-\frac{1}{\Delta z_N^2}+i\frac{\alpha t}{\Delta z_{N1}^2}\right)\Psi_1+\left\{\frac{-(z+z_0-v_xt)}{\Delta z_N^2}+i\left[k_z+\frac{\alpha t(z+z_0-v_zt)}{\Delta z_{N1}^2}\right]\right\}^2\Psi_1 \\ &+ \left(-\frac{1}{\Delta z_P^2}+i\frac{\alpha t}{\Delta z_{P1}^2}\right)\Psi_2+\left\{\frac{-(z-z_0+v_zt)}{\Delta z_P^2}+i\left[-k_z+\frac{\alpha t(z-z_0+v_zt)}{\Delta z_{P1}^2}\right]\right\}^2\Psi_2\end{aligned} \tag{5.31}$$

Finally we replace (5.28) and (5.30) into (3.105). We also replace (5.29) and (5.31) in (3.113).

For plotting, we are going to use the formula (5.32)

$$Q(x,y,z,t)=Q_x(x,y,z,t)+Q_z(x,y,z,t) \tag{5.32}$$

To get the quantum trajectories, first we are going to solve the nonlinear coupled differential equations for the trajectories by inserting (3.137) and (3.138) into (3.122) using the fourth-order RK method (see section 5.4.1) with fixed step size in a Fortran 77 program (see section 5.4.2). The data points produced by this program are excerpted in a file. We will then use these data points to plot trajectories with Maple 2015.

## 5.2 Constants

In the Maple 2015 computational plots, we have kept the components of the velocities of the Gaussian wave packets as $v_x = v_z = 0\, m.s^{-1}$ and $v_y = 1.3\times 10^8\, m.s^{-1}$.

The separation between the centres of the two-pinhole and hence the Gaussian wave functions are:

i. $\Psi_1$ starts at: $(x=-x_0, z=0, y=0)$ and moves to the right and up.

ii. $\Psi_2$ starts at: $(x=x_0, z=0, y=0)$ and moves to the left and up.

with the $x$-distance of the center of the pinhole from the origin $x_0 = 5\times 10^{-7}\, m$ when the $z$-distance of the center of the pinhole from the origin $z_0 = 0\, m$.

The separation between the pinhole screen and the detecting screen is $y = 0.195m$.

$\Delta x_{N0}$ and $\Delta z_{N0}$ are the widths of the Gaussian wave packet $\Psi_1$ while $\Delta x_{P0}$ and $\Delta z_{P0}$ are the widths of the Gaussian wave packet $\Psi_2$. We consider this case:

i. Equal widths: $\Delta x_{N0} = 7{\times}10^{-8}m$, $\Delta z_{N0} = \Delta x_{N0}$, $\Delta x_{P0} = \Delta x_{N0}$ and $\Delta z_{P0} = \Delta x_{P0}$

ii. Unequal widths: $\Delta x_{N0} = 7 \times 10^{-8}\ m$, $\Delta z_{N0} = \Delta x_{N0}$, $\Delta x_{P0} = c \times \Delta x_{N0}$ and $\Delta z_{P0} = \Delta x_{P0}$

where $c$ is a constant ($c \in R$ and $c \neq 1$)

$\tilde{R}_1 = \cos^2 b$ is the amplitude of the Gaussian wave packet $\Psi_1$ and $\tilde{R}_2 = \sin^2 b$ is the amplitude of the Gaussian wave packet $\Psi_2$ where $b$ is an angle. We consider these following cases:

i. Equal amplitude: The only choice that we can make so that the amplitude $\tilde{R}_1 = \tilde{R}_2$ is $b = \frac{\pi}{4}$.

ii. Unequal amplitude: We choose a value $b \neq \frac{\pi}{4}$.

The other constants are

i. The parameter $NSQ = 1.372675283 \times 10^{16}$

ii. The Planck constant $h = 6.6260755 \times 10^{-34}\ Js$

iii. The mass of the electron $m = 9.10938356 \times 10^{-31}\ kg$

iv. The magnitude of $x$-wavenumber $k_x = 1.295696717 \times 10^{6}\ m^{-1}$

v. The magnitude of $y$-wavenumber $k_y = 0$

vi. The magnitude of $z$-wavenumber $k_z = 0$

1. when $k_x = 1.295696717 \times 10^{6}\ m^{-1}$

The Maple 2015 program to produce the plots of the intensity, the intensity contour, the quantum potential and the quantum potential contour follows.

## 5.3 Intensity, Intensity Contour, Quantum Potential and Quantum Potential Contour

The intensity and the quantum potential in the $2-D$ $XZ$ Gaussian Wave Packets are functions of $x$, $y$, $z$ and $t$. We note that the $y$-behaviour is represented by a plane-wave, $Q_y = 0$, while $Q_x$ and $Q_z$ depend only on $x$, $z$ and $t$. Similarly, the intensity does not depend on $y$. This means that the values of the intensity and the quantum potential in the $xy$-plane at a given instant of time are the same from $y = -\infty$ to $y = +\infty$. Since the intensity and the quantum potential change in time, the electron 'sees' evolving values of these quantities. All the plots below show what the electron 'sees' at a particular instant of time $t$ and a particular position $x$, $y$, $z$.

We proceeded two ways to represent the intensity and the quantum potential.

i. We produced animations of the intensity and the quantum potential of six frames. These animations are produced in the $xz$-plane and show the form of the intensity and the quantum potential that the electron 'sees' at each instant of time as it moves along its trajectory.

ii. We produced animations of the intensity contour and the quantum potential contour in the $xz$-plane. These results are presented by placing three $2-D$ $xz$-slices (three frames of the animation) along the $t$-axis, i.e., we pick out three slices of a fully three dimensional density plot.

### 5.3.1 Program to plot intensity, intensity contour, quantum potential and quantum potential contour for Einstein's two-pinhole experiment for a $2-D$ XZ Gaussian wave packet

```
> restart;
> with(plots) :

> NSQ := 1.372675283 10^16 :

> b := Pi/3.8 :
>
> R1T:=cos(b)*cos(b) :
>
> R2T:=sin(b)*sin(b) :
>
> X0 := 5·10^-7 :
>
> Z0 := 0 :
>
> h:=6.6260755*10^(-34) :
> hb:=h/(2*Pi) :
> m:=9.10938356*10^(-31) :
> AL := hb/m :

> kx := 1.295698717 ·10^6 :
> kz := 0 :
> ky := 0 :
> OMX := hb * kx^2 / (2 * m) :
> OMZ := hb * kz^2 / (2 * m) :
> Vx:=AL*kx:
> Vz := AL * kz :
>
> DXN0 := 7·10^(-8) :

> DZN0 := DXN0 :
>
> DXP0 := 0.8 · DXN0 :
>
> DZP0 := DXP0 :
```

```
> ANX := (t)->( 2·π / (DXN0^2 + I·AL·t) )^.5 :
> ANZ := (t)->( 2·π / (DZN0^2 + I·AL·t) )^.5 :
> APX := (t)->( 2·π / (DXP0^2 + I·AL·t) )^.5 :
> APZ := (t)->( 2·π / (DZP0^2 + I·AL·t) )^.5 :
> DXNSQ:=(t)->DXN0^2+AL^2*t^2/DXN0^2:
> DXPSQ := (t)->DXP0^2 + AL^2 * t^2/DXP0^2 :
> DZNSQ := (t)->DZN0^2 + AL^2 * t^2/DZN0^2 :
> DZPSQ := (t)->DZP0^2 + AL^2 * t^2/DZP0^2 :
> DXN1SQ:=(t)->DXN0^4+AL^2*t^2:
> DXP1SQ := (t)->DXP0^4 + AL^2 * t^2 :

> DZN1SQ := (t)->DZN0^4 + AL^2 * t^2 :
> DZP1SQ := (t)->DZP0^4 + AL^2 * t^2 :

> S1X := (x,t)-> AL·t·(x + X0 - Vx*t)^2 / (2·DXN1SQ(t)) + kx·(x + X0) + ky·y - OMX·t :
> S1Z := (z,t)-> AL·t·(z + Z0 - Vz*t)^2 / (2·DZN1SQ(t)) + kz·(z + Z0) + ky·y - OMZ·t :
> S2X := (x,t)-> AL·t·(x - X0 + Vx*t)^2 / (2·DXP1SQ(t)) - kx·(x-X0) + ky·y - OMX·t :
> S2Z := (z,t)-> AL·t·(z - Z0 + Vz*t)^2 / (2·DZP1SQ(t)) - kz·(z - Z0) + ky·y - OMZ·t :
> PSI1 := (x,z,t)->exp(-(x + X0 - Vx*t)^2/(2*DXNSQ(t)))*exp(-(z + Z0 - Vz*t)^2/(2
      *DZNSQ(t)))·ANX(t)·ANZ(t)·R1T^2*exp(I·(S1X(x,t) + S1Z(z,t))) :
> PSI2 := (x,z,t)->exp(-(x - X0 + Vx*t)^2/(2*DXPSQ(t)))*exp(-(z - Z0 + Vz*t)^2/(2
      *DZPSQ(t)))·APX(t)·APZ(t)·R2T^2*exp(I·(S2X(x,t) + S2Z(z,t))) :
> RSQ := (x,z,t)->conjugate(PSI1(x,z,t))·PSI1(x,z,t) + conjugate(PSI2(x,z,t))·PSI2(x,z,t)
      + conjugate(PSI1(x,z,t))·PSI2(x,z,t) + conjugate(PSI2(x,z,t))·PSI1(x,z,t) :
> RSQN := (x,z,t)->RSQ(x,z,t)/NSQ :
xxxxxxxxxxxxxxxxxxxxxxxxxx copy end  xxxxxxxxxxxxxxxxxxxxxxxxxxxxxxxxxxxxxxxxxxx
INTENSITY PLOT
> #opts1:=thickness = 2 , numpoints = 10000, lightmodel = light4, axes = frame, orientation = [
      -100, 70, 5], colorscheme = ["Pink", "Blue"], view = [-3.5·10^-6..3.5·10^-6, -3.5·10^-6..3.5
      ·10^-6, 0..1.8·10^11] :
> opts2 := thickness = 2 , numpoints = 10000, lightmodel = light4, axes = frame, orientation = [
```

$$-100,\ 70,\ 5\ ],\ view = [\ -3.5\cdot 10^{-6}..3.5\cdot 10^{-6}, -3.5\cdot 10^{-6}..3.5\cdot 10^{-6}, 0..1.8\cdot 10^{11}\ ]:$$

> #S1 := plots[animate](plot3d, [RSQN(x, z, t), x = 3.5·10^-6..-3.5·10^-6, z = -3.5·10^-6..3.5·10^-6, opts2], t = 0..2.6923076·10^-9, frames = 6)

> #display(S1)

> #display(S1, orientation = [ −90, 90, 0])

**CONTOUR PLOT IS "INT_DEN_B_1"**

> [RSQAY(x, z, y, t), x = -4·10^-6..4·10^-6, z = -4·10^-6..4·10^-6, style = patchnogrid, colour = "Red", axes = frame], t = 0..1.6·10^-9 :

> RSQAY := (x, z, y, t) → RSQ(x, z, t) :

> #Int_den_b_1 := plots[animate](densityplot, [RSQAY(x, z, y, t), x = -4·10^-6..4·10^-6, z = -4·10^-6..4·10^-6, style = patchnogrid, axes = frame, color = "Blue", brightness = 0.7, contrast = 0.7], t = 0..1.6·10^-9, scaling = constrained, frames = 6 )

> #display(Int_den_b_1)

> $$DPSIX := (x, z, t) \rightarrow \left( \frac{-(x + X0 - Vx*t)}{DXNSQ(t)} + I\cdot\left( kx + \frac{AL\cdot t\cdot (x + X0 - Vx*t)}{2\cdot DXN1SQ(t)} \right) \right)\cdot PSI1(x, z, t) + \left( \frac{-(x - X0 + Vx*t)}{DXPSQ(t)} + I\cdot\left( -kx + \frac{AL\cdot t\cdot (x - X0 + Vx*t)}{2\cdot DXP1SQ(t)} \right) \right)\cdot PSI2(x, z, t) :$$

> $$DPSIZ := (x, z, t) \rightarrow \left( \frac{-(z + Z0 - Vz*t)}{DZNSQ(t)} + I\cdot\left( kz + \frac{AL\cdot t\cdot (z + Z0 - Vz*t)}{2\cdot DZN1SQ(t)} \right) \right)\cdot PSI1(x, z, t) + \left( \frac{-(z - Z0 + Vz*t)}{DZPSQ(t)} + I\cdot\left( -kz + \frac{AL\cdot t\cdot (z - Z0 + Vx*t)}{2\cdot DZP1SQ(t)} \right) \right)\cdot PSI2(x, z, t) :$$

> $$DDPSIX := (x, z, t) \rightarrow \left( \left( \frac{-1}{DXNSQ(t)} + I\cdot\left( \frac{AL\cdot t}{DXN1SQ(t)} \right) \right) + \left( \frac{-(x + X0 - Vx*t)}{DXNSQ(t)} + I\cdot\left( kx + \frac{AL\cdot t\cdot (x + X0 - Vx*t)}{2\cdot DXN1SQ(t)} \right) \right)^2 \right)\cdot PSI1(x, z, t) + \left( \left( \frac{-1}{DXPSQ(t)} + I\cdot\left( \frac{AL\cdot t}{DXP1SQ(t)} \right) \right) + \left( \frac{-(x - X0 + Vx*t)}{DXPSQ(t)} + I\cdot\left( -kx + \frac{AL\cdot t\cdot (x - X0 + Vx*t)}{2\cdot DXP1SQ(t)} \right) \right)^2 \right)\cdot PSI2(x, z, t) :$$

> $$DDPSIZ := (x, z, t) \rightarrow \left( \left( \frac{-1}{DZNSQ(t)} + I\cdot\left( \frac{AL\cdot t}{DZN1SQ(t)} \right) \right) + \left( \frac{-(z + Z0 - Vz*t)}{DZNSQ(t)} + I\cdot\left( kz + \frac{AL\cdot t\cdot (z + Z0 - Vz*t)}{2\cdot DZN1SQ(t)} \right) \right)^2 \right)\cdot PSI1(x, z, t) + \left( \left( \frac{-1}{DZPSQ(t)} + I\cdot\left( \frac{AL\cdot t}{DZP1SQ(t)} \right) \right) + \left( \frac{-(z - Z0 + Vz*t)}{DZPSQ(t)} + I\cdot\left( -kz + \frac{AL\cdot t\cdot (z - Z0 + Vz*t)}{2\cdot DZP1SQ(t)} \right) \right)^2 \right)\cdot PSI2(x, z, t) :$$

> PSI := (x, z, t) → PSI1(x, z, t) + PSI2(x, z, t) :

> $$QPX := (x, z, t) \rightarrow -hb^2/(2*m)\cdot\left( \left( \frac{1}{2\cdot conjugate(PSI(x, z, t))}\cdot conjugate(DDPSIX(x, z, t)) + \frac{1}{2\cdot PSI(x, z, t)}\cdot DDPSIX(x, z, t) + \frac{1}{conjugate(PSI(x, z, t))\cdot PSI(x, z, t)} \right.\right.$$

$$\cdot conjugate(DPSIX(x,z,t))\cdot DPSIX(x,z,t)\Big) - \left(\frac{1}{2\cdot conjugate(PSI(x,z,t))}\right.$$
$$\left.\cdot conjugate(DPSIX(x,z,t)) + \frac{1}{2\cdot PSI(x,z,t)}\cdot DPSIX(x,z,t)\right)^2\Big) :$$

> $QPZ := (x,z,t) \rightarrow -hb\text{^}2/(2*m)\cdot\left(\left(\frac{1}{2\cdot conjugate(PSI(x,z,t))}\cdot conjugate(DDPSIZ(x,z,t))\right.\right.$
$$+ \frac{1}{2\cdot PSI(x,z,t)}\cdot DDPSIZ(x,z,t) + \frac{1}{conjugate(PSI(x,z,t))\cdot PSI(x,z,t)}$$
$$\cdot conjugate(DPSIZ(x,z,t))\cdot DPSIZ(x,z,t)\Big) - \left(\frac{1}{2\cdot conjugate(PSI(x,z,t))}\right.$$
$$\left.\left.\cdot conjugate(DPSIZ(x,z,t)) + \frac{1}{2\cdot PSI(x,z,t)}\cdot DPSIZ(x,z,t)\right)^2\right) :$$

> $QP := (x,z,t) \rightarrow QPX(x,z,t) + QPZ(x,z,t) :$

**QUANTUM POTENTIAL PLOT**

> $\#optsk1 := thickness = 2,\ numpoints = 10000,\ lightmodel = light4,\ axes = frame,\ orientation = [-100, 70, 5],\ colorscheme = ["Red", "White"],\ view = [-3.5\cdot10^{-6}..3.5\cdot10^{-6}, -3.5\cdot10^{-6}..3.5\cdot10^{-6}, -1\cdot10^{-22}..1\cdot10^{-23}] :$

> $optsk1 := thickness = 2,\ numpoints = 10000,\ lightmodel = light4,\ axes = frame,\ orientation = [-100, 70, 5],\ view = [-3.5\cdot10^{-6}..3.5\cdot10^{-6}, -3.5\cdot10^{-6}..3.5\cdot10^{-6}, -1.5\cdot10^{-22}..1\cdot10^{-23}] :$

> $\#k1 := plots[animate](plot3d, [QP(x,z,t),\ x = -3.5\cdot10^{-6}..3.5\cdot10^{-6},\ z = -3.5\cdot10^{-6}..3.5\cdot10^{-6}, optsk1],\ t = 0..2.6923076\cdot10^{-9}, frames = 6)$

> $\#display(k1)$

> $\#display(k1, orientation = [-90, 90, 0])$

>

**CONTOUR PLOT "QP_CON_FR_NC_1"**

> $QPY := (x,z,y,t) \rightarrow QP(x,z,t) :$

> $\#QP\_con\_fr\_nc\_1 := plots[animate](contourplot, [QPY(x,z,y,t),\ x = -3\cdot10^{-6}..3\cdot10^{-6},\ z = -3\cdot10^{-6}..3\cdot10^{-6}, style = patchnogrid, axes = frame, color = "Blue"],\ t = 0..1.6\cdot10^{-9}, scaling = constrained,\ frames = 6)$

> $\#QP\_con\_fr\_nc\_1 := plots[animate](contourplot, [QPY(x,z,y,t),\ x = -3\cdot10^{-6}..3\cdot10^{-6},\ z = -3\cdot10^{-6}..3\cdot10^{-6}, filledregions = true, axes = frame], t = 0..1.6\cdot10^{-9}, scaling = constrained, frames = 6)$

> $\#QP\_con\_fr\_nc\_1 := plots[animate](contourplot, [QPY(x,z,t),\ x = -3.5\cdot10^{-6}..3.5\cdot10^{-6},\ z = -3.5\cdot10^{-6}..3.5\cdot10^{-6}, optsQP\_con\_fr\_nc\_1],\ t = 0..2.6923076\cdot10^{-9}, frames = 6)$

> $\#display(QP\_con\_fr\_nc\_1)$

>

### 5.3.2 Intensity plots

#### EWEA

The animation sequence for the intensity for EWEA is shown in Figure 5.1.

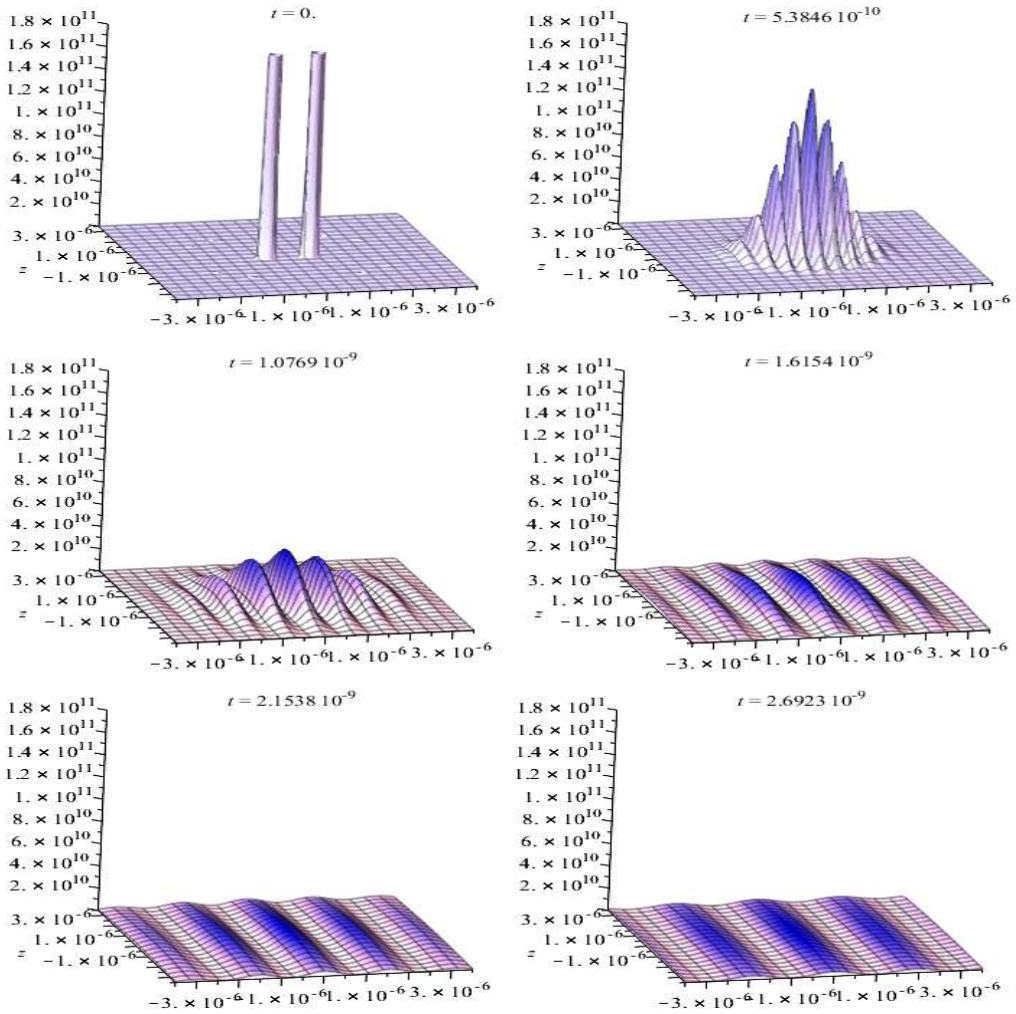


Figure 5.1: *Maple 2015 electron intensity plot in Einstein's two-pinhole interference experiment with EWEA modeled by* $2-D$ *Gaussian wave packets. The angle* $b = \frac{\pi}{4}$

The animation ranges are $x = -3.5 \times 10^{-6}$ to $3.5 \times 10^{-6}\, m$, $z = -3.5 \times 10^{-6}$ to $3.5 \times 10^{-6}\, m$, $R^2 = 0$ to $1.8 \times 10^{11}\, Jm^{-2}s^{-1}$ and $t = 0$ to $2.6923 \times 10^{-9}\, s$. The orientation of the figure is $\theta = -100°$, $\varphi = 70°$ and $\psi = 5°$. The plots show the time evolution of the intensity in the $xz$-plane. The first frame ($t = 0\, s$) shows the Gaussian peaks at the two pinholes. Frames two ($t = 5.3846 \times 10^{-10}\, s$) and three ($t = 1.0769 \times 10^{-9}\, s$) show the spreading Gaussian packets beginning to overlap and also show the beginning of the formation of interference fringes. Frames four ($t = 1.6154 \times 10^{-9}\, s$) to five ($t = 2.1538 \times 10^{-9}\, s$) show the time evolution of distinct interference fringes. The sixth frame ($t = 2.6923 \times 10^{-9}\, s$) shows a fully formed interference pattern.

By changing the orientation of Figure 5.1 to Figure 5.2 with $\theta = -90°$, $\varphi = 90°$ and $\psi = 0°$, it becomes easy to make an approximate calculation of the visibility (V) of the central fringe by taking readings from 'face-on' plots. In fact, a quantitative formulation for which-way detection has been developed on the basis of theoretical [34] and experimental [35] investigations of BPC during the past two decades, leading to a wave-particle duality relation covering both sharp and intermediate stages expressed as

$$V^2 + K^2 \leq 1 \tag{5.33}$$

where the two complementary measurements are $0 \leq V \leq 1$, the visibility or contrast of the interference pattern and $0 \leq K \leq 1$ the which-way knowledge corresponding to which-way information. The visibility is given by

$$V = \frac{I_{max} - I_{min}}{I_{max} + I_{min}} \tag{5.34}$$

where $I_{max}$ is the maximum intensity of a bright fringe and $I_{min}$ is the minimum intensity of the adjacent dark fringe.

Therefore by considering the sixth frame of Figure 5.2, we see that the maximum intensity $I_{max} = 1 \times 10^{10}\, Jm^{-2}s^{-1}$ and the minimum intensity $I_{min} = 0\, Jm^{-2}s^{-1}$. By calculating the visibility using equation (5.34) we obtain $V_{EWEA} = 1$. Thus from equation (5.33) we obtain $K = 0$, meaning that the fringes are perfectly visible (sharp wave-like behavior) and we do not have any information about it.

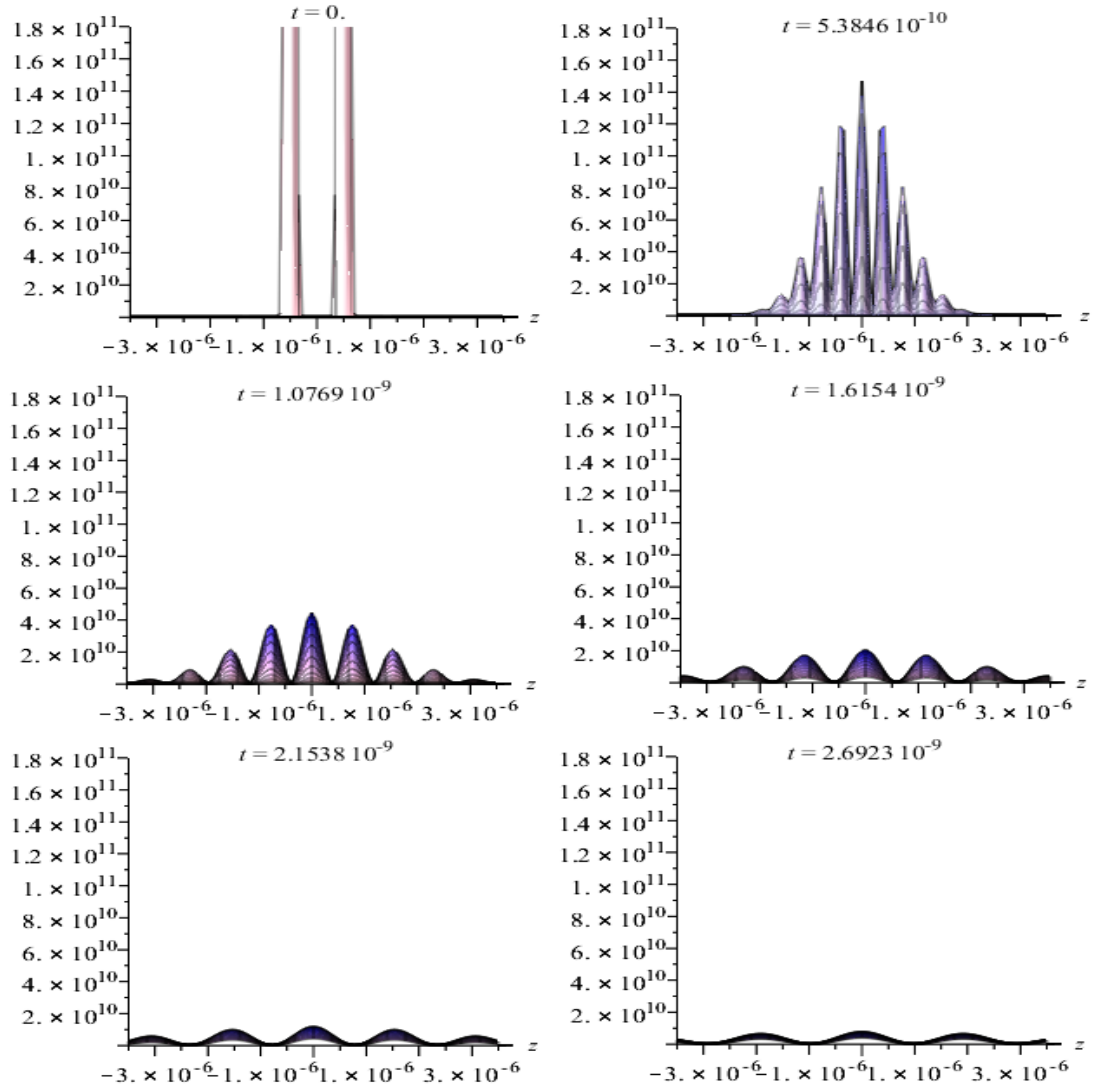


Figure 5.2: *Maple 2015 electron intensity plot in Einstein's two-pinhole interference experiment with EWEA modeled by* $2-D$ *Gaussian wave packets, but with different orientation.*

**EWUA**

The animation sequence for the intensity for EWUA is shown in Figure 5.3.

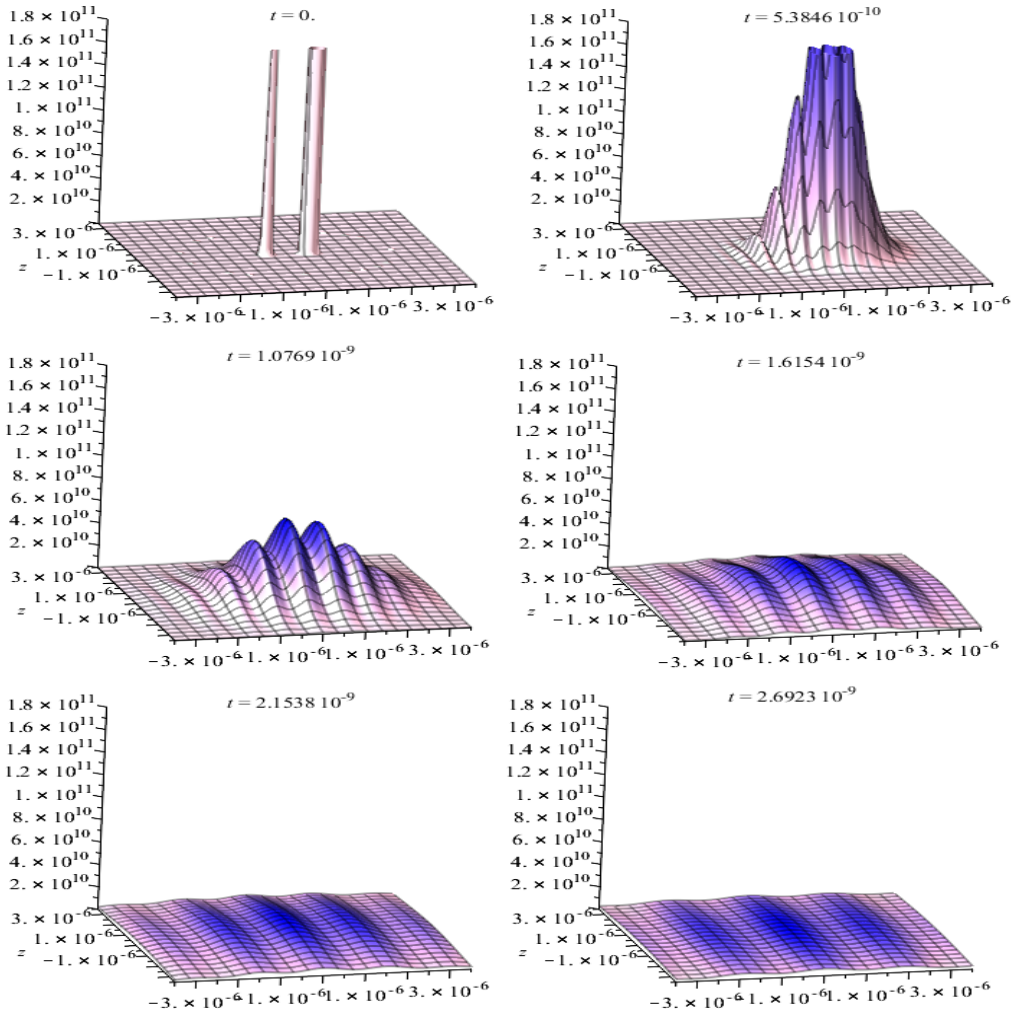


Figure 5.3: *Maple 2015 electron intensity plot in Einstein's two-pinhole interference experiment with EWUA modeled by* $2-D$ *Gaussian wave packets. The angle* $b = \frac{\pi}{3}$

The animation ranges are $x = -3.5 \times 10^{-6}$ to $3.5 \times 10^{-6}\ m$, $z = -3.5 \times 10^{-6}$ to $3.5 \times 10^{-6}\ m$, $R^2 = 0$ to $1.8 \times 10^{11}\ Jm^{-2}s^{-1}$ and $t = 0$ to $2.6923 \times 10^{-9}\ s$. The orientation of the figure is $\theta = -100°$, $\varphi = 70°$ and $\psi = 5°$. By choosing the angle $b = \frac{\pi}{3}$ we have increased in the intensity through the first pinhole $(+x_0)$ from $\frac{1}{2}$ to $\frac{3}{4}$ and a reduction in the intensity at the second pinhole $(-x_0)$ from $\frac{1}{2}$ to $\frac{1}{4}$. We observe from Figure 5.3 that as the Gaussian wave-packets begin to combine to form a single peak envelope with interference fringes beginning to form, the intensity peak is shifted toward the larger intensity (the first pinhole $(+x_0)$). This shift becomes less pronounced, almost disappearing, as the interference fringes become more distinct as in the last frame.

By considering the sixth frame of Figure 5.4 as previously, we see that the maximum intensity $I_{max} = 9 \times 10^{10}\ Jm^{-2}s^{-1}$ and the minimum intensity $I_{min} = 4 \times 10^{10}\ Jm^{-2}s^{-1}$. The visibility hence becomes after calculation $V_{EWUA} = 0.4 < V_{EWEA}$. Thus we see that fringe visibility $V_{EWUA}$ is reduced.

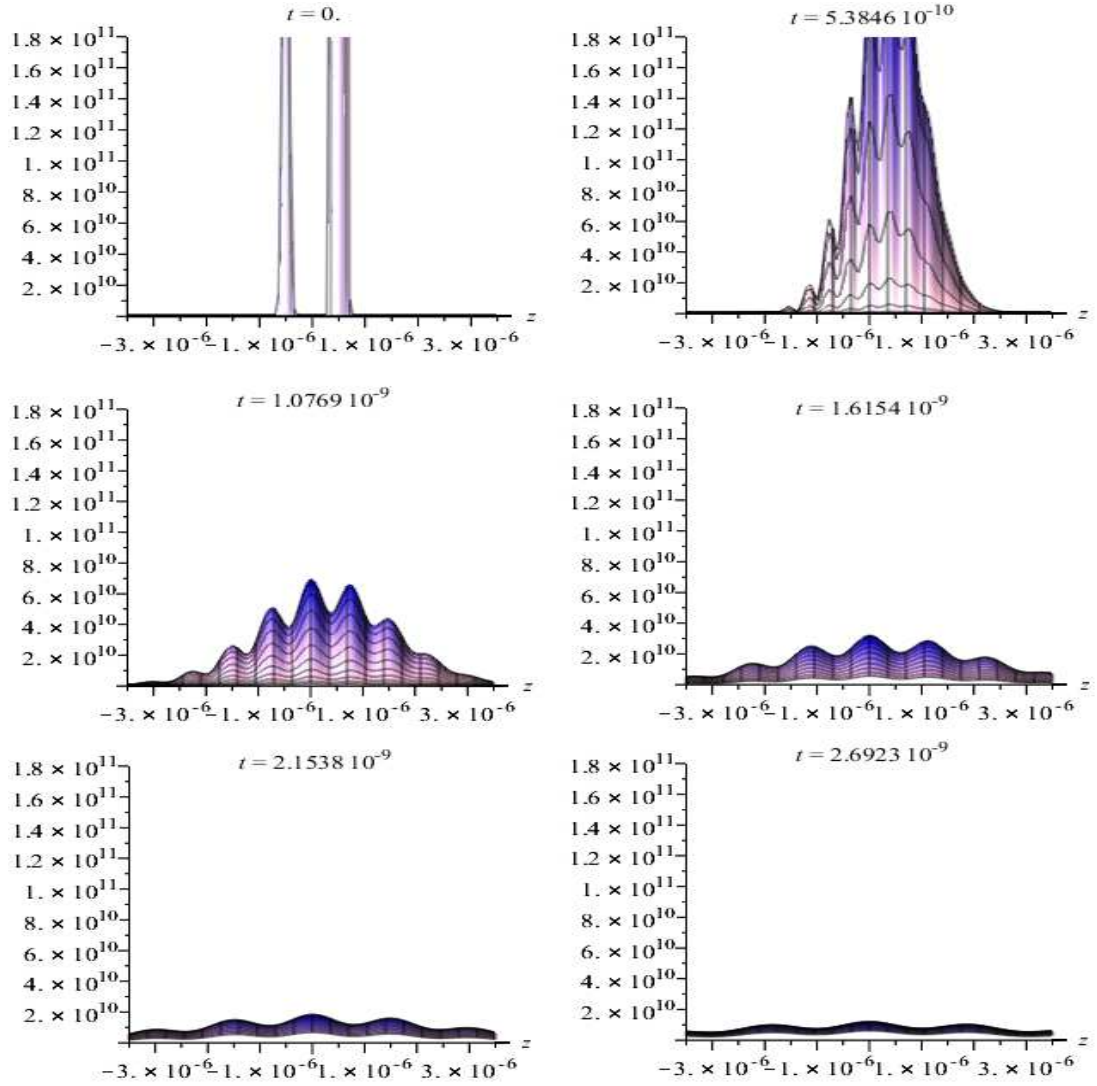


Figure 5.4: *Maple 2015 electron intensity plot in Einstein's two-pinhole interference experiment with EWUA modeled by* $2-D$ *Gaussian wave packets, but with different orientation.*

**UWEA**

The animation sequence for the intensity for UWEA is shown in Figure 5.5.

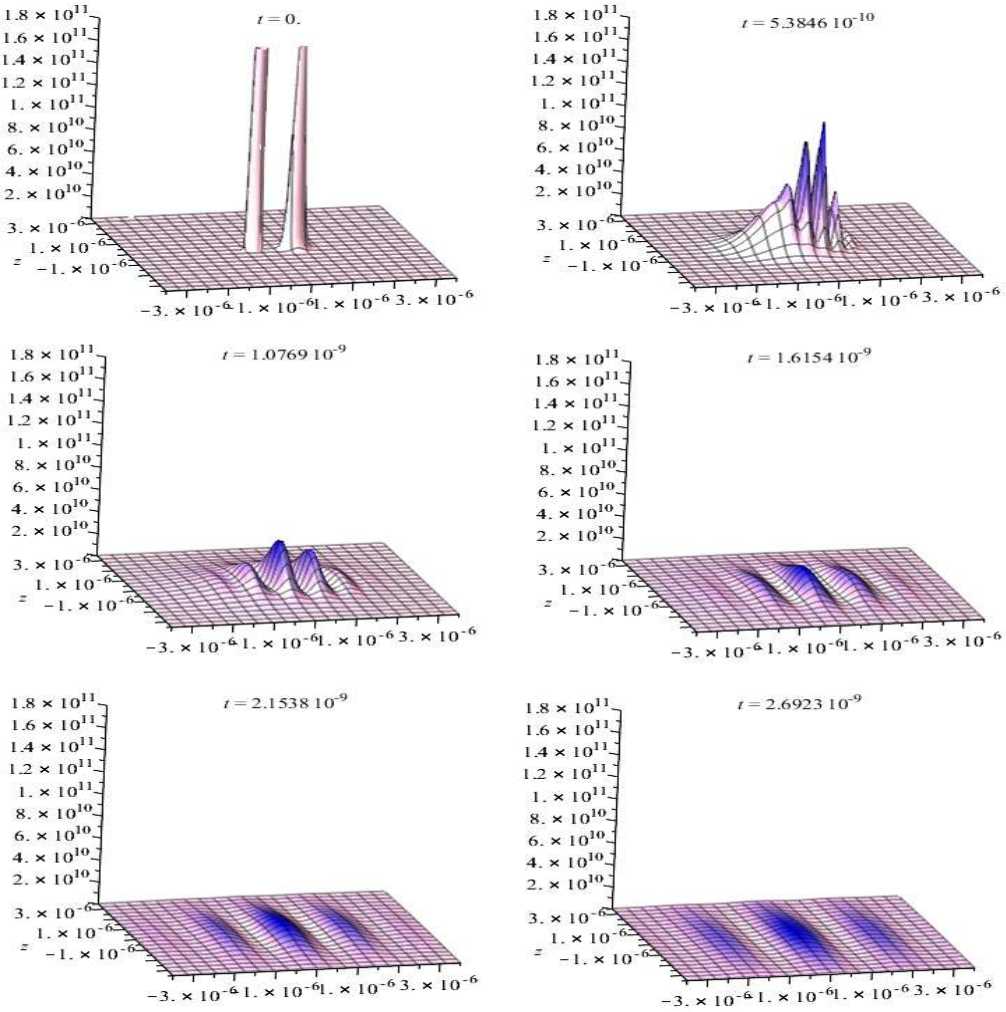


Figure 5.5: *Maple 2015 electron intensity plot in Einstein's two-pinhole interference experiment with UWEA modeled by* $2-D$ *Gaussian wave packets. The width* $\Delta x_{P0} = 2.4\Delta x_{N0}$

The animation ranges are $x = -3.5 \times 10^{-6}$ to $3.5 \times 10^{-6}\ m$, $z = -3.5 \times 10^{-6}$ to $3.5 \times 10^{-6}\ m$, $R^2 = 0$ to $1.8 \times 10^{11}\ Jm^{-2}s^{-1}$ and $t = 0$ to $2.6923 \times 10^{-9}\ s$. The orientation of the figure is $\theta = -100°$, $\varphi = 70°$ and $\psi = 5°$. We note that the width of the $+x_0$ Gaussian wave-packet is 2.4 times that of the $-x_0$ Gaussian wave-packet. The first frame clearly shows the narrower $-x_0$ wave-packet. A narrower wave-packet spreads more rapidly than a wider packet, as seen in the second frame. The more rapid spread of the narrower wave-packet results in the wave-packets beginning to overlap on $+x$-side, as is shown in the second frame. As the wave-packets spread, the interference pattern becomes ever more distinct. Though becoming a little more symmetrical about $x = 0$, the fringe pattern is shifted toward the $+x$-side, with the fringes on the $+x$-side being slightly more pronounced.

The visibility of the central fringe for this case can be calculated by considering the sixth frame of Figure 5.6 with the maximum intensity $I_{max} = 0.8 \times 10^{10}\ Jm^{-2}s^{-1}$ and the minimum intensity $I_{min} = 0.1 \times 10^{10}\ Jm^{-2}s^{-1}$. The visibility hence becomes after calculation $V_{EWUA} = 0.7 < V_{EWEA}$. We see that the visibility is less than in the EWEA case, but greater than in the EWUA case.

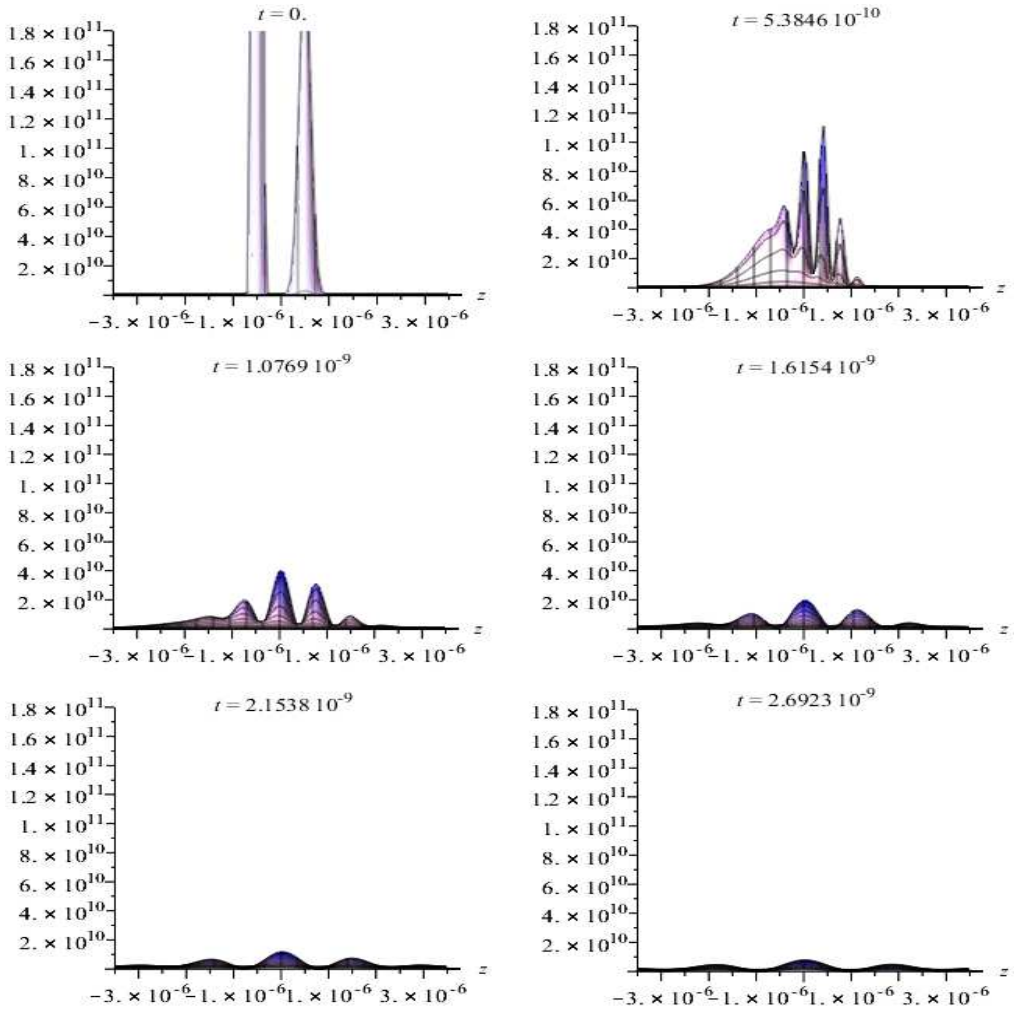


Figure 5.6: *Maple 2015 electron intensity plot in Einstein's two-pinhole interference experiment with UWEA modeled by* $2-D$ *Gaussian wave packets, but with different orientation.*

**UWUA**

The animation sequence for the intensity for UWUA is shown in Figure 5.7.

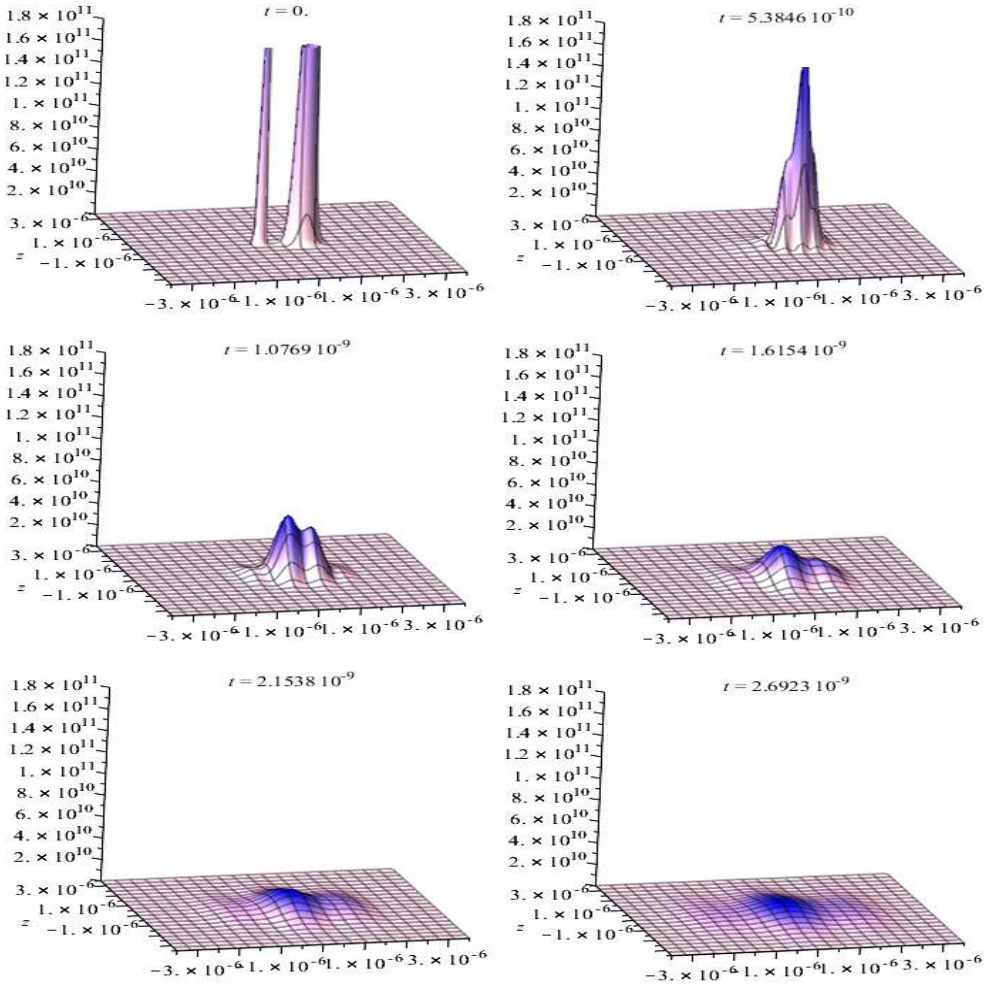


Figure 5.7: *Maple 2015 electron intensity plot in Einstein's two-pinhole interference experiment with UWUA modeled by* $2-D$ *Gaussian wave packets.* $b = \frac{\pi}{3}$ *and* $\Delta x_{P0} = 3\Delta x_{N0}$

The animation ranges are $x = -3.5 \times 10^{-6}$ to $3.5 \times 10^{-6}\, m$, $z = -3.5 \times 10^{-6}$ to $3.5 \times 10^{-6}\, m$, $R^2 = 0$ to $1.8 \times 10^{11}\, Jm^{-2}s^{-1}$ and $t = 0$ to $2.6923 \times 10^{-9}\, s$. The orientation of the figure is $\theta = -100°$, $\varphi = 70°$ and $\psi = 5°$. We note that the width of the $+x_0$ Gaussian wave-packet is 3 times that of the $-x_0$ Gaussian wave-packet and By choosing the angle $b = \frac{\pi}{3}$ we have increased in the intensity through the first pinhole $(+x_0)$ from $\frac{1}{2}$ to $\frac{3}{4}$. We observe from Figure 5.7 that from the first to the sixth frame there is reduction in interference. This reduction in interference is interpreted as in the classical case in terms of wave profiles with reduced coherence. The reduction of interference for this case is attributed to partial particle behaviour and partial wave-behaviour. The partial particle behaviour is attributed to the increase in knowledge of the electrons path in the sense that an electron it is more likely to pass through the larger pinhole or the pinhole with the larger intensity.

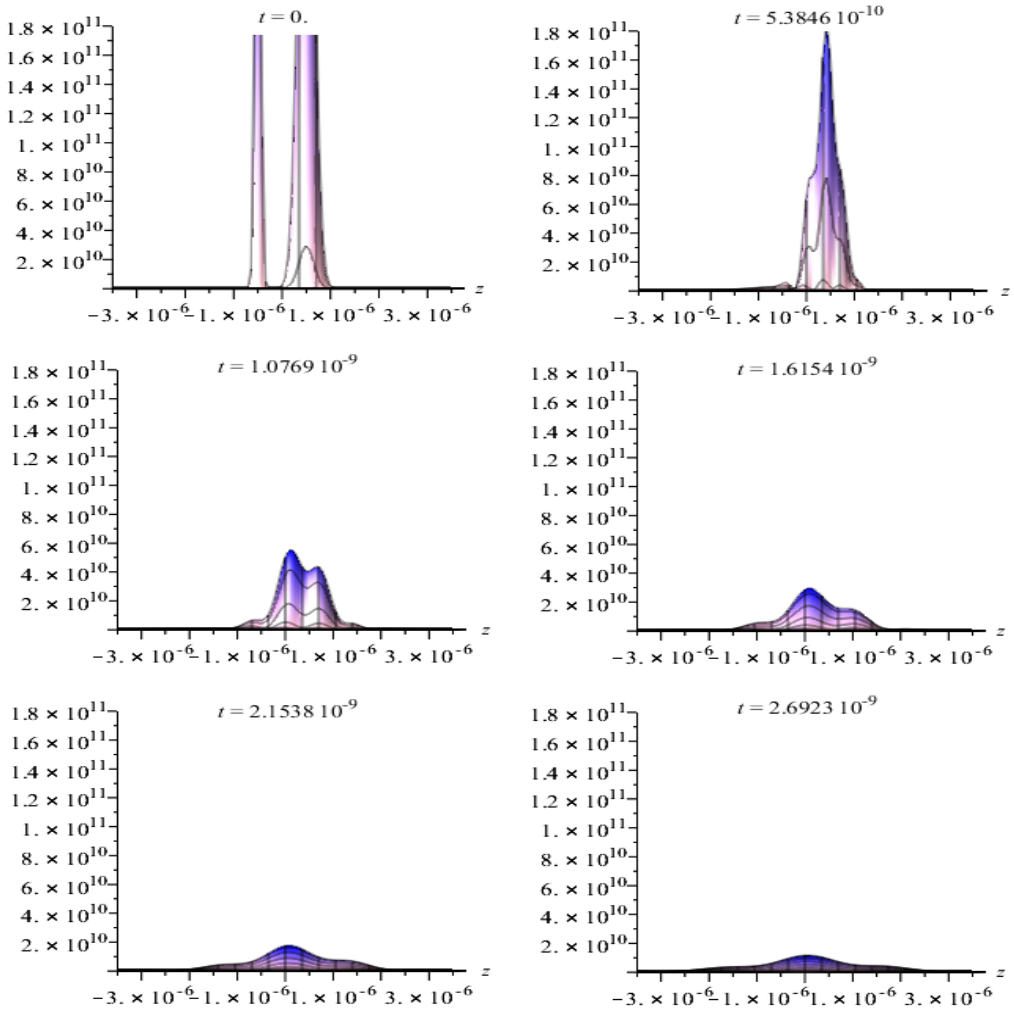


Figure 5.8: *Maple 2015 electron intensity plot in Einstein's two-pinhole interference experiment with UWUA modeled by* $2-D$ *Gaussian wave packets, but with different orientation.*

**Note**

We may note that the peak intensity for the UWEA case (see Figure (5.5)) is greater than the peak intensities for the EWEA (see Figure (5.1)), the EWUA (see Figure (5.3)) and the UWUA (see Figure (5.7)) cases. The smallest peak intensity is the UWUA case. This is because the normalization factor for the wavefunction $\Psi$ is different for each case, with that for the UWEA case being the least, resulting in the largest peak intensity. However the peak intensity is not the indicator of fringe visibility so that the fringe visibility for the UWEA case, calculated by the formula is less than for the EWEA case,as expected.

### 5.3.3 Quantum Potential Plots

#### EWEA

The animation sequence for the quantum potential for EWEA is shown in Figure 5.9.

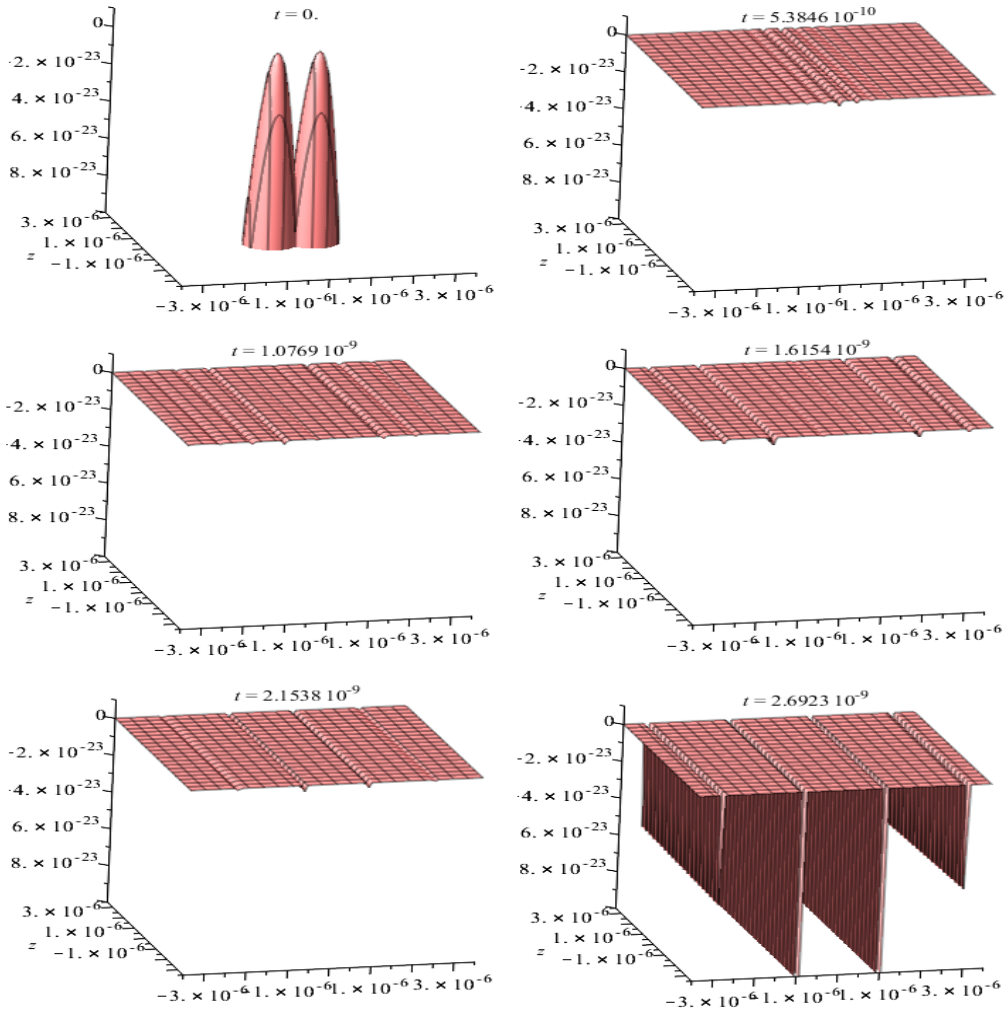


Figure 5.9: *Maple 2015 electron quantum potential in Einstein's two-pinhole experiment in* $2-D$ *for EWEA.*

The animation sequence for the quantum potential for EWEA is shown in Figure 5.9. The animation ranges are $x = -3.5 \times 10^{-6}$ to $3.5 \times 10^{-6}\, m$, $z = -3.5 \times 10^{-6}$ to $3.5 \times 10^{-6}\, m$, $Q = -10 \times 10^{-23}\, J$ to $0\, J$ and $t = 0$ to $2.6923 \times 10^{-9}\, s$. The orientation of the figure is $\theta = -100°$, $\varphi = 70°$ and $\psi = 5°$. The first frame shows that the quantum potential is restricted to the width of the two pinholes. The second frame shows the beginning of the formation of quantum potential plateaus and valleys corresponding to the beginning of the overlap of the Gaussian wave packets. Subsequent frames show the continued widening of the plateaus and the deepening of the valleys. The final frame, as mentioned, shows clear plateau and valley formation. The gradient of the quantum potential gives rise to a quantum force. Where the gradient is zero, as on the flat plateaus, the quantum force is zero and electrons progress along their trajectory to a bright fringe on the detecting screen unhindered. At the edges of the plateaus the quantum potential slopes steeply down to the valleys. The steep gradient of these slopes gives rise to a large quantum force that pushes particles with trajectories along these slopes to adjacent plateaus, after which they proceed unhindered to a bright fringe on the detecting screen. In this way, the quantum potential guides the electrons to the bright fringes and prevents electrons reaching the dark fringes.

**EWUA**

The animation sequence for the quantum potential for EWUA is shown in Figure 5.10.

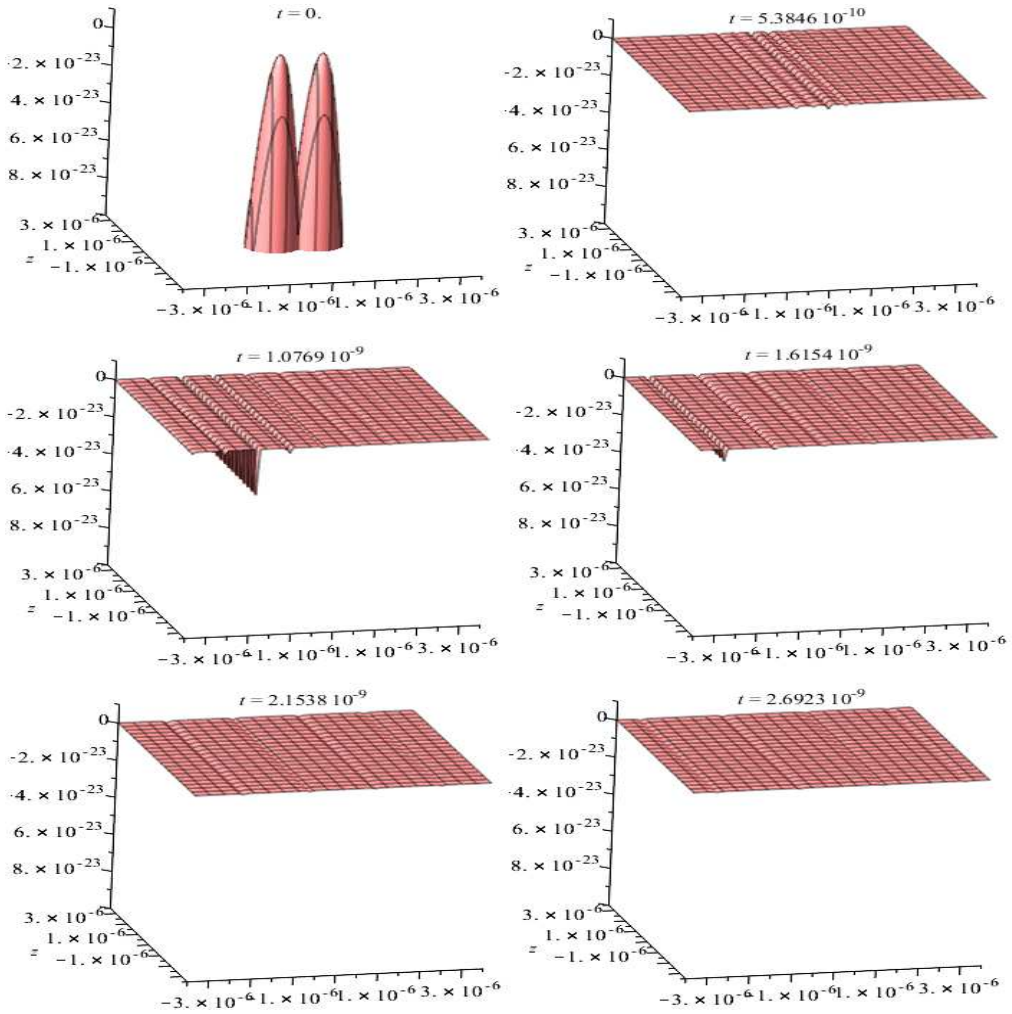


Figure 5.10: *Maple 2015 electron quantum potential in Einstein's two-pinhole experiment in* $2-D$ *for EWUA. The angle* $b = \dfrac{\pi}{3.8}$

The animation sequence for the quantum potential for EWUA is shown in Figure 5.10. The animation ranges are $x = -3.5 \times 10^{-6}$ to $3.5 \times 10^{-6}\, m$, $z = -3.5 \times 10^{-6}$ to $3.5 \times 10^{-6}\, m$, $Q = -10 \times 10^{-23}\, J$ to $0\, J$ and $t = 0$ to $2.6923 \times 10^{-9}\, s$. The orientation of the figure is $\theta = -100°$, $\varphi = 70°$ and $\psi = 5°$. The quantum potential in the early frames peaks on the side of the lower intensity $-x_0$-pinhole. This behaviour is most pronounced in frames two and three. As the peaks and valleys become more pronounced, the envelope peak spreads and flattens as shown in frames 5 and 6. However, the valleys on the side of the lower intensity $-x_0$-pinhole are deeper. The gradient of quantum potential sloping down to the deeper valleys is greater giving rise to a stronger quantum force. This results in the formation of more distinct fringes on the side of the lower intensity pinhole.

**UWEA**

The animation sequence for the quantum potential for UWEA is shown in Figure 5.11.

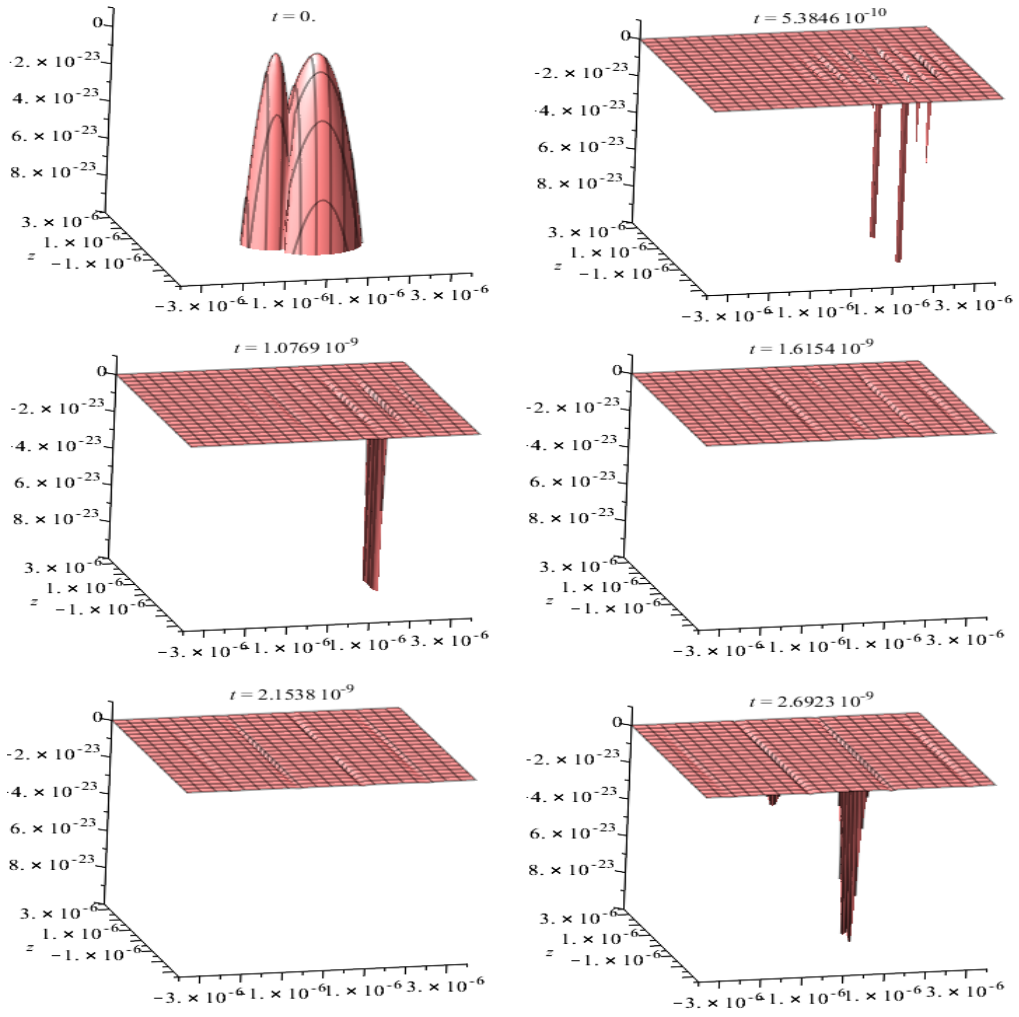


Figure 5.11: *Maple 2015 electron quantum potential in Einstein's two-pinhole experiment in* $2-D$ *for UWEA. The width* $\Delta x_{P0} = 1.4\Delta x_{N0}$

The animation sequence for the quantum potential for UWEA is shown in Figure 5.11. The animation ranges are $x = -3.5 \times 10^{-6}$ to $3.5 \times 10^{-6}$ $m$, $z = -3.5 \times 10^{-6}$ to $3.5 \times 10^{-6}$ $m$, $Q = -10 \times 10^{-23}$ $J$ to $0$ $J$ and $t = 0$ to $2.6923 \times 10^{-9}$ $s$. The orientation of the figure is $\theta = -100°$, $\varphi = 70°$ and $\psi = 5°$. The first frame shows the difference in size of the pinholes, while the second frame shows the more rapid spread of the narrower wave-packet. The overlap of the wave-packets, as for the intensity, begins on the $+x$-side, as does the formation of plateaus and valleys. Subsequent frames show the skewed formation to the $+x$-side of plateaus and valleys. The shift to the $+x$-side is maintained even in the last frame, even though the pattern looks more symmetrical. This can be seen by noticing that in the last frame there are three quantum potential peaks on the $+x$-side, compared to two peaks on the $-x$-side.

**UWUA**

The animation sequence for the quantum potential for UWUA is shown in Figure 5.12.

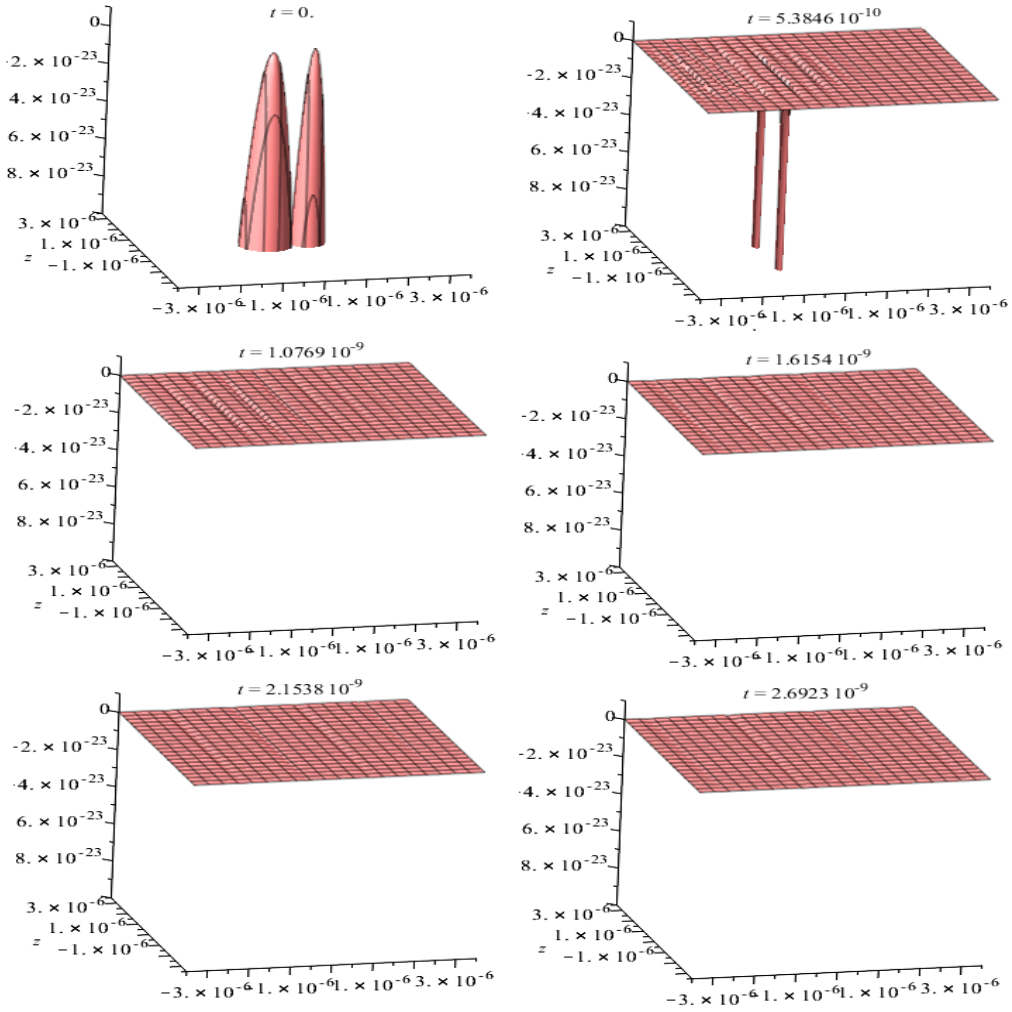


Figure 5.12: *Maple 2015 electron quantum potential in Einstein's two-pinhole experiment in* $2-D$ *for UWUA. The angle* $b = \dfrac{\pi}{3.8}$ *and The width* $\Delta x_{P0} = 0.8\Delta x_{N0}$

The animation sequence for the quantum potential for UWUA is shown in Figure 5.12. The animation ranges are $x = -3.5 \times 10^{-6}$ to $3.5 \times 10^{-6}\ m$, $z = -3.5 \times 10^{-6}$ to $3.5 \times 10^{-6}\ m$, $Q = -10 \times 10^{-23}\ J$ to $0\ J$ and $t = 0$ to $2.6923 \times 10^{-9}\ s$. We note that the width of the $+x_0$ Gaussian wave-packet is 0.8 times that of the $-x_0$ Gaussian wave-packet and the angle $b = \dfrac{\pi}{3.8}$. We observe from Figure 5.12 that from the first to the sixth frame there is reduction in interference. This reduction of interference is attributed to partial particle behaviour and partial wave-behaviour.

### 5.3.4 Intensity Contour Plots or Density Plot of the Intensity

#### EWEA

A sequence of density plots (3 slices of a $3D$-plot) of the intensity for EWEA is shown in Figure 5.13. The plot ranges are $x = -4 \times 10^{-6}$ to $4 \times 10^{-6}\ m$, $z = -4 \times 10^{-6}$ to $4 \times 10^{-6}\ m$ and $t = 0\ s$ to $1.6000 * 10^{-9}\ m\ s$. The first $xz$-slice shows the high intensity emerging from the two pinholes, the middle $xz$-slice shows the beginning of the formation of interference as the Gaussian packets begin to overlap, while the final $xz$-slice shows a fully formed interference pattern.

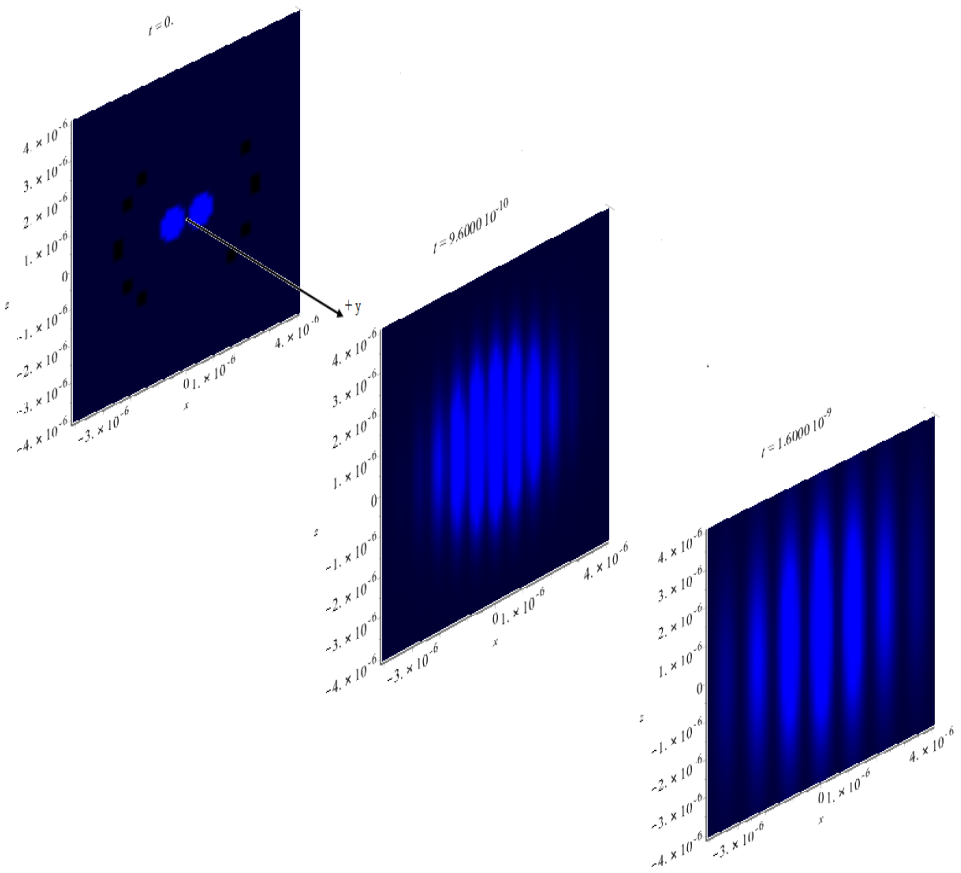


Figure 5.13: *A sequence of density plots (3 slices of a 3D-plot) of the intensity in a two-pinhole interference experiment with EWEA modeled by* $2-D$ *Gaussian wave-packets.*

**EWUA**

A sequence of density plots (3 slices of a 3D-plot) of the intensity for EWUA is shown in Figure 5.14. The plot ranges are $x = -4 \times 10^{-6}$ to $4 \times 10^{-6}$ $m$, $z = -4 \times 10^{-6}$ to $4 \times 10^{-6}$ $m$ and $t = 0$ to $1.6000 * 10^{-9}$ $s$. The intensity is reduced by noticing that the dark bands are not as distinct as for the EWEA case.

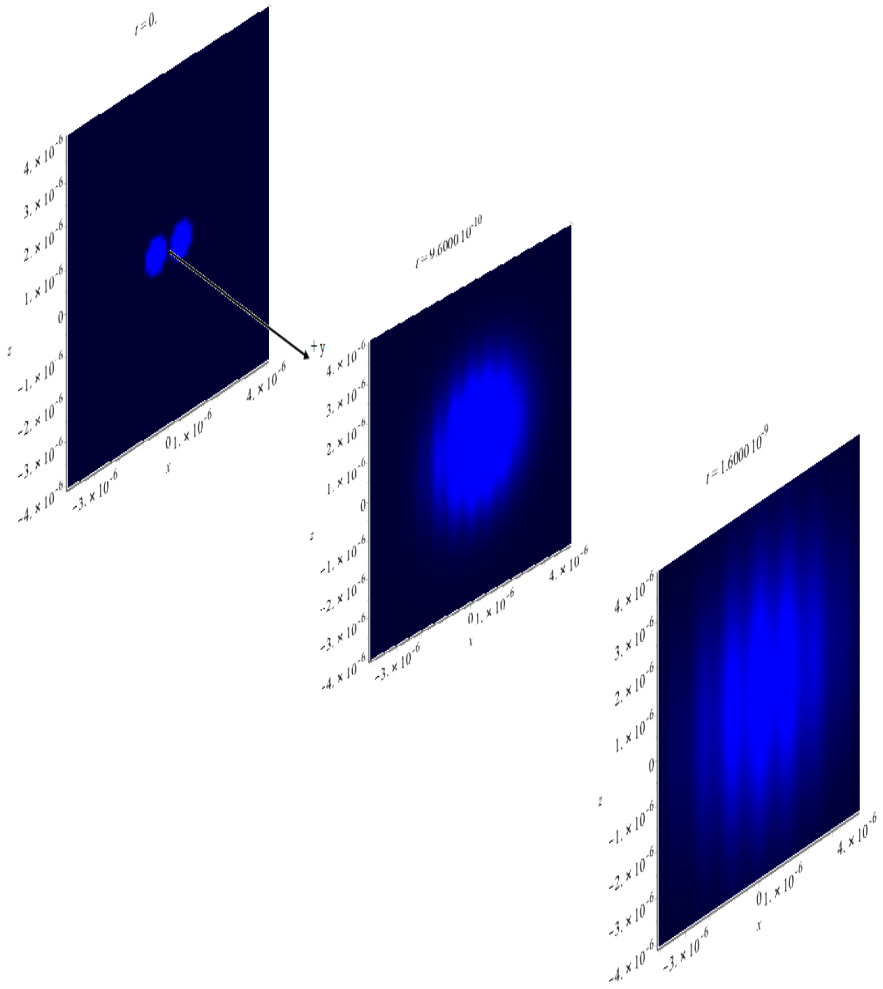

Figure 5.14: *A sequence of density plots (3 slices of a 3D-plot) of the intensity in a two-pinhole interference experiment with EWUA modeled by* $2-D$ *Gaussian wave-packets.*

**UWEA**

A sequence of density plots (3 slices of a 3D-plot) of the intensity for UWEA is shown in Figure 5.15. The plot ranges are $x = -4 \times 10^{-6}$ to $4 \times 10^{-6}$ $m$, $z = -4 \times 10^{-6}$ to $4 \times 10^{-6}$ $m$ and $t = 0$ $s$ to $1.6000 * 10^{-9}$ $s$. The first slice clearly shows the difference in the size of the pinholes, while the second slice shows interference fringes beginning to form on the $+x$-side. The final slice shows that the interference pattern develops into a more symmetric form, though still shifted more to the $+x$-side. The dark bands are less distinct than in the EWEA case, reflecting the reduction in fringe visibility for this case.

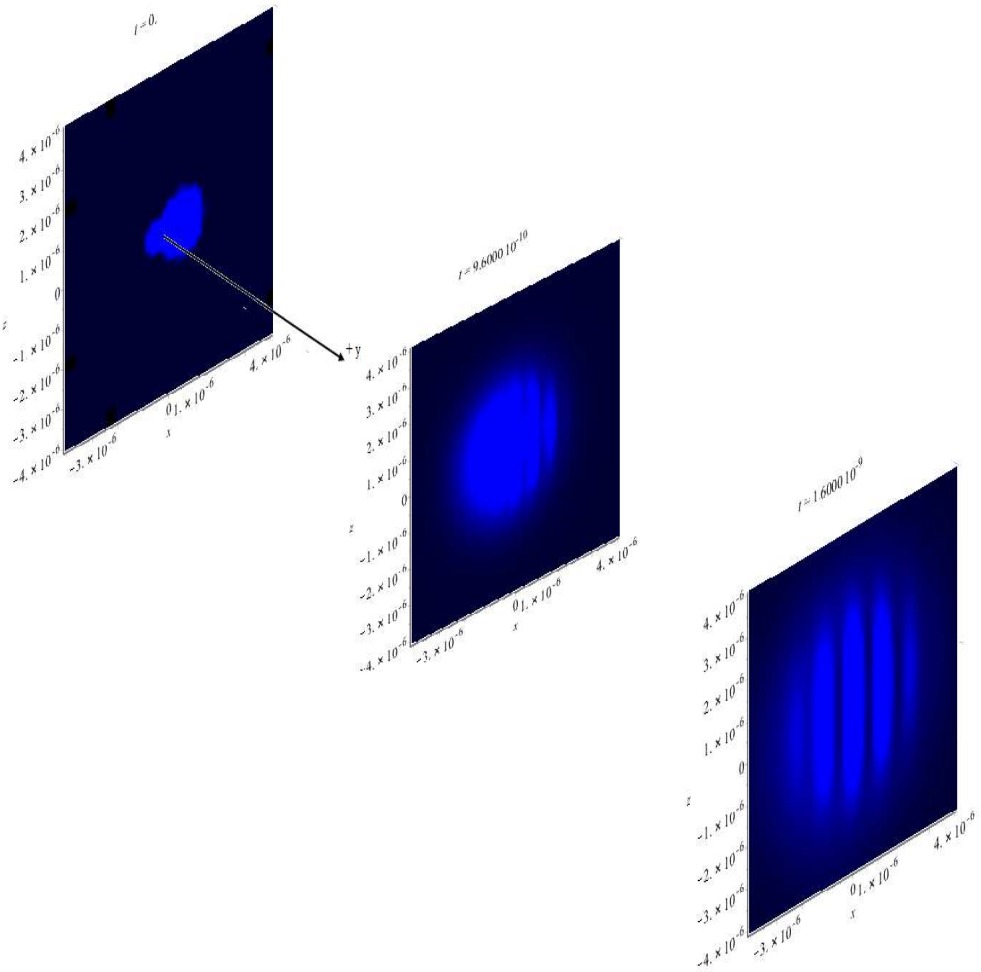

Figure 5.15: *A sequence of density plots (3 slices of a 3D-plot) of the intensity in a two-pinhole interference experiment with UWEA modeled by* $2 - D$ *Gaussian wave-packets.*

**UWUA**

A sequence of density plots (3 slices of a 3D-plot) of the intensity for UWUA is shown in Figure 5.16. The plot ranges are $x = -4 \times 10^{-6}$ to $4 \times 10^{-6}$ $m$, $z = -4 \times 10^{-6}$ to $4 \times 10^{-6}$ $m$ and $t = 0s$ to $1.6000 * 10^{-9}$ $s$. The intensity is reduced by noticing that the dark bands are not distinct.

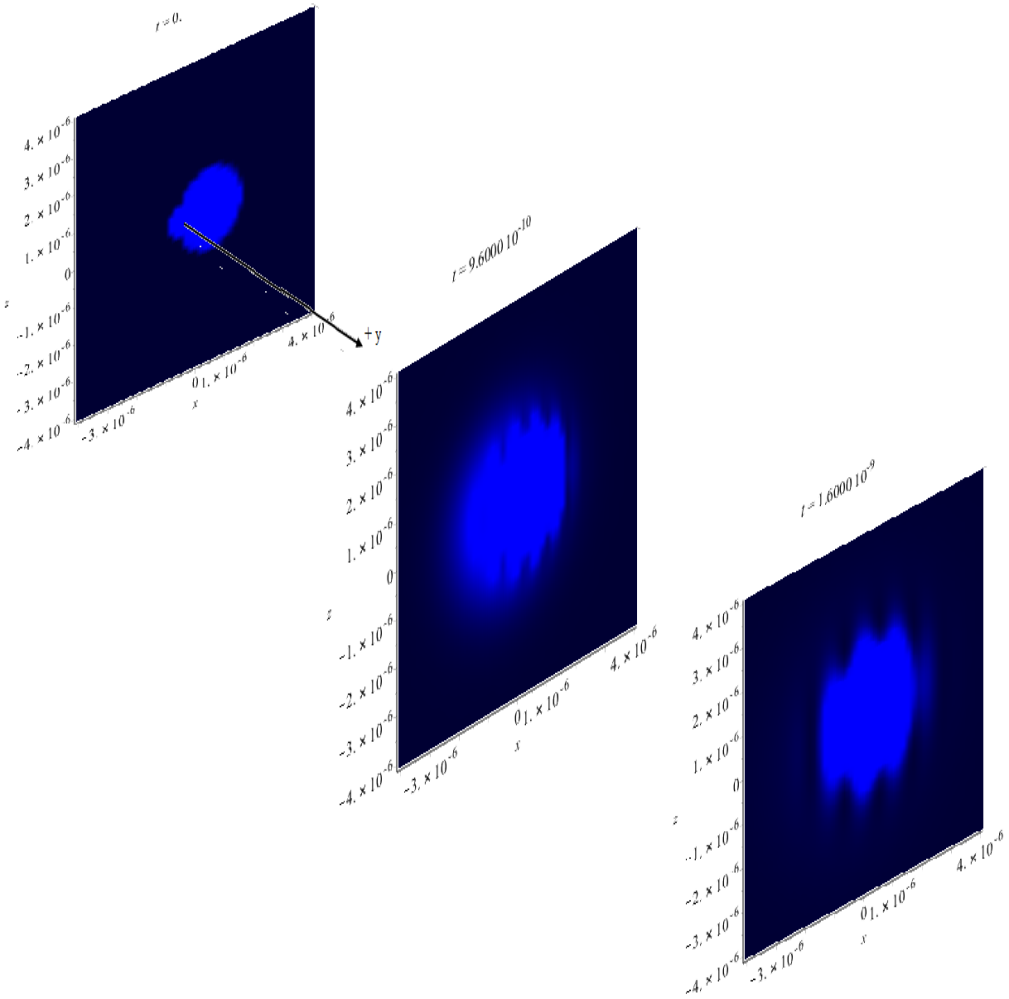


Figure 5.16: *A sequence of density plots (3 slices of a 3D-plot) of the intensity in a two-pinhole interference experiment with UWUA modeled by* $2 - D$ *Gaussian wave-packets.*

### 5.3.5 Quantum Potential Contour plots or Density Plot of the Quantum Potential

**EWEA**

A sequence of density plots (3 slices of a $3D$-plot) of the quantum potential for EWEA is shown in Figure 5.17. The plot ranges are $x = -3 \times 10^{-6}$ to $3 \times 10^{-6}\, m$, $z = -3 \times 10^{-6}$ to $3 \times 10^{-6}\, m$ and $t = 0\, s$ to $1.6000 * 10^{-9}\, s$. When producing the density animation we found that part of the image in the $t = \ 0s$ frame was missing, hence, we have left out this frame, beginning instead with the $t = 3 \times 10^{-10}\, s$ frame. The reason for the missing image is not clear, but is most likely due to the density plotting algorithm not handling difficult numbers very well, unlike the $3-D$ plotting algorithm. The first slice shows the beginning of the overlap of the Gaussian packets and the beginning of plateau and valley formation. The middle slice shows the more developed plateaus and valleys, while the final slice shows distinct plateaus and valleys. The wide bright blue bands indicate the quantum potential plateaus where the quantum force is zero. The narrower dark bands show the quantum potential sloping down to the valleys, slopes were electrons experience a strong quantum force. The darker the bands the steeper the quantum potential slopes.

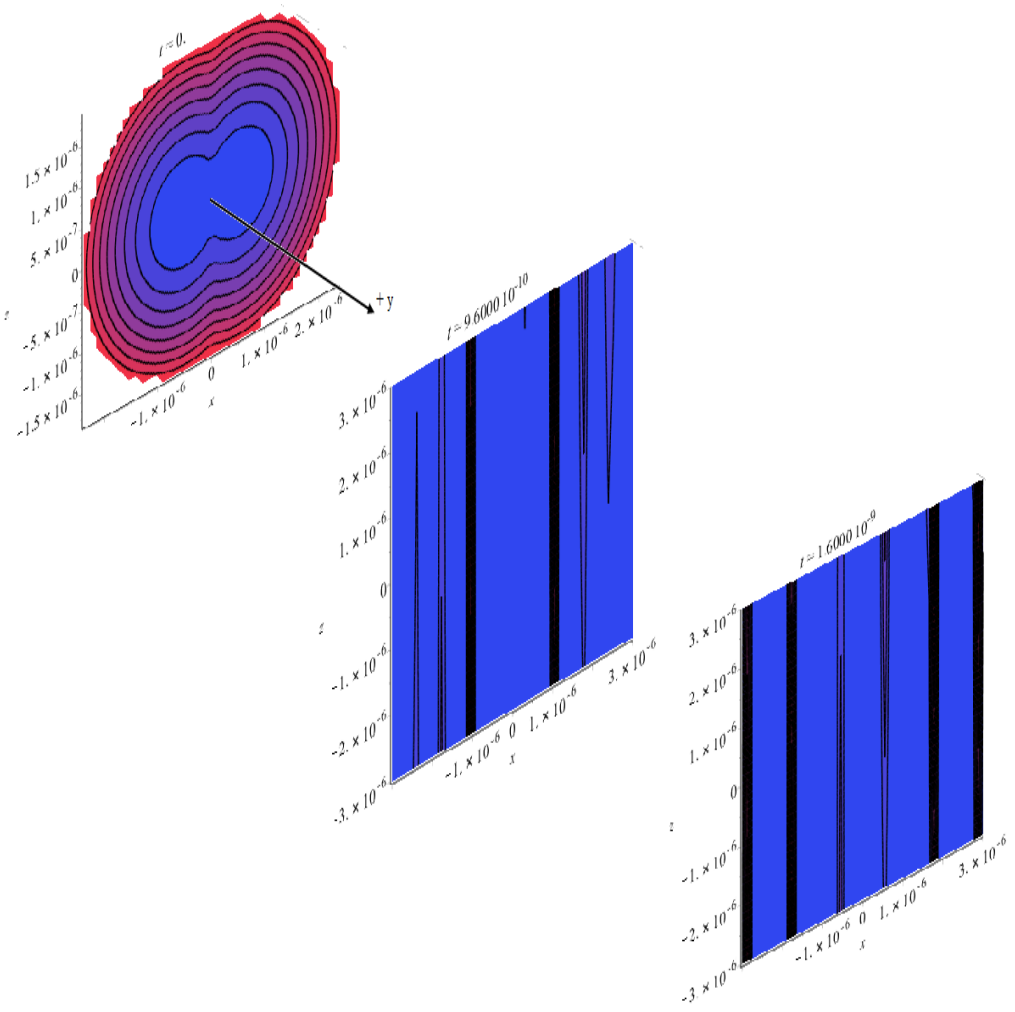


Figure 5.17: *A sequence of density plots (3 slices of a 3D-plot) of the quantum potential in a two-pinhole interference experiment with EWEA modeled by* $2-D$ *Gaussian wave-packets.*

**EWUA**

A sequence of density plots (3 slices of a $3D$-plot) of the quantum potential for EWUA is shown in Figure 5.18. The plot ranges are $x = -3 \times 10^{-6}$ to $3 \times 10^{-6}\, m$, $z = -3 \times 10^{-6}$ to $3 \times 10^{-6}\, m$ and $t = 0\, s$ to $1.6000 * 10^{-9}\, s$. As for the EWEA case, the first slice is not shown because the image is badly formed. The second slice clearly shows that the deeper valleys indicated by blacker bands are on the side of lower intensity $-x_0$-pinhole. In the final $t = 1.5 \times 10^{-9}\, s$ slice, the peaks and valleys even out though a slight bias to deeper valleys on the $-x_0$ side is still discernible.

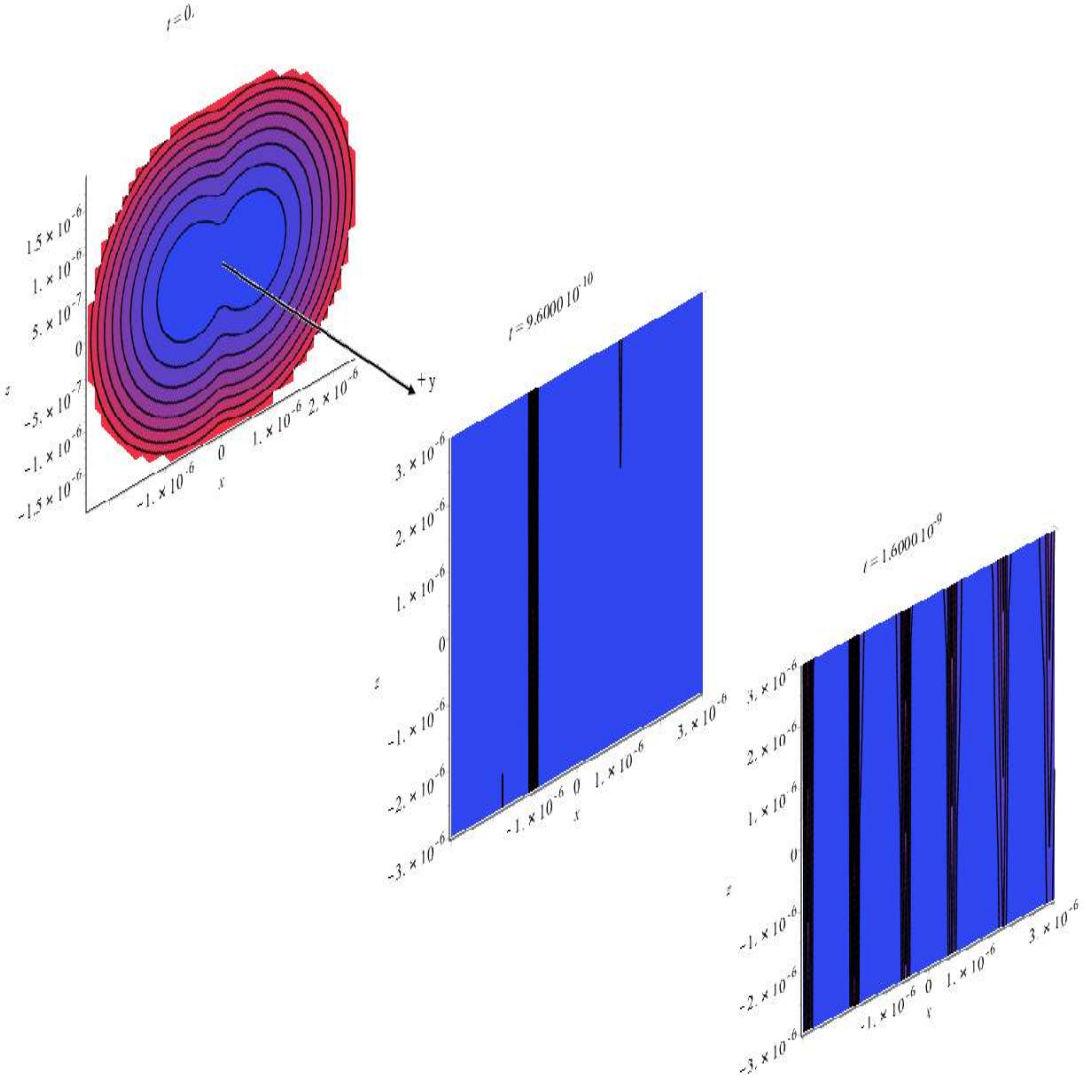


Figure 5.18: *A sequence of density plots (3 slices of a 3D-plot) of the quantum potential in a two-pinhole interference experiment with EWUA modeled by* $2-D$ *Gaussian wave-packets.*

**UWEA**

A sequence of density plots (3 slices of a 3D-plot) of the quantum potential for UWEA is shown in Figure 5.19. The plot ranges are $x = -3 \times 10^{-6}$ to $3 \times 10^{-6}\, m$, $z = -3 \times 10^{-6}$ to $3 \times 10^{-6}\, m$ and $t = 0\, s$ to $1.6000 * 10^{-9}\, s$. As with the quantum potential density plots for the EWUA case, the image in the first slice is problematic. This time, the image is complete but it does not reflect the two-pinhole structure. As before, this is probably because the density plotting algorithm does not handle difficult numbers very well. The middle slice shows the early formation of plateaus and valleys skewed to the $+x$-side, with the plateau regions narrower than the valley regions. In the final slice, the plateau regions become wider than the valley regions, but are less distinct as compared to the EWEA case, or even as compared to the EWUA case. Despite this, the fringe visibility is greater than for the EWUA case, though of course, less than for EWEA case, as we saw above. Again, the shift of quantum potential peaks to the +x-side can be seen.

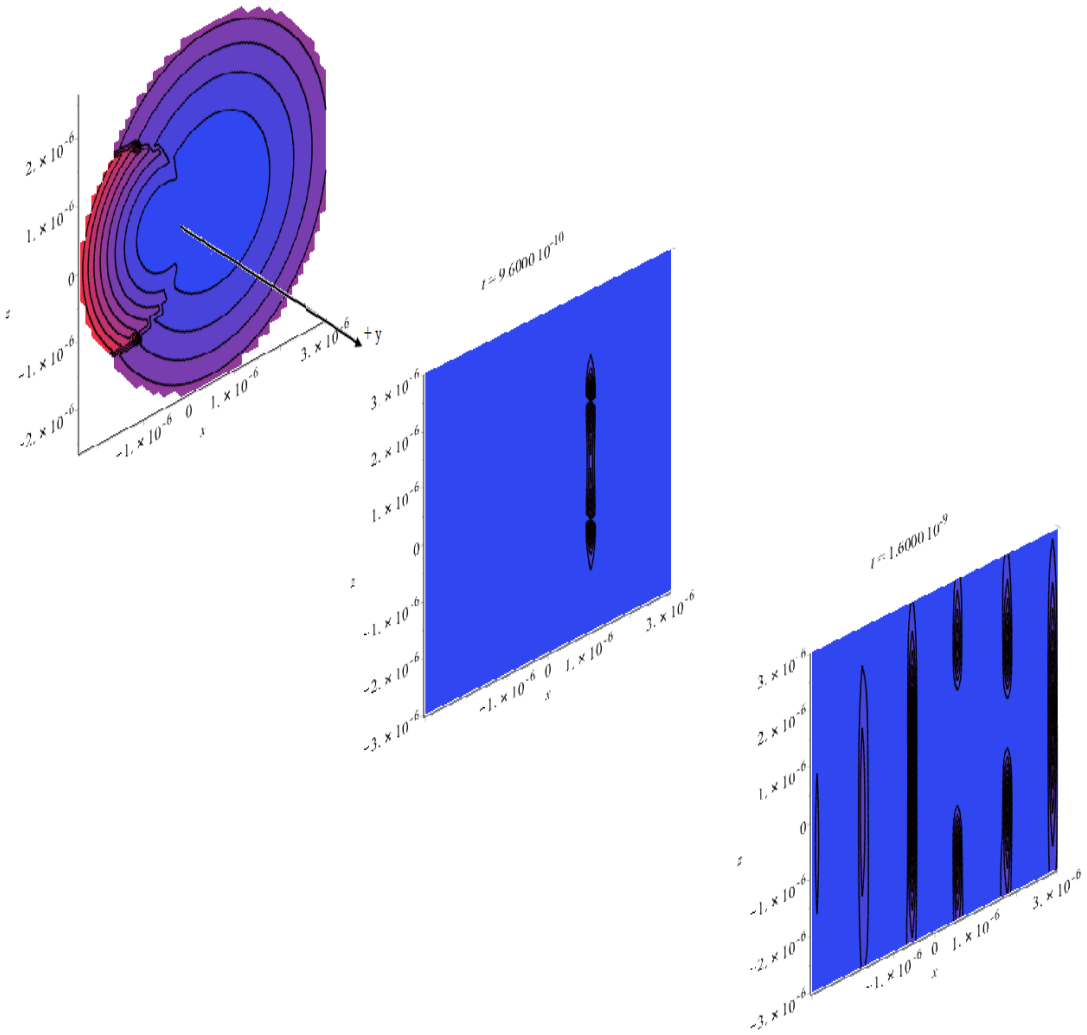


Figure 5.19: *A sequence of density plots (3 slices of a 3D-plot) of the quantum potential in a two-pinhole interference experiment with UWEA modeled by* $2-D$ *Gaussian wave-packets.*

**UWUA**

A sequence of density plots (3 slices of a 3D-plot) of the quantum potential for UWUA is shown in Figure 5.20. The plot ranges are $x = -3 \times 10^{-6}$ to $3 \times 10^{-6}\, m$, $z = -3 \times 10^{-6}$ to $3 \times 10^{-6}\, m$ and $t = 0\, s$ to $1.6000 * 10^{-9}\, s$. There is a reduction in interference of the quantum potential which can be interpreted as in the classical case, in terms of wave profiles with reduced coherence.

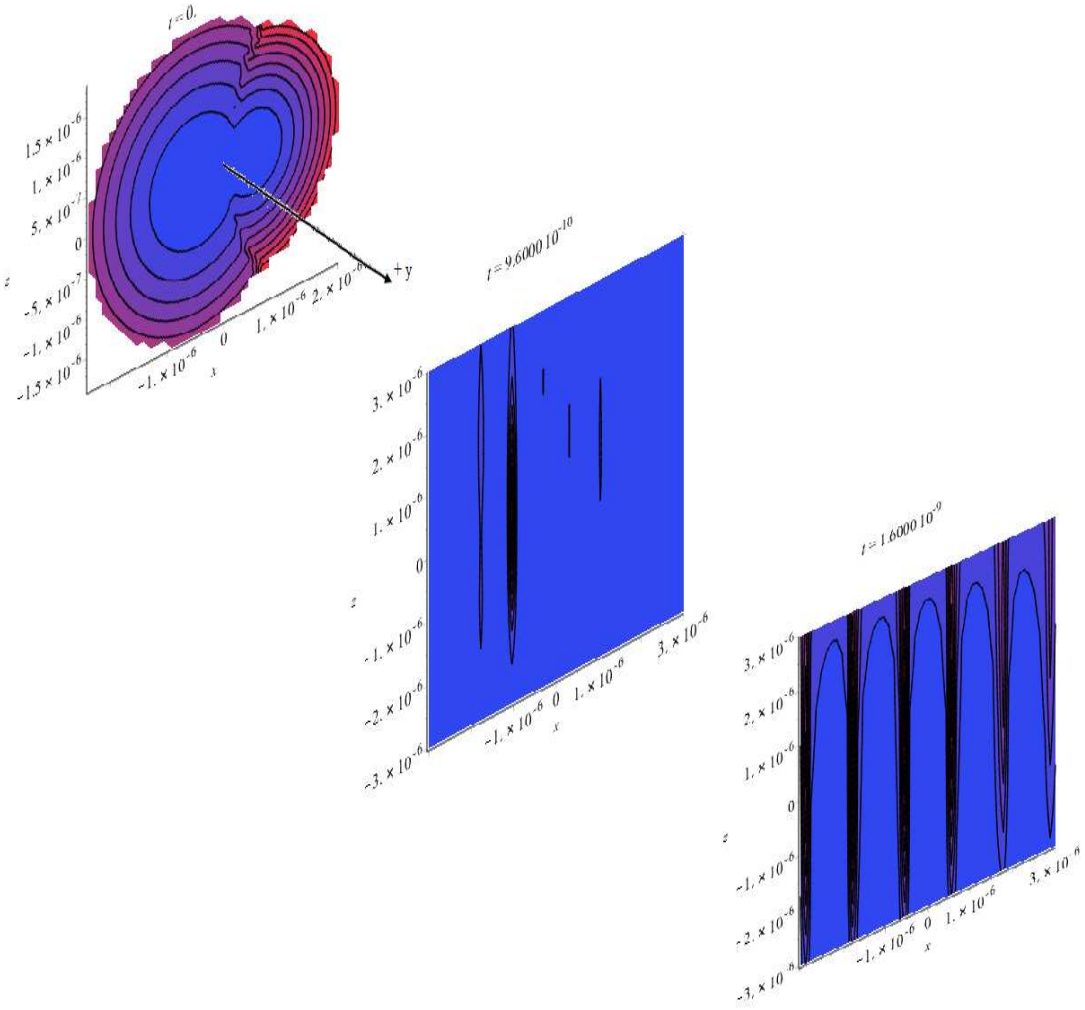


Figure 5.20: *A sequence of density plots (3 slices of a 3D-plot) of the quantum potential in a two-pinhole interference experiment with UWUA modeled by* $2-D$ *Gaussian wave-packets.*

## 5.4 Trajectories

### 5.4.1 Numerical Solution of Systems of Differential Equations Using the Adapted RK Method

The $m\,th$-order system of first-order initial-value problems is expressed in the form

$$\begin{cases} \dfrac{du_1}{dt} = f_1(t, u_1, u_2, ..., u_m), \\ \dfrac{du_2}{dt} = f_2(t, u_1, u_2, ..., u_m), \\ \qquad\qquad . \\ \qquad\qquad . \\ \qquad\qquad . \\ \dfrac{du_m}{dt} = f_m(t, u_1, u_2, ..., u_m) \end{cases} \tag{5.35}$$

for $a \leq t \leq b$, with the initial conditions:

$$\begin{cases} u_1(a) = \alpha_1, \\ u_1(a) = \alpha_2, \\ \qquad . \\ \qquad . \\ \qquad . \\ u_m(a) = \alpha_m \end{cases} \tag{5.36}$$

In our particular case, the second-order system of first-order initial-value problems is expressed by equations (3.137) and (3.138) for $0 \leq t \leq 1.5 \times 10^{-9}$, with the initial conditions:

$$\begin{cases} x(0) = \alpha_1 = 0.5 \times 10^{-6} \\ z(0) = \alpha_2 = 0 \end{cases} \tag{5.37}$$

The objective is to find $m$ functions $u_1, ..., u_m$ that satisfy the system of differential equations as well as the initial conditions (in our particular case, the two functions to be found are $x$ and $z$).

To discuss the existence and uniqueness of the solutions to systems of equations, we need to extend the definition of the Lipschitz condition to functions of several variables.

**Definition 1** : *The function $f(t, y_1, ..., y_m)$, defined on the set*

$$D = \{(t, u_1, ..., u_m) \mid a \leq t \leq b, -\infty < u_i < \infty, for\ each\ i = 1, 2, ..., m\}$$

*is said to satisfy a Lipschitz condition on $D$ in the variables $u_1, u_1, ..., u_m$ if a constant $L > 0$ exists with the property that*

$$\mid f(t, u_1, ..., u_m) - f(t, z_1, ..., z_m) \mid \leq L \sum_{j=1}^{m} \mid u_j - z_j \mid \tag{5.38}$$

*for all $(t, u_1, ..., u_m)$ and $(t, z_1, ..., z_m)$ in $D$.*

By using the Mean Value Theorem, it can be shown that if $f$ and its first partial derivatives are continuous on $D$ and if

$$\left| \frac{\partial f(t, u_1, ..., u_m)}{\partial u_i} \right| \leq L \tag{5.39}$$

for each $i = 1, 2, ..., m$ and all $(t, u_1, ..., u_m)$ in $D$, then $f$ satisfies a Lipschitz condition on $D$ with Lipschitz constant $L$(see ([36], p.283). A basic existence and uniqueness theorem follows.

**Theorem 1** : *Suppose*

$$D = \{(t, u_1, ..., u_m) \mid a \leq t \leq b, -\infty < u_i < \infty, for\ each\ i = 1, 2, ..., m\}$$

*and let $f_i(t, u_1, ..., u_m)$, for each $i = 1, 2, ..., m$, be continuous on $D$ and satisfy a Lipschitz condition there. The system of first-order differential equations (5.35), subject to the initial conditions (5.36), has a unique solution $u_1(t), ..., u_m(t)$ for $a \leq t \leq b$.*

Methods to solve systems of first-order differential equations are simply generalizations of the methods for a single first-order equation.

For example, the classical RK of order four given by

$$
\begin{aligned}
w_0 &= \alpha, \\
k_1 &= h \times f(t_i, w_i), \\
k_2 &= h \times f\left(t_i + \frac{h}{2}, w_i + \frac{k_1}{2}\right), \\
k_3 &= h \times f\left(t_i + \frac{h}{2}, w_i + \frac{k_2}{2}\right), \\
k_4 &= h \times f(t_{i+1}, w_i + k_3), \qquad (5.40)
\end{aligned}
$$

and $w_{i+1} = w_i + \frac{1}{6}[k_1 + 2k_2 + 2k_3 + k_4]$ for each $i = 0, 1, ..., N-1$, used to solve the first-order initial-value problem

$$y' = f(t, y), a \leq t \leq b, y(a) = \alpha, \qquad (5.41)$$

can be generalized as follows. Let an integer $N > 0$ be chosen and set $h = b - a/N$. Partition the interval $[a, b]$ into $N$ subintervals with the mesh points

$$t_j = a + jh \; for \; each \; j = 0, 1, ..., N.$$

Use the notation $w_{ij}$ to denote an approximation to $u_i(t_j)$ for each $j = 0, 1, ..., N$ and $i = 1, 2, ..., m$, that is, $w_{ij}$ will approximate the $i\,th$ solution $u_i(t)$ of (5.35) at the $j\,th$ mesh point $t_j$. For the initial conditions, set

$$
\begin{aligned}
w_{1,0} &= \alpha_1, \; w_{2,0} = \alpha_2, \; ..., \; w_{m,0} = \alpha_m, \\
k_{1,i} &= h \times f_i(t_j, w_{1,j}, ..., w_{m,j}), \\
k_{2,i} &= h \times f_i\left(t_j + \frac{h}{2}, w_{1,j} + \frac{k_{1,1}}{2}, w_{2,j} + \frac{k_{1,2}}{2}, ..., w_{m,j} + \frac{k_{1,m}}{2}\right), \\
k_{3,i} &= h \times f_i\left(t_j + \frac{h}{2}, w_{1,j} + \frac{k_{2,1}}{2}, w_{2,j} + \frac{k_{2,2}}{2}, ..., w_{m,j} + \frac{k_{2,m}}{2}\right), \\
k_{4,i} &= h \times f_i(t_j + h, w_{1,j} + k_{3,1}, w_{2,j} + k_{3,2}, ..., w_{m,j} + k_{3,m}), \qquad (5.42)
\end{aligned}
$$

and $w_{i,j+1} = w_{i,j} + \frac{1}{6}[k_{1,i} + 2k_{2,i} + 2k_{3,i} + k_{4,i}]$ for each $i = 1, 2, ..., m$.

Note that $k_{1,1}, k_{1,2}, ..., k_{1,m}$ must all be computed before $k_{2,1}$ can be determined. In

general, each $k_{l,1}, k_{l,2}, ..., k_{l,m}$ must be computed before any of the expressions $k_{l+1,i}$.

Hence, to approximate the solution of the $mth$-order system of first-order initial-value problems

$$u_j^{'} = f_j(t, u_1, ..., u_m), a \leq t \leq b, u_j(a) = \alpha_j, j = 1, 2, ..., m$$

at $(n+1)$ equally spaced numbers in the interval $[a, b]$, we are going to use the following algorithm:

**RK for systems of differential equations algorithm**

INPUT endpoints $a, b$; number of equations $m$; integer $N$;
initial conditions $\alpha_1, ..., \alpha_m$.

OUTPUT approximations $w_j$ to $u_j(t)$ at the $(N+1)$ values of $t$.

Step 1 Set $h = (b-a)/N$; $t = a$.

Step 2 For $j = 1, 2, ..., m$ set $w_j = \alpha_j$.

Step 3 OUTPUT $(t, w_1, ..., w_m)$.

Step 4 For $i = 1, 2, ..., N$ do steps $5 - 11$.

Step 5 For $j = 1, ..., m$ set
$k_{1,j} = h \times f_j(t, w_1, ..., w_m)$.
Step 6 For $j = 1, ..., m$ set
$k_{2,j} = h \times f_j\left(t + \frac{h}{2}, w_1 + \frac{k_{1,1}}{2}, w_2 + \frac{k_{1,2}}{2}, ..., w_m + \frac{k_{1,m}}{2}\right)$.
Step 7 For $j = 1, ..., m$ set
$k_{3,j} = h \times f_j\left(t + \frac{h}{2}, w_1 + \frac{k_{2,1}}{2}, w_2 + \frac{k_{2,2}}{2}, ..., w_m + \frac{k_{2,m}}{2}\right)$.
Step 8 For $j = 1, ..., m$ set
$k_{4,j} = h \times f_j(t + h, w_1 + k_{3,1}, w_2 + k_{3,2}, ..., w_m + k_{3,m})$.
Step 9 For $j = 1, ..., m$
set $w_j = w_j + \frac{1}{6}[k_{1,j} + 2k_{2,j} + 2k_{3,j} + k_{4,j}]$.
Step 10 Set $t = a + ih$
Step 11 OUTPUT $(t, w_1, ..., w_m)$.

Step 12 STOP.

### 5.4.2 Trajectories Fortran 77 program of electron trajectories in Einstein's two-pinhole experiment in $2-D$

```
 program Traj2slit using S_formula for left trajectories
 implicit none
 integer i,j
 double precision t,x,h,hi,xi,ti, x0x,z0z
 double precision z,zi, pppi, dzinc, dznew
 double precision dx0, dz0
integer p1,u1,u2,u3,u4,u5
integer u6, u7,u8,u9, u10
integer u11,u12,u13,u14,u15
integer u16, u17,u18,u19, u20
integer u21, u22,u23,u24, u25
integer u26, u27,u28,u29, u30
integer u31, u32,u33,u34, u35
integer u36, u37,u38,u39, u40
parameter (p1=87,u1=1, u2=2,u3=3,u4=4,u5=5)
parameter (u6=86, u7=7,u8=8,u9=9, u10=10)
parameter (u11=11, u12=12,u13=13,u14=14,u15=15)
parameter (u16=16, u17=17,u18=18,u19=19, u20=20)
parameter (u21=21, u22=22,u23=23,u24=24, u25=25)
parameter (u26=26, u27=27,u28=28,u29=29, u30=30)
parameter (u31=31, u32=32,u33=33,u34=34, u35=35)
parameter (u36=36, u37=37,u38=38,u39=39, u40=40)
parameter(pppi=3.141592654)
open(p1, file='inixtnega.txt', form='formatted', status='new')
open(u1, file='pan2Strajfm81a', form='formatted', status='new')
open(u2, file='pan2Strajfm82a', form='formatted', status='new')
open(u3, file='pan2Strajfm83a', form='formatted', status='new')
open(u4, file='pan2Strajfm84a', form='formatted', status='new')
open(u5, file='pan2Strajfm85a', form='formatted', status='new')
open(u6, file='pan2Strajfm86a', form='formatted', status='new')
open(u7, file='pan2Strajfm87a', form='formatted', status='new')
open(u8, file='pan2Strajfm88a', form='formatted', status='new')
open(u9, file='pan2Strajfm89a', form='formatted', status='new')
open(u10, file='pan2Strajfm90a', form='formatted', status='new')
open(u11, file='pan2Strajfm91a', form='formatted', status='new')
open(u12, file='pan2Strajfm92a', form='formatted', status='new')
open(u13, file='pan2Strajfm93a', form='formatted', status='new')
open(u14, file='pan2Strajfm94a', form='formatted', status='new')
open(u15, file='pan2Strajfm95a', form='formatted', status='new')
open(u16, file='pan2Strajfm96a', form='formatted', status='new')
open(u17, file='pan2Strajfm97a', form='formatted', status='new')
open(u18, file='pan2Strajfm98a', form='formatted', status='new')
open(u19, file='pan2Strajfm99a', form='formatted', status='new')
open(u20, file='pan2Strajfm100a', form='formatted', status='new')
open(u21, file='pan2Strajfm101a', form='formatted', status='new')
open(u22, file='pan2Strajfm102a', form='formatted', status='new')
open(u23, file='pan2Strajfm103a', form='formatted', status='new')
open(u24, file='pan2Strajfm104a', form='formatted', status='new')
open(u25, file='pan2Strajfm105a', form='formatted', status='new')
open(u26, file='pan2Strajfm106a', form='formatted', status='new')
open(u27, file='pan2Strajfm107a', form='formatted', status='new')
open(u28, file='pan2Strajfm108a', form='formatted', status='new')
```

```
open(u29, file='pan2Strajfm109a', form='formatted', status='new')
open(u30, file='pan2Strajfm110a', form='formatted', status='new')
open(u31, file='pan2Strajfm111a', form='formatted', status='new')
open(u32, file='pan2Strajfm112a', form='formatted', status='new')
open(u33, file='pan2Strajfm113a', form='formatted', status='new')
open(u34, file='pan2Strajfm114a', form='formatted', status='new')
open(u35, file='pan2Strajfm115a', form='formatted', status='new')
open(u36, file='pan2Strajfm116a', form='formatted', status='new')
open(u37, file='pan2Strajfm117a', form='formatted', status='new')
open(u38, file='pan2Strajfm118a', form='formatted', status='new')
open(u39, file='pan2Strajfm119a', form='formatted', status='new')
open(u40, file='pan2Strajfm120a', form='formatted', status='new')
 z0z=0
 x0x=5D-7
 dx0=1.4D-7
 dz0=dx0
 ti=0
 dzinc=dz0/39
 xi=-x0x-dx0/2
 zi=z0z-dz0/2
 h=(1.5D-9)/200
 t=ti
 x=xi
 z=zi
 do 2000 i=1,40
 t=t
 x=x
 z=z
 write(p1,400) 'i=',i,'t=',t,'x=',x,'z=',z
 do  1000 j=1,200
 if (i.EQ.1 )  then
 write(u1,500) t,x,z
 elseif (i .EQ. 2) then
 write(u2,500) t,x,z
 elseif (i .EQ. 3) then
 write(u3,500) t,x,z
 elseif (i .EQ. 4) then
 write(u4,500) t,x,z
 elseif (i .EQ. 5) then
 write(u5,500) t,x,z
 elseif (i .EQ. 6) then
 write(u6,500) t,x,z
 elseif (i .EQ. 7) then
 write(u7,500) t,x,z
 elseif (i .EQ. 8) then
 write(u8,500) t,x,z
 elseif (i .EQ. 9) then
 write(u9,500) t,x,z
 elseif (i.EQ.10 )  then
 write(u10,500) t,x,z
 elseif (i .EQ. 11) then
 write(u11,500) t,x,z
```

```
elseif (i .EQ. 12) then
write(u12,500) t,x,z
elseif (i .EQ. 13) then
write(u13,500) t,x,z
elseif (i .EQ. 14) then
write(u14,500) t,x,z
elseif (i .EQ. 15) then
write(u15,500) t,x,z
elseif (i .EQ. 16) then
write(u16,500) t,x,z
elseif (i .EQ. 17) then
write(u17,500) t,x,z
elseif (i .EQ. 18) then
write(u18,500) t,x,z
elseif (i .EQ. 19) then
write(u19,500) t,x,z
elseif (i .EQ. 20) then
write(u20,500) t,x,z
elseif (i .EQ. 21) then
write(u21,500) t,x,z
elseif (i .EQ. 22) then
write(u22,500) t,x,z
elseif (i .EQ. 23) then
write(u23,500) t,x,z
elseif (i .EQ. 24) then
write(u24,500) t,x,z
elseif (i .EQ. 25) then
write(u25,500) t,x,z
elseif (i .EQ. 26) then
write(u26,500) t,x,z
elseif (i .EQ. 27) then
write(u27,500) t,x,z
elseif (i .EQ. 28) then
write(u28,500) t,x,z
elseif (i .EQ. 29) then
write(u29,500) t,x,z
elseif (i .EQ. 30) then
write(u30,500) t,x,z
elseif (i .EQ. 31) then
write(u31,500) t,x,z
elseif (i .EQ. 32) then
write(u32,500) t,x,z
elseif (i .EQ. 33) then
write(u33,500) t,x,z
elseif (i .EQ. 34) then
write(u34,500) t,x,z
elseif (i .EQ. 35) then
write(u35,500) t,x,z
elseif (i .EQ. 36) then
write(u36,500) t,x,z
elseif (i .EQ. 37) then
write(u37,500) t,x,z
```

```
      elseif (i .EQ. 38) then
      write(u38,500) t,x,z
      elseif (i .EQ. 39) then
      write(u39,500) t,x,z
      else
      write(u40,500) t,x,z
      endif
      call incrementxz(t,x,z,h)
      x=x
      z=z
      t=t+h
1000    continue
      t=0
      dznew=i*dzinc
      x=-x0x-dx0/2
      z=z0z-dz0/2+dznew
2000    continue
400     format(A,I2,X,A,(E16.8),X,A,(E16.8),X,A,(E16.8))
500     format(3(E16.8))
      close(unit=p1)
      close(unit=u1)
      close(unit=u2)
      close(unit=u3)
      close(unit=u4)
      close(unit=u5)
      close(unit=u6)
      close(unit=u7)
      close(unit=u8)
      close(unit=u9)
      close(unit=u10)
      close(unit=u11)
      close(unit=u12)
      close(unit=u13)
      close(unit=u14)
      close(unit=u15)
      close(unit=u16)
      close(unit=u17)
      close(unit=u18)
      close(unit=u19)
      close(unit=u20)
      close(unit=u21)
      close(unit=u22)
      close(unit=u23)
      close(unit=u24)
      close(unit=u25)
      close(unit=u26)
      close(unit=u27)
      close(unit=u28)
      close(unit=u29)
      close(unit=u30)
      close(unit=u31)
      close(unit=u32)
```

```
 close(unit=u33)
 close(unit=u34)
 close(unit=u35)
 close(unit=u36)
 close(unit=u37)
 close(unit=u38)
 close(unit=u39)
 close(unit=u40)
 Stop
 End
 double precision function sx(t,x,z)
 double precision t,x,z
 double precision ppi,dxn0, dxp0,x0,kx
 double precision dzn0, dzp0, z0,kz,vz
 double precision chi,b,al,vx
 double precision dxn,dxn1,dxp,dxp1,r1,r2
 double precision dzn,dzn1,dzp,dzp1
 double precision s12, f1x, f2x, f3x, f4x, f5x, f6x
 double precision bt1, bt2, th12
 parameter(ppi=3.141592654)
 parameter(dxn0=0.7D-7)
 parameter(dxp0=dxn0)
 parameter(x0=5D-7)
 parameter(z0=0)
 parameter(kx=1.295697844D6)
 parameter(kz=0)
 parameter(chi=0)
 parameter(al=1.157677314D-4)
 b=ppi/4
 dzn0=dxn0
 dzp0=dxp0
 vx=al*kx
 vz=al*kz
 dxn=dxn0*dxn0+al*al*t*t/dxn0/dxn0
 dxp=dxp0*dxp0+al*al*t*t/dxp0/dxp0
 dzn=dzn0*dzn0+al*al*t*t/dzn0/dzn0
 dzp=dzp0*dzp0+al*al*t*t/dzp0/dzp0
 dxn1=dxn0*dxn0*dxn0*dxn0+al*al*t*t
 dxp1=dxp0*dxp0*dxp0*dxp0+al*al*t*t
 dzn1=dzn0*dzn0*dzn0*dzn0+al*al*t*t
 dzp1=dzp0*dzp0*dzp0*dzp0+al*al*t*t
 bt1=sqrt(4*ppi*ppi/dxn1)
 bt2=sqrt(4*ppi*ppi/dxp1)
 th12=(   atan(-al*t/dxn0/dxn0) -  atan(-al*t/dxp0/dxp0)  )/2
 r1=bt1*cos(b)*cos(b)*exp( -(x+x0-vx*t)*(x+x0-vx*t)/(2*dxn) )
+                *exp( -(z+z0-vz*t)*(z+z0-vz*t)/(2*dzn) )
 r2=bt2*sin(b)*sin(b)*exp( -(x-x0+vx*t)*(x-x0+vx*t)/(2*dxp)   )
+                *exp( -(z-z0+vz*t)*(z-z0+vz*t)/(2*dzp)   )
 s12=2*th12+2*kx*x + 2*kz*z + chi
+    +al*t*(x+x0-vx*t)*(x+x0-vx*t)/(2*dxn1)
+    -al*t*(x-x0+vx*t)*(x-x0+vx*t)/(2*dxp1)
+    +al*t*(z+z0-vz*t)*(z+z0-vz*t)/(2*dzn1)
```

```
+     -al*t*(z-z0+vz*t)*(z-z0+vz*t)/(2*dzp1)
  f1x=r1*r1+r2*r2+2*r1*r2*cos(s12)
  f2x=x*r1*r2*sin(s12)*(dxn-dxp)/dxn/dxp
  f3x=al*t*x*(  r1*r1*dxp1  +  r2*r2*dxn1
+             +r1*r2*cos(s12)*(dxn1+dxp1)  )/dxn1/dxp1
  f4x=(x0-vx*t)*r1*r2*sin(s12)*(dxp+dxn)/dxn/dxp
  f5x=al*t*(x0-vx*t)*(  r1*r1*dxp1 - r2*r2*dxn1
+           + r1*r2*cos(s12)*(dxp1-dxn1) )/dxn1/dxp1
  f6x=kx*(r1*r1-r2*r2)
  sx= al*(   f5x+f6x-f4x  + f3x +f2x)/f1x
  return
  end
  double precision function sz(t,x,z)
  double precision t,x,z
  double precision ppi,dxn0, dxp0,x0,kx
  double precision dzn0, dzp0, z0,kz,vz
  double precision chi,b,al,vx
  double precision dxn,dxn1,dxp,dxp1,r1,r2
  double precision dzn,dzn1,dzp,dzp1
  double precision s12, f1x, f2x, f3x, f4x, f5x, f6x
  double precision bt1, bt2, th12
  parameter(ppi=3.141592654)
  parameter(dxn0=0.7D-7)
  parameter(dxp0=dxn0)
  parameter(x0=5D-7)
  parameter(z0=0)
  parameter(kx=1.295697844D6)
  parameter(kz=0)
  parameter(chi=0)
  parameter(al=1.157677314D-4)
  b=ppi/4
  dzn0=dxn0
  dzp0=dxp0
  vx=al*kx
  vz=al*kz
  dxn=dxn0*dxn0+al*al*t*t/dxn0/dxn0
  dxp=dxp0*dxp0+al*al*t*t/dxp0/dxp0
  dzn=dzn0*dzn0+al*al*t*t/dzn0/dzn0
  dzp=dzp0*dzp0+al*al*t*t/dzp0/dzp0
  dxn1=dxn0*dxn0*dxn0*dxn0+al*al*t*t
  dxp1=dxp0*dxp0*dxp0*dxp0+al*al*t*t
  dzn1=dzn0*dzn0*dzn0*dzn0+al*al*t*t
  dzp1=dzp0*dzp0*dzp0*dzp0+al*al*t*t
  bt1=sqrt(4*ppi*ppi/dxn1)
  bt2=sqrt(4*ppi*ppi/dxp1)
  th12=(   atan(-al*t/dxn0/dxn0) -  atan(-al*t/dxp0/dxp0)  )/2
  r1=bt1*cos(b)*cos(b)*exp( -(x+x0-vx*t)*(x+x0-vx*t)/(2*dxn) )
+                  *exp( -(z+z0-vz*t)*(z+z0-vz*t)/(2*dzn) )
  r2=bt2*sin(b)*sin(b)*exp( -(x-x0+vx*t)*(x-x0+vx*t)/(2*dxp)   )
+                  *exp( -(z-z0+vz*t)*(z-z0+vz*t)/(2*dzp)   )
  s12=2*th12+2*kx*x + 2*kz*z + chi
+     +al*t*(x+x0-vx*t)*(x+x0-vx*t)/(2*dxn1)
```

```
+     -al*t*(x-x0+vx*t)*(x-x0+vx*t)/(2*dxp1)
+     +al*t*(z+z0-vz*t)*(z+z0-vz*t)/(2*dzn1)
+     -al*t*(z-z0+vz*t)*(z-z0+vz*t)/(2*dzp1)
  f1z=r1*r1+r2*r2+2*r1*r2*cos(s12)
  f2z=z*r1*r2*sin(s12)*(dzn-dzp)/dzn/dzp
  f3z=al*t*z*(  r1*r1*dzp1  +  r2*r2*dzn1
+             +r1*r2*cos(s12)*(dzn1+dzp1)  )/dzn1/dzp1
  f4z=(z0-vz*t)*r1*r2*sin(s12)*(dzp+dzn)/dzn/dzp
  f5z=al*t*(z0-vz*t)*(  r1*r1*dzp1 - r2*r2*dzn1
+           + r1*r2*cos(s12)*(dzp1-dzn1) )/dzn1/dzp1
  f6z=kz*(r1*r1-r2*r2)
  sz= al*(  f5z+f6z-f4z + f3z+f2z ) /f1z
  return
  end
   subroutine incrementxz(t,x,z,h)
   double precision t,x,z,h,sx,sz
   double precision k1x,k2x,k3x,k4x
   double precision k1z,k2z,k3z,k4z
   double precision a,b,c
   a=t
   b=x
   c=z
   k1x=h*sx(a,b,c)
   k1z=h*sz(a,b,c)
   a=t+h/2
   b=x+k1x/2
   c=z+k1z/2
   k2x=h*sx(a,b,c)
   k2z=h*sz(a,b,c)
   b=x+k2x/2
   c=z+k2z/2
   k3x=h*sx(a,b,c)
   k3z=h*sz(a,b,c)
   a=t+h
   b=x+k3x
   c=z+k3z
   k4x=h*sx(a,b,c)
   k4z=h*sz(a,b,c)
   x=x+(1.0/6.0)*(k1x+2*k2x+2*k3x+k4x)
   z=z+(1.0/6.0)*(k1z+2*k2z+2*k3z+k4z)
   return
   end
```

### 5.4.3 Plot of electron trajectories in Einstein's two-pinhole experiment in $2-D$

**EWEA**

The trajectories for EWEA is shown in Figure 5.21. The trajectory ranges are $x = -4 \times 10^{-6}$ to $4 \times 10^{-6}\ m$, $z = -4 \times 10^{-6}$ to $4 \times 10^{-6}\ m$ and $t = 0\ s$ to $1.5000 * 10^{-9}\ s$. Though the axes are labeled at the edges, the plots correspond to axes with their origin placed centrally between the pinholes. We have chosen to label the axis at the edges of the plot frame in order to show the trajectories clearly. In a real experiment, the initial position of the electrons can lie anywhere within the pinholes. But, to clearly show the behaviour of the trajectories we have chosen square initial positions within each pinhole. It is clear, that interference occurs only along the $x$-direction; there is no interference along the $z$-direction. We also see clearly how the quantum potential (and $S$-field) guides the electron trajectories to the bright fringes. Electrons whose trajectories lie within the quantum potential plateaus, therefore experiencing no quantum force, move along straight trajectories to the bright fringes. Electrons whose trajectories lie along the quantum potential slopes are pushed by the quantum force to an adjacent plateau, thereafter proceeding along straight trajectories to the bright fringes.

By changing the orientation of Figure (5.21) we obtain Figure (5.22) which retain the characteristic features of the two-slit modeled by $1-D$ Gaussian wave packets case (see Figure 4.3).

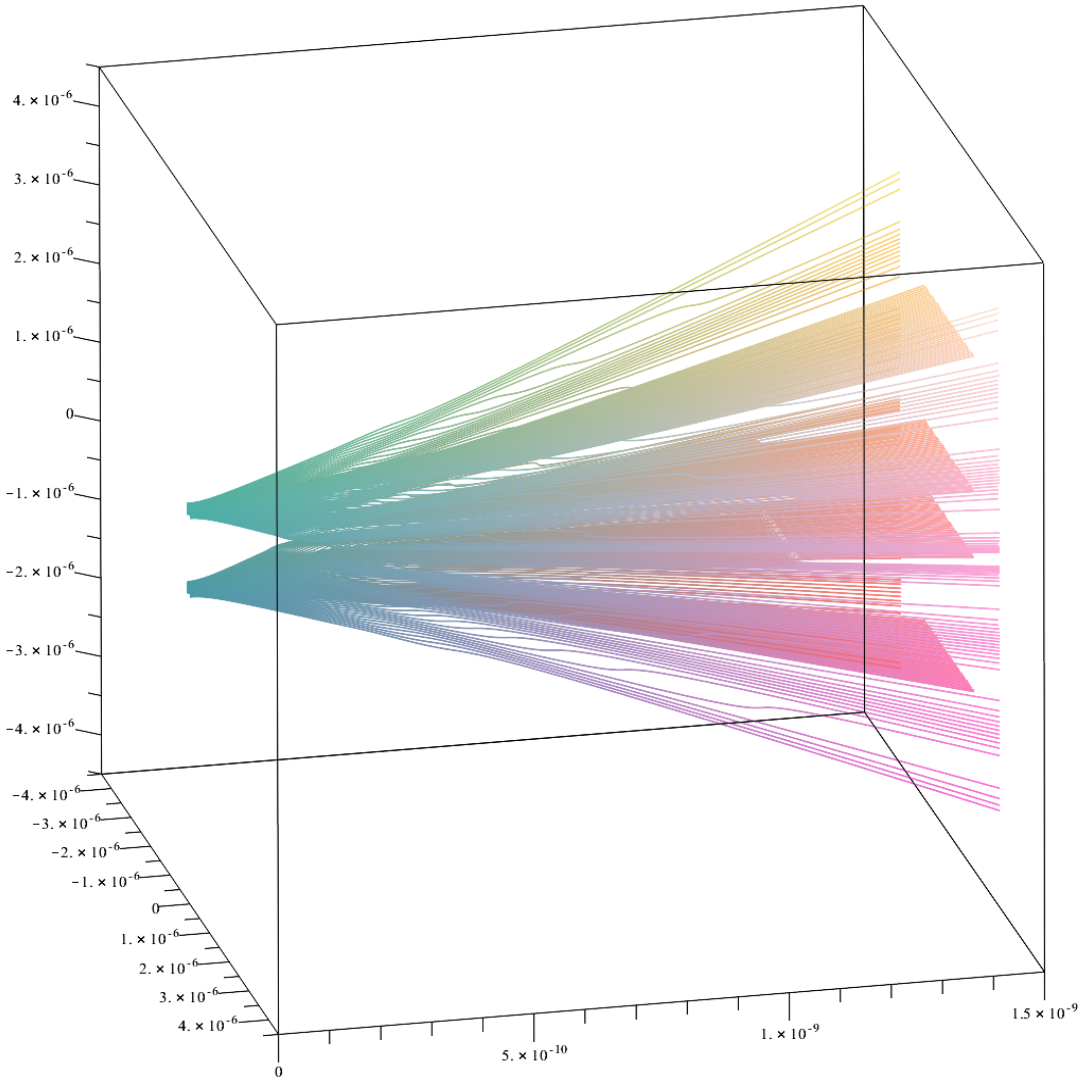


Figure 5.21: *Maple 2015 electron trajectories in Einstein's two-pinhole experiment in* $2-D$*, from the pinholes up to the detecting screen along the* $y$*-axis. Orientation:* $\theta = -95°$, $\varphi = -20°$ *and* $\psi = 14°$

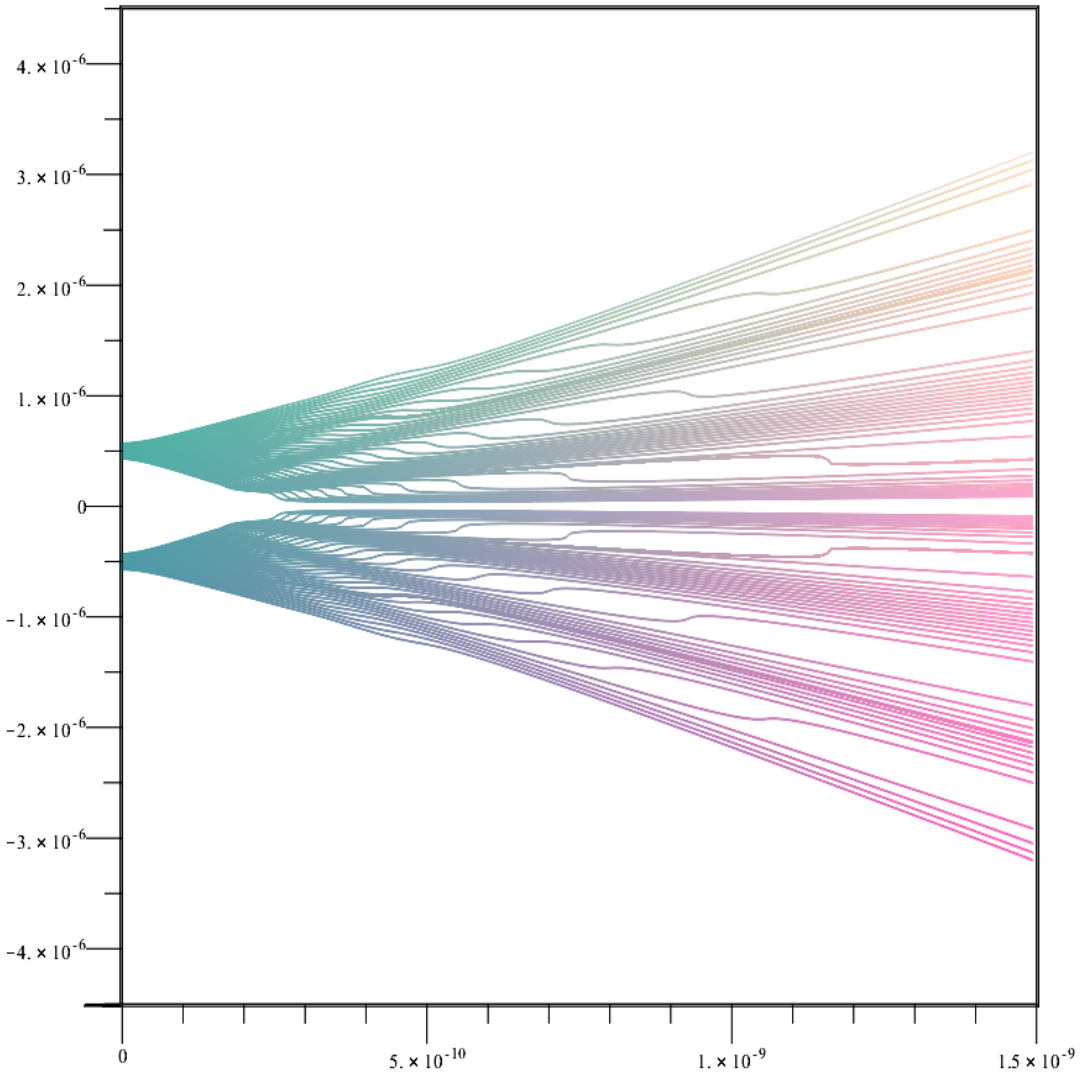


Figure 5.22: *Maple 2015 electron trajectories in Einstein's two-pinhole experiment in* $2-D$*, from the pinholes up to the detecting screen along the* $y$*-axis, but with orientation:* $\theta = -90°$*,* $\varphi = 0°$ *and* $\psi = 0°$*.*

**EWUA**

The trajectories for EWUA are shown in Figure 5.23. The trajectory ranges are $x = -4 \times 10^{-6}$ to $4 \times 10^{-6}\ m$, $z = -4 \times 10^{-6}$ to $4 \times 10^{-6}\ m$ and $t = 0\ s$ to $1.5000 * 10^{-9}\ s$. We notice that some electron trajectories reach what were the dark regions for the case of EWEA. This indicates the reduction of fringe visibility that we saw above in the intensity plots for this case. We also notice that this reduced intensity is less pronounced on the side of the lower intensity $-x_0$-pinhole, so that interference fringes on this side are more distinct, a feature we noted above for the quantum potential for this case. The overall reduction in visibility is clear to see.

In Figure 5.24, we have plotted EWUA case in $XY$-plane. We observe that there is no longer symmetry among the electron trajectories and the symmetric line has shifted downward.

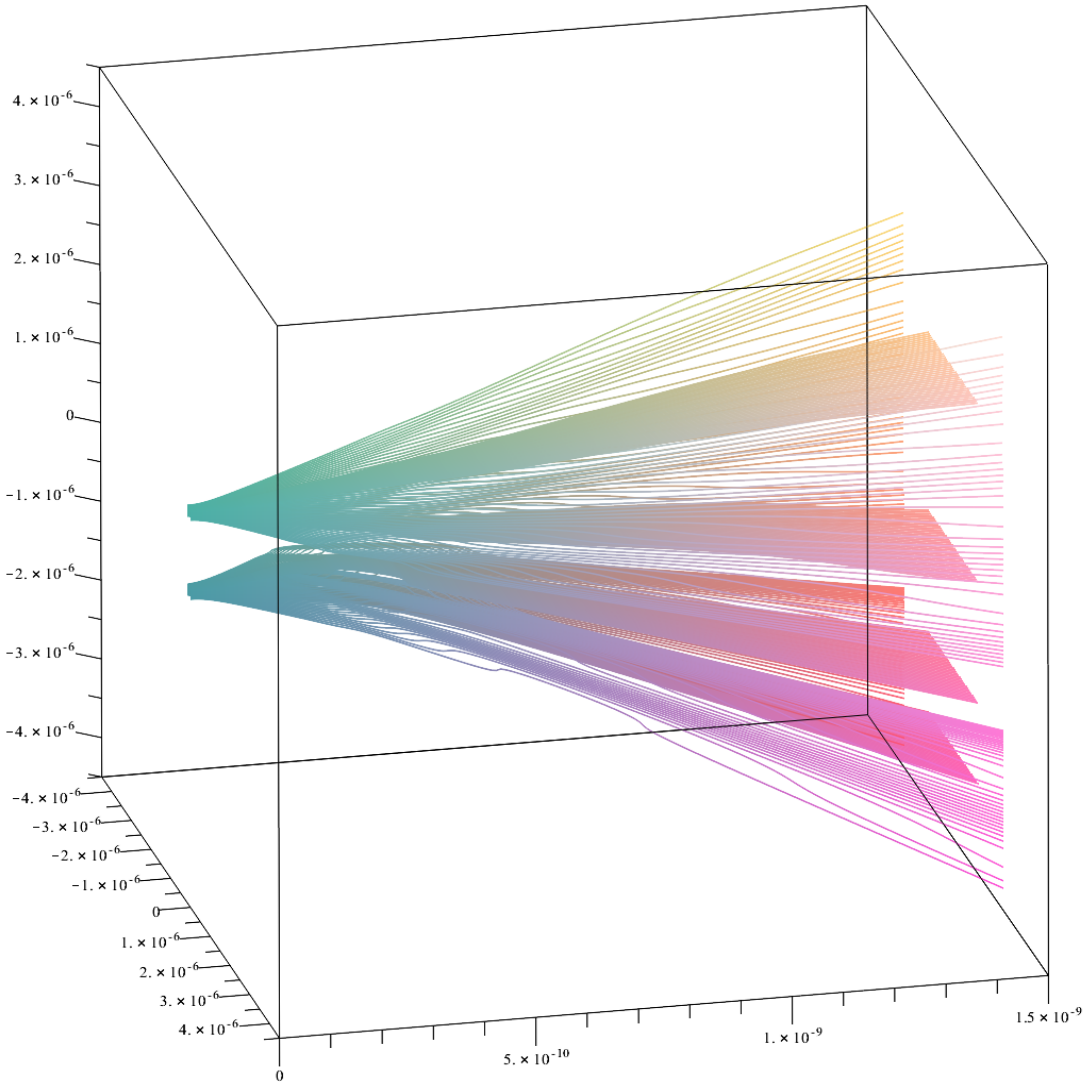


Figure 5.23: *Maple 2015 electron trajectories in Einstein's two-pinhole experiment in* $2-D$*, from the pinholes up to the detecting screen along the* $y$*-axis. Orientation:* $\theta = -95°$, $\varphi = -20°$ *and* $\psi = 14°$. Amplitude $b = \frac{\pi}{3}$

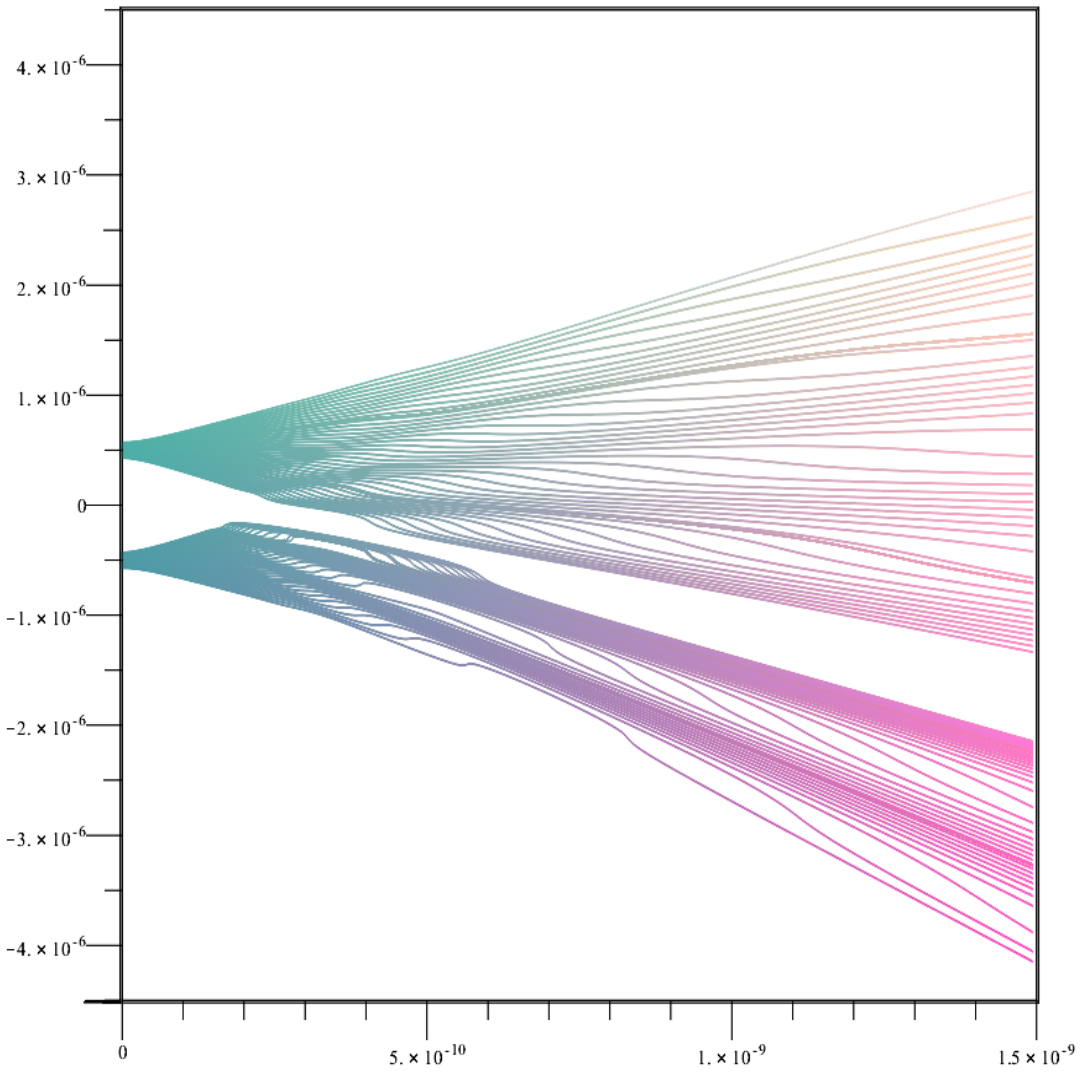


Figure 5.24: *Maple 2015 electron trajectories in Einstein's two-pinhole experiment in* $2-D$*, from the pinholes up to the detecting screen along the* $y$*-axis, but with orientation:* $\theta = -90°$*,* $\varphi = 0°$ *and* $\psi = 0°$*.*

**UWEA**

The trajectories for UWEA is shown in Figure 5.25. The trajectory ranges are $x = -4 \times 10^{-6}$ to $4 \times 10^{-6}\ m$, $z = -4 \times 10^{-6}$ to $4 \times 10^{-6}\ m$ and $t = 0\ s$ to $1.5000 * 10^{-9}\ s$. The electron trajectories clearly show the rapid spread of the narrower $-x_0$-Gaussian wave-packet. It can also be seen that electron trajectories from the $-x_0$-pinhole are more evenly spread on the detecting screen parallel to the xaxis than for the EWEA case, indicating a reduced interference pattern. The electron trajectories from the $+x_0$-pinhole, spread much less. Though only one bright and one dark fringe is shown on the $+x$-side, they appear more distinct than on the $-x$-side, reflecting the shift of the interference fringes to the $+x$-side.

In Figure 5.26, we have plotted UWEA case in $XY$-plane. We observe that there is no longer symmetry among the electron trajectories and the symmetric line has shifted upward.

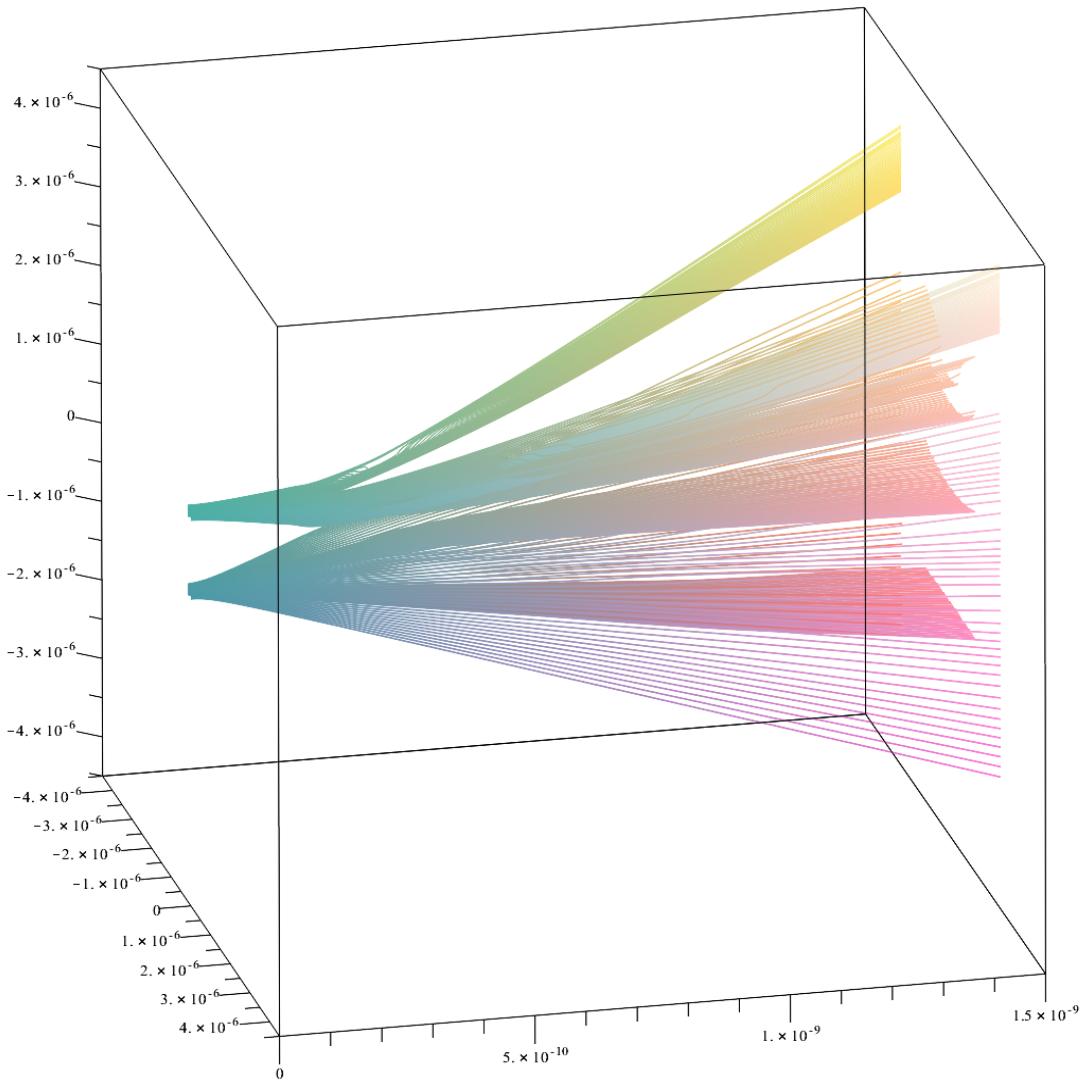


Figure 5.25: *Maple 2015 electron trajectories in Einstein's two-pinhole experiment in* $2-D$*, from the pinholes up to the detecting screen along the y-axis. Orientation:* $\theta = -95°$, $\varphi = -20°$ *and* $\psi = 14°$. Width $\Delta x_{P0} = 2\Delta x_{N0}$

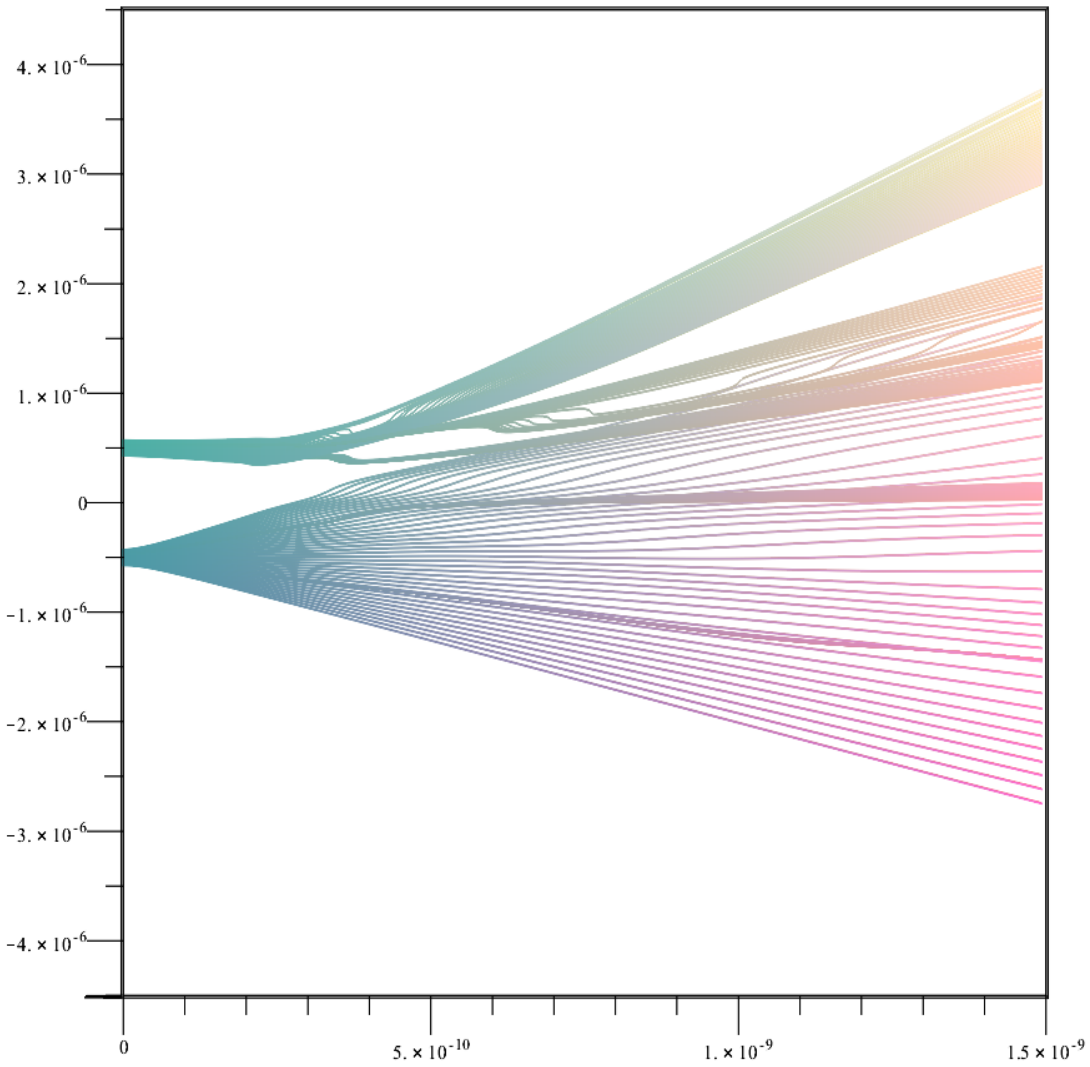


Figure 5.26: *Maple 2015 electron trajectories in Einstein's two-pinhole experiment in* $2-D$*, from the pinholes up to the detecting screen along the* $y$*-axis, but with orientation:* $\theta = -90°$*,* $\varphi = 0°$ *and* $\psi = 0°$*.*

**UWUA**

The trajectories for UWUA is shown in Figure 5.27. The trajectory ranges are $x = -4 \times 10^{-6}$ to $4 \times 10^{-6}\ m$, $z = -4 \times 10^{-6}$ to $4 \times 10^{-6}\ m$ and $t = 0\ s$ to $1.5000 * 10^{-9}\ s$. There is a reduction in interference of the electron trajectories which can be interpreted as in the classical case, in terms of wave profiles with reduced coherence.

In Figure 5.28, we have plotted UWUA case in $XY$-plane. We observe that there electron trajectories are concentrated near the symmetric line.

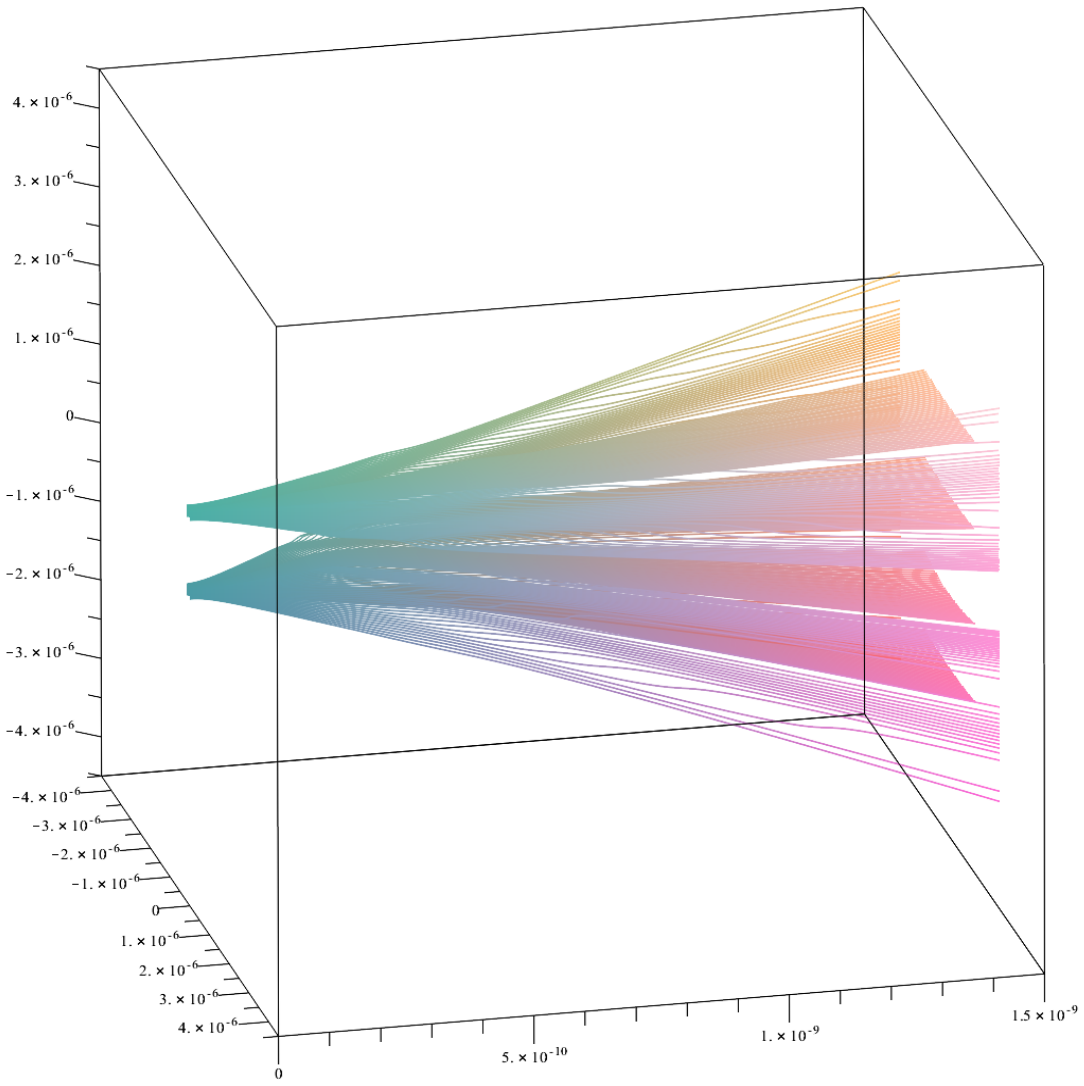


Figure 5.27: *Maple 2015 electron trajectories in Einstein's two-pinhole experiment in* $2-D$*, from the pinholes up to the detecting screen along the y-axis. Orientation:* $\theta = -95°$, $\varphi = -20°$ *and* $\psi = 14°$. Amplitude $b = \frac{\pi}{3}$ and width $\Delta x_{P0} = 1.4\Delta x_{N0}$.

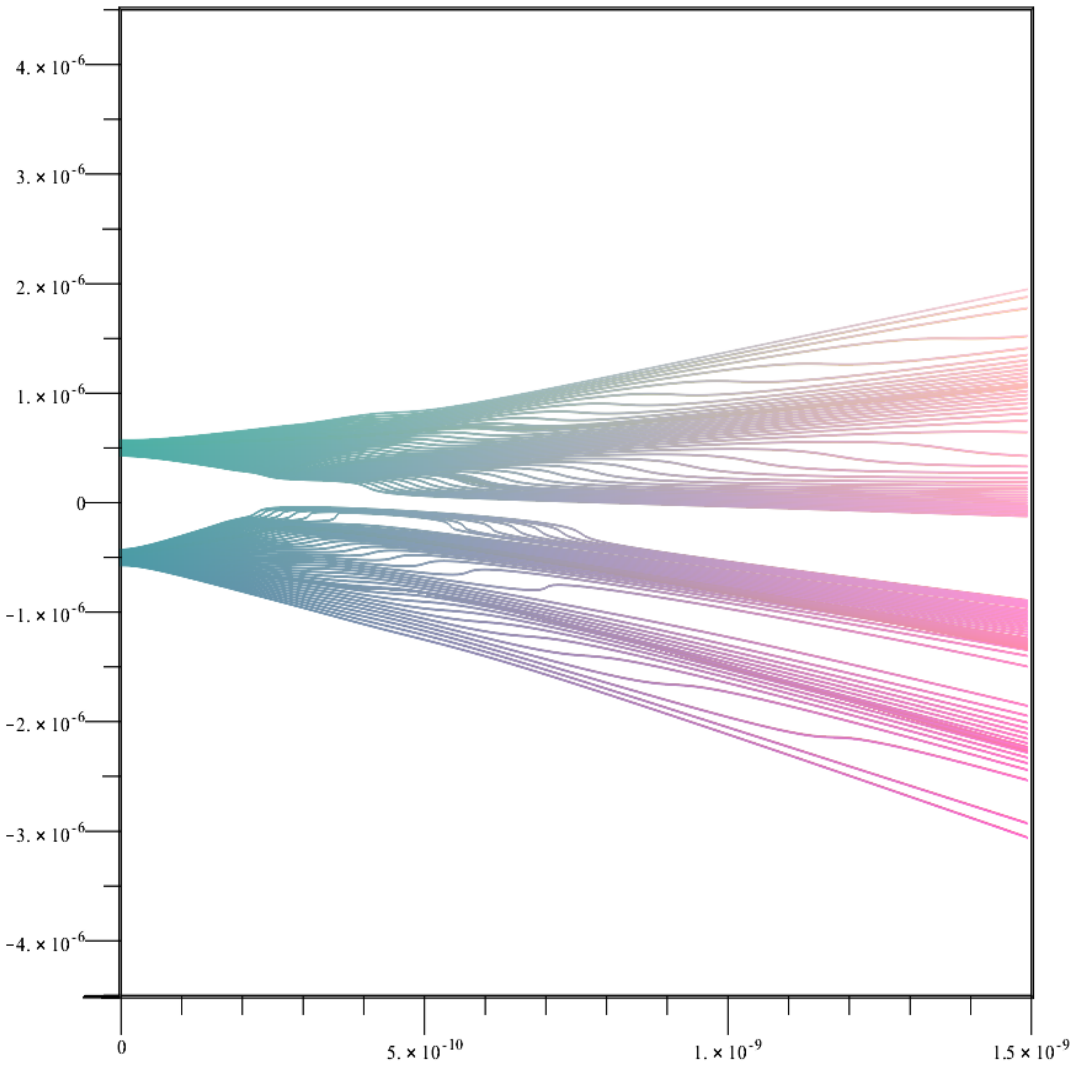


Figure 5.28: *Maple 2015 electron trajectories in Einstein's two-pinhole experiment in* $2-D$*, from the pinholes up to the detecting screen along the* $y$*-axis, but with orientation:* $\theta = -90°$*,* $\varphi = 0°$ *and* $\psi = 0°$*.*

# Chapter 6

# Conclusion

From our results we can say that we have succeeded in the following objectives:

(1) To reproduce existing $1-D$ Gaussian model of the two-slit experiment using the three software packages Maple 2015, Mathematica 10.0 and Matlab R2015a. After comparing we concluded that Maple produced the best results, so Maple was therefore selected to use to reproduce the $2-D$ Gaussian model.

(2) To derive the formula for the intensity, the quantum potential and the equations for the trajectories needed to provide the model of the two pinhole experiment using $2-D$ Gaussian wave packets.

(3) To derive the coupled nonlinear differential equation (3.137) and (3.138) used to obtain the trajectories plot,

(4) To write a program in Fortran 77 to solve the coupled nonlinear differential equation (see section 5.4.2) which describe the trajectories, i.e., to produce the data values needed to plot the trajectories,

(5) To write the Maple programs to produce intensity (Figure 5.1), quantum potential (Figure 5.9), intensity contour (Figure 5.13), quantum potential contour (Figure 5.17) and trajectories plots (Figure 5.21) using $2-D$ Gaussian wave packet for EWEA, EWUA, UWEA and UWUA cases.

(6) To see the distictive kinked behavior of the electron trajectories in directions parallel to the x-axis. There is no interference in the vertical z-direction.

The model of the two-slit and two-pinhole experiment apply to quantum objects that satisfy the Schrödinger equation such electron, neutron, proton and atom. However, the electromagnetic field is not described by the Schrödinger equation so we cannot use the Bohm-de Broglie CI to model the two-slit experiment for the electromagnetic field.

Instead the electromagnetic field is described by the second-quantized Maxwell equations. Therefore to model the two-slit experiment we need to use the CI of the electromagnetic field (CIEM). This is particularly relevant since a recent experiment by Kocsis et al [37] have managed to experimentally observe what they call photon trajectories by using the weak measurement protocol of Aharanov, Albert and Vaidman (see [38] for further references). But according to CIEM, what Kcosis et al. observed were not photon trajectories but electromagnetic field flow lines. A model of the two-slit experiment for photons based on CIEM will confirm the latter assertion. We therefore hope that such a model can be produced in future work.

# Bibliography


[1] Dewdney, C.: PhD Thesis, University of London (1983)

[2] C. Philippidis, C. Dewdney and B. J. Hiley: Quantum Interference and the Quantum Potential. Department of Physics, Birkbeck College, University of London, Malet Street, London WC1E 7HX. (1978)

[3] von Neumann, J.: Mathematische Grundlagen der Quantemechanik. Springer, Berlin (1932). English translation: Mathematica 10.0l Foundations of Quantum Mechanics, trans. by R. T. Beyer (Princeton University Press, Princeton, 1955)

[4] Possible test of the reality of superluminal phase waves and particle phase space motions in the Einstein-de Broglie-Bohm causal stochastic interpretation of quantum mechanics Vigier, J.P., Foundations of Physics, vol.24, no.1, p.61-83, 1994

[5] Bohm, D., Schiller, R. and Tiomno, J.: A Causal interpretation of the Pauli Equation (A). Suppl. Nuovo Cimento, N.1 (1955).

[6] T. Takabayasi: On the Formulation of Quantum Mechanics associated with Classical Pictures. Progress of Theor. Phvs., Vol. 8, No; 2, (1952)

[7] J .S.BELL: On the Eisntein Podolsky Rosen paradox. Physics Vol.1,No.3, pp.195-200, (1964)

[8] JeanMerker: La rigueur chez Von Neumann Seminaire EPIPHYMATHS (1991)

[9] Bell: On the Problem of Hidden Variables in Quantum Mechanics. Rev. Mod. Phys. Vol. 38. No;3 (1966)

[10] Shimony, A. (1989). Found. Phys., 19, 1425-9.

[11] Alain Aspect, Philippe Grangier, and Gerard Roger. Experimental Realization of Einstein-Podolsky-Rosen-Bohm Gedankenexperiment. Phys. Rev. Lett., Vol. 49, No; 2, (1982).

[12] Michel et Darrigol, Olivier (eds.), Erwin Schrödinger. Philosophy and the birth of quantum mechanics. Philosophie et naissance de la mecanique quantique, Editions Frontieres, Paris, 1993

[13] Jammer, M.: The Philosophy of Quantum Mechanics: The Interpretations of Quantum Mechanics in Historical Perspective. Wiley, New York (1974)

[14] Landau L D and Lifshitz E M Fluid Mechanics 1959

[15] Louis De Broglie *L'interpretation de la mecanique ondulatoire*. Le journal de physique et le radium. Tome 20. (1959)

[16] Wootters, W.K., Zurek, W.H.: Complementarity in the double-slit experiment: quantum nonseparability and a quantitative statement of Bohr's principle. Phys. Rev. D19, 473-484 (1979)

[17] P.N. Kaloyerou: Critique of Quantum Optical Experimental Refutations of Bohr's Principle of Complementarity, of the Wootters-Zurek Principle of Complementarity, and of the Particle-Wave Dulity Relation, Found. Phys. V46, No2 (2016)

[18] Jafari Matehkolaee & Mehdi *Understanding the measurement theory in quantum mechanics* (2011)

[19] J. von Neumann *Mathematica 10.0l Foundations of Quantum Mechanics* (1988)

[20] Franco Selleri. Le grand debat de la theorie quantique (1986)

[21] Bohm, D. and Hiley, B.J. The Undivided Universe: An Ontological Interpretation of Quantum Theory. London: Routledge (1993).

[22] Bohm, D.: A suggested interpretation of the quantum theory in Terms of "hidden" variables. I. Phys. Rev.85, 166-179 (1952)

[23] Einstein, A. . In Albert Einstein: Philosopher-Scientist, ed. P. A. Schilpp, pp. 1-95 and 663-88. La Salle, 111: Open Court. (1949)

[24] Schrödinger, E. (1935b). Naturwissenschaften, 23, 807-12, 823-8, 844-9 (English translation in Wheeler and Zurek (1983)).

[25] J. S. Bell, Speakable and Unspeakable in Quantum Mechanics, chapter 2, Cambridge University Press, Cambridge, (1987).

[26] Bohr, N. Atomic physics and human knowledge. New York: Wiley. (1958)

[27] Paavo Pylkkanen, B. J. Hiley, Ilkka Pattiniemi, arXiv:1405.4772v1 [quant-ph] , Bohm's approach to Quantum Mechanics and Individuality (2014)

[28] G. Iannaccone, G. Curatola, G. Fiori: Effective Bohm Quantum Potential for device simulators based on drift-diffusion and energy transport, Simulation of Semiconductor Processes and Devices, 2004, vol. (2004)

[29] Eric R. Bittner: Quantum tunneling dynamics using hydrodynamic trajectories, arXiv:quant-ph/0001119v2, (2000)

[30] E. Gindensberger, C. Meier, J.A. Beswick: Mixing quantum and classical dynamics using Bohmian trajectories, Journal of Chemical Physics, vol. 113, no. 21, (2000)

[31] Jeremy B. Maddox, Eric R. Bittner: Estimating Bohm's quantum force using Bayesian statistics, Journal of Chemical Physics, vol. 119, no. 13, (2003)

[32] D. Bohm, Quantum Theory. Prentice-Hall, Inc., New York, (1951)

[33] D Home and P N Kaloyerou, New twist to Einstein's two-slit experiment: complementarity vis-a-vis the causal interpretation. J.Phys. Math.Gen.22 (1989)

[34] A. Nazarkin, G. Korn, Phys. Rev. Lett. 8EOT, 4748 (1999)

[35] M. Y. Shverdin, D. R. Walker, D. D. Yavuz, G. Y. Yin, S. E. Harris, in OSA Trends in Optics and Photonics Series (TOPS) Vol. 96, Conference on Lasers and ElectroOptics (CLEO) (Optical Society of America, Washington, DC, 2004), Post-deadline paper CPDC1

[36] R.L. Burden and T.D. Faires, Numerical Analysis. Publishing Company, Boston, (1989).

[37] Kocsis S, Braverman B, Ravets S, Stevens MJ, Mirin R P, Shalm L K and Steinberg AM 2011 Observing the trajectories of a single photon using weak measurement Science 332 1170.

[38] Kaloyerou PN 2017 A brief overview and some comments on the weak measurement protocol Phys. Astron. Int. J. 5 1-7.

**END**